Molecular, Cellular, and Industrial Aspects of *Oedogonium* Cellulose

By

Michael Piotrowski

A dissertation submitted in partial fulfillment of

the requirements for the degree of

Doctor of Philosophy

(Botany)

at the

UNIVERSITY OF WISCONSIN-MADISON

2019

Date of final oral examination: 12/17/2019

This dissertation is approved by the following members of the Final Oral Committee:

Linda Graham, Professor, Botany

Donna Fernandez, Professor, Botany

Kenneth Sytsma, Professor, Botany

Donald Waller, Professor Botany

Alan W. Rudie, Supervisory Research Chemist, U.S. Forest Service, Forest Products Laboratory

Acknowledgements

I would like to acknowledge people who guided my research. First of all my graduate committee – Dr. Linda Graham, Dr. Donna Fernandez, Dr. Kenneth Sytsma, Dr. Don Waller, and Dr. Alan Rudie - for their continued support and efforts in bringing this thesis to fruition.

My thanks also go to current and former members of the Graham, including Dr. James Graham, Dr. Lee Wilcox, Dr. Shahrizim Zulkifly, Dr. Christopher Cardona-Correa, Jennifer Knack, Michael Braus, Dr. Anchittha Satjarak, and Elizabeth Phillippi for support and company. I am also grateful to Marie Trest who helped me with algal culturing techniques, and Dr. Heather Owen (UW Milwaukee) for guidance with microscopy techniques.

Appreciation also goes out for the financial support I received from the Botany Department in the form of teaching assistantships, research support from a USDA grant awarded to AlgaExperts (currently Algenomics, LLC), and research lab computing equipment funded by NSF DEB111- 9944 (awarded to Dr. Linda Graham). I very much appreciate Sarah Friedrich's assistance with figures for portions of this thesis that have been or are yet to be submitted for publication.

Lastly, I thank my family for being my biggest supporters, not letting me quit when I became overwhelmed, listening to me babble on for endless hours about my head/heartaches, and making me smile.

Thank you all.

Abstract

Chlorophyte algae are important components of aquatic and terrestrial ecosystems worldwide, the chlorophyte *Oedogonium* being particularly rich in species, abundant, and globally widespread. *Oedogonium* and many other chlorophytes, like plants and closely related streptophyte algae, produce cellulose-rich cell walls that have been employed in industrial applications. In the present study, a draft genome for our lab's isolate of *Oedogonium* (Lake Mendota strain) was employed to generate sequences for five marker genes for taxonomic characterization, and to characterize *CesA* sequences inferred to encode proteins involved in cellulose biosynthesis, for phylogenetic comparison to *CesA*s known for other chlorophytes. Some *Oedogonium* Lake Mendota strain *CesA* sequences appear to have diverged even earlier than those of prasinophytes, representing the earliest-diverging lineages of green algae. This result may help to explain unusual macromolecular features of cellulose produced by this strain. Other *CesA* sequences filtered from the Lake Mendota strain draft genome were distributed more broadly though-out the chlorophyte tree, but did not match those known for two other *Oedogonium* species. This thesis also reports the results of growth experiments designed to foster industrial-level production of *Oedogonium* cellulose at wastewater treatment facilities that provide nutrient-rich water. Results revealed a strong impact of temperature, but also that production in temperate locales is feasible. A final thesis component employed quantitative imaging methods to test a hypothesis that the unusual macromolecular structure of the cell wall of *Oedogonium* Lake Mendota strain confers resistance to microbial attachment, a feature of potential ecological and industrial importance. Results indicated that natural microbial populations on the low-texture cellulosic cell wall surfaces of the *Oedogonium* Lake Mendota strain were an order of magnitude lower than microbial populations present on the higher-

texture cellulosic surfaces of two ecologically- and structurally-similar green algal species. In summary, the thesis displays the results of molecular, cellular, and experimental growth approaches to cellulose production by an ecologically important chlorophyte.

Table of contents

Chapter 1. Introduction to the chlorophyte *Oedogonium*, chlorophyte celluloses and cellulose synthase genes, and the potential for their use in industrial applications

This chapter provides an overview and rationale for three research studies that make up this thesis. This overview consists of three sections, the first of which focuses on the organismal system under study–the green algal genus *Oedogonium*. A second section concerns the cellulose-rich cell wall produced by the study organism, cellulose biosynthesis genes, and inferred cellulose biosynthesis proteins, the focus of thesis Chapter 2. The third section of this overview concerns the potential for industrial cultivation of *Oedogonium* and applications of cellulose extracted from it, related to thesis Chapters 3 and 4. Please note that for readability, this overview includes representative literature citations; more extensive literature coverage has been provided in the following three chapters.

I. The chlorophyte Oedogonium

This section begins with a summary of information about evolutionary relationships, morphology, ecology, and taxonomy of the chlorophyte algal genus *Oedogonium*. The section then focuses on a particular strain of *Oedogonium* that was employed for research work described in other chapters of this thesis.

The green algae are commonly classified into one of two phyla: 1) Streptophyta that also includes the embryophytic (land) plants, and 2) Chlorophyta. The Chlorophyta includes multiple early-diverging lineages of unicellular prasinophytes plus core chlorophytes, most grouped into classes Ulvophyceae, Trebouxiophyceae, or Chlorophyceae (Fig. 1).

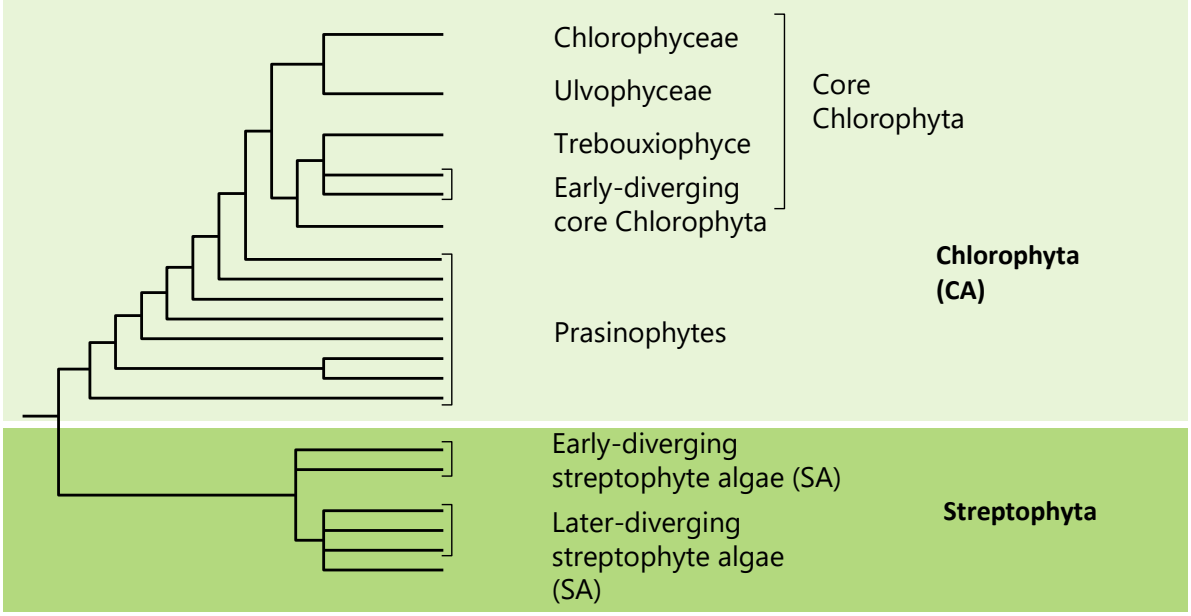

Fig. 1. Phylogeny of the green algae (from Graham et al. 2016).

According to Fucikova et al. (2019), the green algal class Chlorophyceae is a monophyletic group that includes members having diverse types of body structure, illustrated by unicellular *Chlamydomonas*, colonial *Volvox*, coenocytes such as *Protosiphon*, and branched or unbranched filaments illustrated by order Oedogoniales. Considered to be a monophyletic group, the Oedogoniales are most closely related to Chaetophorales and Chaetopeltidales (Buchheim et al. 2011, Fang et al. 2018). Cellulose-rich cell walls are common, but not universal among chlorophyceans; for example, cell walls in the *Chlamydomonas-Volvox* complex lack cellulose. The cell walls of Oedogoniales are known to be cellulose-rich (Estevez et al. 2008; Domozych et al. 2012).

Oedogoniales are characterized by a distinctive set of structural features: uninucleate cells; a parietal, reticulate plastid containing many pyrenoids; an unusual form of cytokinesis involving precocious development of cell wall rings; asexual zoospores produced one per vegetative cell; stephanokont (multiple flagella occur in a ring) zoospores and sperm, and

oogamous sexual reproduction with zygotic meiosis (Graham et al. 2016). Asexual reproduction can also occur by fragmentation, with the result that population growth can occur rapidly.

Genus *Oedogonium* takes its name from the Greek “oidos,” meaning swelling + Greek “gonos, meaning offspring, reflecting production of oogonia and zygotes that are generally larger than vegetative cells. *Oedogonium* is an unbranched filament that commonly occurs in freshwater periphyton, attached by means of specialized basal holdfast cells (Fig. 2a), or as floating masses in temperate-tropical freshwaters world-wide.

For genomic and industrial research described in chapters 2 and 3 of this thesis, a unialgal isolate of *Oedogonium* was made from the periphyton of Lake Mendota (Dane Co., WI, USA) (43°06’24”N, 89°25’29”W). In addition to *Oedogonium*, Lake Mendota periphyton typically includes the branched filamentous genus *Cladophora* and filamentous zygnematalean algae, often tangled together. Isolates of *Oedogonium* can be made by using dissecting microscope and fine forceps to select and transfer algal filaments to well-plates containing a growth medium designed to mimic the nutrient status of hypereutrophic Lake Mendota, then monitoring wells for production of large swimming zoospores, which can be isolated and grown in the laboratory to generate experimental biomass. Because previous experimental studies (Machlis 1973) demonstrated that *Oedogonium* cultures rendered axenic did not grow well, the cultures employed for thesis studies were not axenic (completely free of bacteria), though bacterial populations were not conspicuous (Fig. 2).

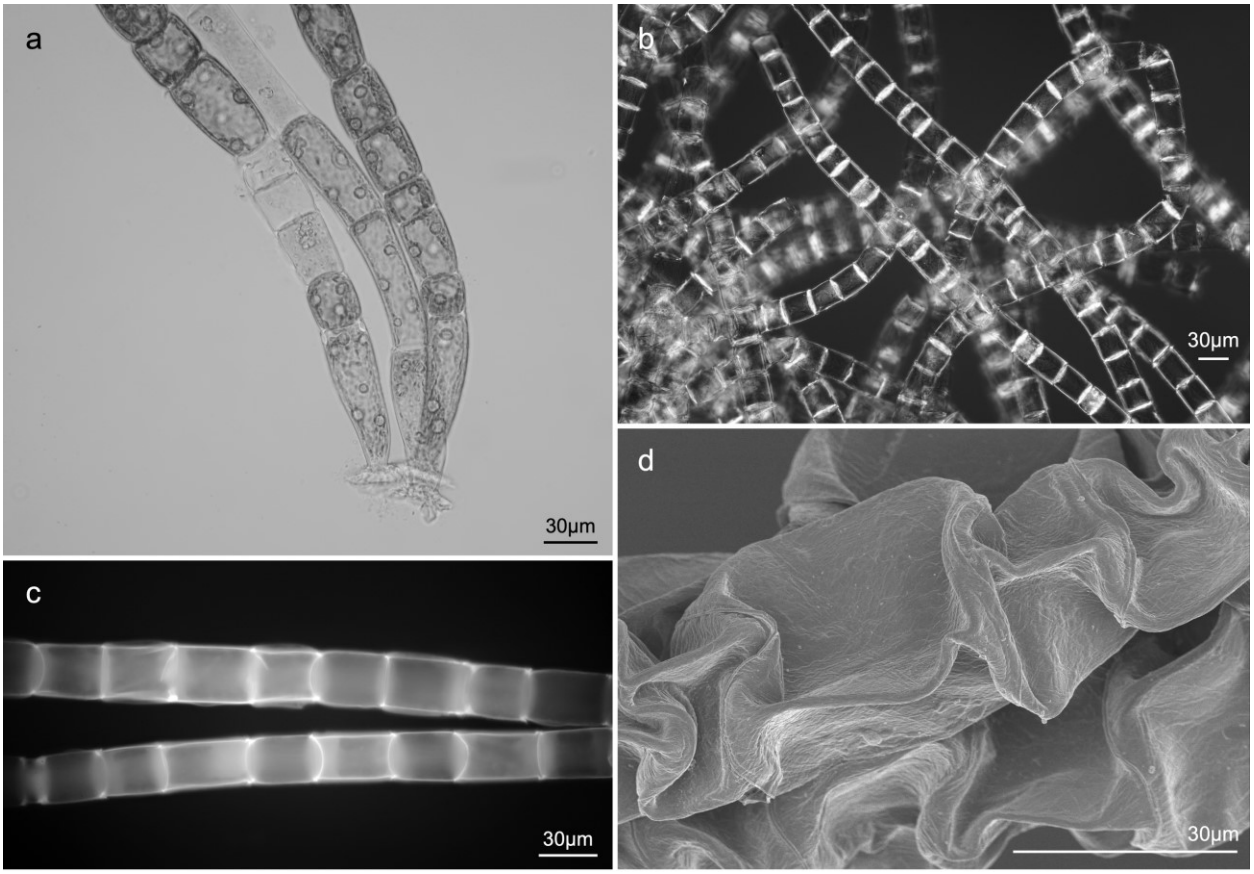

Fig. 2. Unialgal cultures of the *Oedogonium* strain isolated from Lake Mendota for use in molecular and industrial growth studies described in this thesis. a. Unbranched filaments attach to substrata by specialized holdfast cells. b. Cell walls are rich in cellulose, indicated by birefringence as viewed with crossed-polarizers. c. When treated with the fluorochrome Calcofluor White, cell walls fluoresce blue-white, a reaction typical of cellulose. d. When viewed with use of scanning electron microscopy, cell wall surfaces appear relatively smooth by comparison to the more-textured, fibrillar walls of *Cladophora*, other algae, and land plants. Image plate from Piotrowski et al. (2020).

Identifying *Oedogonium* isolates to the species level is challenging because more than 850 species of *Oedogonium* have been named, often from field collections and on the basis of structural or reproductive variation (e.g. Huxley 2003); of these, 569 are currently accepted (Guiry et al. 2019). If key structural or reproductive features are not expressed in cultured isolates, confident classification to the species level by means of morphology alone may not be possible. For example, Lawton et al. (2014) were able to make tentative species assignments based on structural features for only a few of the 11 Australian isolates these researchers had generated for potential industrial application. These authors attempted to characterize isolates with the use of the molecular marker ITS, based upon a previous molecular phylogenetic study of 25 *Oedogonium* accessions, including 12 new Chinese isolates based on "ITS-2" (Mei et al. 2007), but were not able to obtain ITS sequences for all of their isolates, and none of the Australian isolates could be phylogenetically linked with any named *Oedogonium* species for which ITS sequences were then available.

Similarly, we were unable to confidently identify the Lake Mendota *Oedogonium* isolate to the species level based on structural characters expressed in culture. Although filament width was highly consistent (Fig. 2a-c) and congruent with Huxley's (2003) description of *O. capilliforme* Kutzing 1849, the cultured isolate did not express all sexual traits needed for comparison, specifically male gametangia and oospores (zygotes). It is possible that the Lake Mendota isolate represents a female strain of a dioicous species.

For this reason, to characterize the Lake Mendota isolate, we acquired a set of five commonly-used molecular marker sequences: partial sequences of the plastid-coded large subunit of rubisco *rbc*L, and four ribosomal markers: 23S rDNA, 28S rDNA, 18S rDNA, and a sequence that includes part of the 18S ribosomal gene + internal transcribed spacer 1 (ITS1) +

the 5.8S ribosomal RNA gene + internal transcribed spacer 2 (ITS2) + part of the 28S ribosomal gene, previously described as "ITS-2" (Mei et al. 2007). These marker gene sequences were derived from our lab's deep draft genome sequence dataset for the Lake Mendota strain: 1,780 bp length of 18S rDNA was obtained with mean coverage of 1,028-fold; for chloroplast 23S rDNA, 348 bp length was obtained with mean coverage of 39-fold; 2,000 bp length of 28S rDNA was obtained at 868-fold; 1,395 bp length of plastid-encoded *rbc*L was obtained in mean coverage of 71-fold; and a 702 bp length sequence encompassing some 18S rDNA+ITS1+5.8S rDNA+ITS2+some 28S rDNA (for simplicity, ITS1+5.8S rDNA+ITS2) was obtained with mean coverage of 996-fold (Graham et al. 2020). Employing draft genome sequence avoids potential amplification bias that can occur when marker sequences represent amplicons.

Phylogenetic methods, namely maximum likelihood (ML) and Bayesian analyses, were used to compare the Lake Mendota strain with *Oedogonium* accessions currently represented in the NCBI GenBank public databases. Current GenBank information was not sufficient to allow identification of an appropriate outgroup in order to perform a concatenation analysis; no single species or isolate of Oedogoniales was represented in genomic databases by all five of the taxonomic marker sequences we employed, though at least one of these marker sequence types was available in databases for at least one species or isolate of Oedogoniales. It is also the case that concatenation approaches can converge on incorrect species trees (Liu et al. 2019), a particular concern in the case of Oedogoniales because the high diversity of accepted species (>569) is poorly represented in current genomic databases. Consequently, we generated separate trees for each marker. ML and Bayesian phylogenetic analyses revealed that the five gene markers–*rbc*L and four ribosomal DNA regions–could not distinguish the Lake Mendota strain from other *Oedogonium* species or isolates represented in the NCBI GenBank accessed on July

15, 2019. For this reason, the isolate employed for genomic and industrial studies of cellulose production in this thesis (and publications arising) has been denoted as "*Oedogonium* sp. Lake Mendota strain." The new marker sequences for *Oedogonium* sp. Lake Mendota strain have been archived in NCBI GenBank: 18S rDNA MN191507; 23S rDNA MN191506; 28S rDNA MN191505; *rbc*L MN205324; ITS1+5.8S rDNA+ITS2 MN191508 (Graham et al. 2020).

II. Chlorophyte celluloses and synthesis genes

This section surveys existing information about cellulose production by chlorophyte algae, focusing on macromolecular differences between chlorophyte celluloses and those of streptophytes (including streptophyte green algae). Such macromolecular differences–based upon differences in cellulose synthesizing complexes encoded by *CesA* genes–affect the potential for industrial applications.

In land plants, particulate cellulose synthesizing complexes–located in the cell membrane–take the form of rosettes of cellulose synthases that spin out relatively fine cellulosic microfibrils (Haigler and Roberts 2019). Plant CesA proteins are glycosyl transferases with catalytic regions involved in synthesizing cellulose microfibrils. Plant CesA proteins also include domains important for CesA-CesA interaction linked to rosette structure (Kumar and Turner 2015). Streptophyte green algae, which are closely related to land plants, likewise produce cellulose synthase rosettes. By contrast, cell wall celluloses produced by other algae (e.g. stramenopiles, red algae, chlorophyte green algae) generate structurally different synthase arrays, typically rectangular in shape, derived from the linear cellulose molecules generated by bacteria, including cyanobacteria (reviewed by Tsekos 1999). Bacterial cellulose synthases, likewise targeted to cell

membranes, are encoded by bacterial-type cellulose synthase genes (*Bcs*). Recent studies have detected evidence that both CesA and Bcs proteins occur in streptophytes (Harholt et al. 2012, Ulvskov et al. 2013). It has been hypothesized that the ancestors of green algae acquired from a cyanobacterial endosymbiont a *Bcs* gene (Nobles et al. 2001) from which *CesA* was later derived (Mikkelsen et al. 2014).

A prior genomic study from our lab that focused on carbohydrate active enzymes of an early-diverging chlorophyte lineage represented by the modern prasinophyte *Pyramimonas parkeae* (Satjarak and Graham 2017) indicated the presence of at least one type of glycosyl transferase (GT). The *P. parkeae* GT gene displayed features common to *Bcs* and land plant *CesA* genes (Fig. 3), a finding consistent with those for some other prasinophytes for which draft genomes have been generated. Evidence that prasinophyte flagellates generally possess the genetic capability to produce cellulose was somewhat surprising, because in other algae and land plants, cellulose is commonly deployed externally during the construction of a cell wall, which is lacking from *P. parkeae*. Even so, these observations suggest that chlorophyceans such as *Oedogonium* likely inherited cellulose-synthesis genes from ancestral green algae.

Fig. 3. Putative cellulose synthase gene from draft nuclear genome of *Pyramimonas parkeae* CCMP726, showing QXXRW domains, Ds residues, and the DSD motif characteristic of catalytic regions of bacterial and embryophyte cellulose synthases. Image from Satjarak and Graham (2017).

SEM observations indicated that cell walls of *Oedogonium* sp. Lake Mendota strain had a noticeably less-fibrillar texture (Fig. 2d) than those of other algae having cellulose-rich cell wall, and that *Oedogonium* cell walls may have high resistance to hydrolysis (Graham et al. 2013). Because the molecular bases of these unusual features are unknown, and because chlorophyte cellulose synthase genes are poorly-studied–largely known from species for which draft whole genome sequence has been obtained (Ulvskov et al. 2013)–we examined our draft genome for the *Oedogonium* sp. Lake Mendota strain for evidence of genes associated with cellulose synthesis, an effort described more fully in Chapter 2 of this thesis.

III. *Potential industrial applications of Oedogonium and its cellulose*

The robust nature of conspicuous *Oedogonium* populations in nature has suggested diverse industrial applications, primarily remediation of waters contaminated by heavy metals or nutrients that would otherwise foster harmful algal blooms. For example, because metals readily adsorb to *Oedogonium* surfaces (Gupta et al. 2008a, 2008b, 2009, 2010; Bakatula 2014), *Oedogonium* has been studied in engineered systems designed to remove heavy metals, as well as N and P from wastewaters to improve water quality before effluent discharge to natural environments (Cole et al. 2014, 2016; Neveux et al. 2016; Roberts et al. 2013, 2018), and at the

same time generate biomass for bioenergy and other industrial applications, reviewed by Lawton et al. (2017).

Cellulose has been cited among various types of useful materials that might be extracted from *Oedogonium* (Piotrowski et al. 2020). Highly-crystalline cellulose extracted from the branched filamentous chlorophyte *Cladophora* has been proposed for a variety of industrial applications (reviewed by Mihranyan 2011), suggesting that *Oedogonium* cellulose may likewise also find industrial uses. Chlorophyte celluloses are known to vary among genera, and to differ from celluloses produced by streptophytes–plants and closely-related charophycean green algae–in biophysical traits (Kubicki et al. 2018) that arise from biochemical differences in the cell membrane proteins that make up cellulose-synthesizing complexes (Tsekos 1999, Polko and Kleiber 2019), which are encoded by *CesA* genes (Kumar and Turner 2015, Chen et al. 2018, Speicher et al. 2018). Rapidly-growing, easily-harvested chlorophyte algae such as *Oedogonium* thus offer the potential for wastewater-linked production of distinctive types of cellulose that may have useful applications.

Previous comparisons of growth performance of different *Oedogonium* isolates have indicated the advisability of employing isolates obtained from geographical areas characterized by high annual variability in annual temperature, which are expected to have broad environmental tolerance (Lawton et al. 2014). In general, for outdoor biomass cultivation, it would seem advisable to employ algal strains for which optimal environmental conditions for growth have evolved to match ambient conditions. Using isolates generated from the same geographical locale for outdoor biomass cultivation would increase the chances that such algal strains have become adapted to local environmental stressors. A master's degree study of cellulose productivity by *Oedogonium* sp. Lake Mendota strain, earlier conducted by the thesis

author in varying environmental conditions in the UW-Madison Biotron facility, indicated high potential for scale-up production of cellulose at a local wastewater treatment facility. In such a case, secondary wastewater effluent supplies mineral nutrients (N, P, inorganic C) and water essential for algal growth, which improves effluent quality while also generating dissolved oxygen useful in primary wastewater treatment and a cellulose crop that could be sold to subsidize costs of effluent remediation. Chapter 3 of this thesis, based on Piotrowski et al. (2020), describes a study designed to determine industrial cultivation feasibility.

Previous observations also suggested a potential application of harvested *Oedogonium* cellulose, based on structural features differing from those of other studied chlorophytes. As noted, *Oedogonium* commonly occurs in natural freshwater periphyton communities together with the ulvophycean chlorophyte *Cladophora*. Our three previous studies of the microbiota or microbiome of *Cladophora* sampled from Lake Mendota had revealed the common occurrence of diverse and abundant epimicrobiota (Zulkifly et al. 2012; Graham et al. 2015; Braus et al. 2017), but such microbiota were not as conspicuous on the wall surfaces of co-occurring *Oedogonium*, particularly natural collections that were morphologically similar to our cultivated Lake Mendota strain (Fig. 4). One possible explanation for the difference in epimicrobiota colonization is that the unusual smoothness of *Oedogonium* cellulose (Fig. 2d) may not foster microbial attachment to the same degree as the more-textured cell walls of *Cladophora*. If *Oedogonium* cellulose, by virtue of differing surface texture, is less subject to microbial colonization than other types of cellulose, useful medical and other industrial applications might be indicated. And, since algal epimicrobiota are known to play important ecological roles, such a difference might also be important in the realm of aquatic ecology. To further explore this difference in epimicrobiota colonization, epimicrobial populations on replicate filaments of

Cladophora and *Oedogonium* sampled from Lake Mendota on the same day in spring 2019 were compared. These epibacterial populations were also compared to those of the similarly-structured (filamentous) streptophyte *Nitella tenuissima* (which does not occur in Lake Mendota) sampled from a different locale for a high-throughput molecular study of epimicrobiota (Knack et al. 2015). These three green algal taxa represent three distinct lineages of green algae that include filamentous species commonly observed in freshwater habitats. SEM and other imaging methods employed for these comparisons are described in Chapter 4 of this thesis.

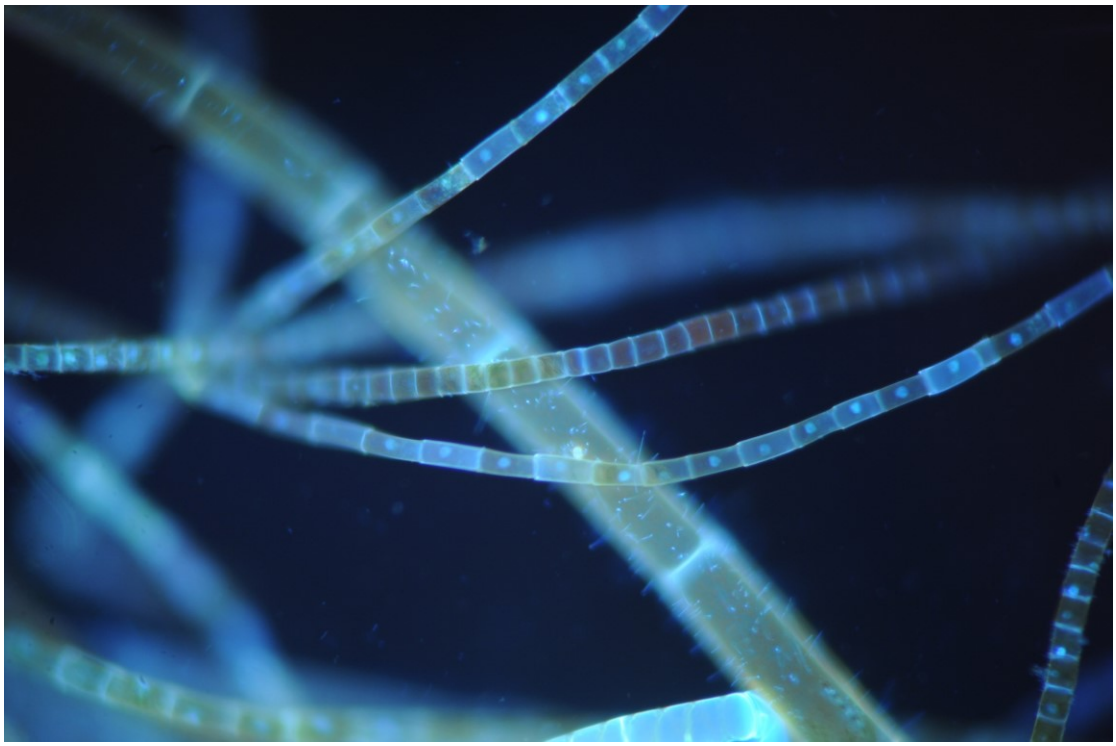

Fig. 4. Periphyton sampled from Lake Mendota in spring, 2019, stained with the DNA-binding fluorochrome DAPI and viewed with UV epifluorescence. Narrower filaments of *Oedogonium* lack obvious colonization by epimicrobiota. By comparison, the wider *Cladophora* filament is coated with diverse types of epimicrobiota. Two of the narrower filaments shown in this view, those having cells whose lengths are consistently greater than cell widths, correspond to our

isolate "*Oedogonium* sp. Lake Mendota strain," which has been distinguished from other molecularly-characterized *Oedogonium* species by five molecular markers (Graham et al. 2020). Other narrow filaments having cells whose lengths and widths are of similar dimensions represent a different (unknown and uncharacterized) species of *Oedogonium* and were not studied.

References

Bakatula, E.N., E.M. Cukrowska, I.M. Weiersbye, L. Mihaly-Cozmuta, A. Peter & H. Tutu. 2014. Biosorption of trace elements from aqueous systems in gold mining sites by the filamentous green algae (*Oedogonium* sp.). *J Geochem Explo*r 144:492-503.

Braus, M.J., T.L. Whitman & L.E. Graham. 2017. Spatiotemporal dynamics of bacterial microbiota and methanotrophic bacteria on lotic *Cladophora glomerata* (Chlorophyta). *J Phycol* 53:1255-1262.

Buchheim, M.A., D.M. Sutherland, T. Schleicher, F. Förster & M. Wolf. 2012. Phylogeny of Oedogoniales, Chaetophorales, and Chaetopeltidales (Chlorophyceae): inferences from sequence-structure analysis of ITS2. *Ann Bot* 109:109-116.

Chen, H.-W., S. Persson, M. Grebe & H.E. McFarlane. 2018. Cellulose synthase during cell plate assembly *Physiol Plant* 164:17-26.

Cole, A.J., L. Mata, N.A. Paul & R. de Nys. 2014. Using CO_2 to enhance carbon capture and biomass applications of freshwater macroalgae. *GCB Bioenergy* 6:637-645.

Cole, A.J., N. Neveux, A. Whelan, J. Morton, M. Vis, R. de Nys & N.A. Paul. 2016. Adding value to the treatment of municipal wastewater through the intensive production of freshwater macroalgae. *Algal Res* 20:100-109.

Domozych, D.S., M. Ciancia, J.U. Fangel, M.D. Mikkelsen, P. Ulskov & W.G.T, Willats. 2012. The cell walls of green algae: a journey through evolution and diversity. *Front Plant Sci* 3:82

Estevez, J.M., P.I. Leonardi & J.S. Alberghina. 2008. Cell wall carbohydrate epitopes in the green alga *Oedogonium bharuchae* f. minor (Oedogoniales, Chlorophyta). *J Phycol* 44:1257-1268.

Fang, L., F. Leliaert, P.M. Novis, Z. Zhang, H. Zhu, G. Liu, D. Penny & B. Zhong. 2018. Improving phylogenetic inference of core Chlorophyta using chloroplast sequences with strong phylogenetic signals and heterogeneous models. *Molecular Phylogenetics and Evolution* 127:248-255.

Fucikova, C., P.O. Lewis, S. Neupane, K.G. Karol & L.A. Lewis. 2019. Order, please! Uncertainty in the ordinal-level classification of Chlorophyceae. *PeerJ* 7:e6899.

Graham, L., M.E. Cook, L.W. Wilcox, J.M. Graham, C.H. Wellman, W. Taylor & L.A. Lewis. 2013. Resistance of filamentous chlorophycean, ulvophycean, and xanthophycean algae to acetolysis: testing Proterozoic and Paleozoic microfossil attributions. *Int J Plant Sci* 174:947-957.

Graham L.E., J.J. Knack, M.E. Graham, J.M. Graham & S. Zulkifly. 2015. A metagenome for lacustrine *Cladophora* (Cladophorales) reveals remarkable diversity of eukaryotic epibionts and genes related to materials cycling. *J Phycol* 51:408-418.

Graham, L.E., J.M. Graham, L.W. Wilcox, L.W. & M.E. Cook. 2016. *Algae*. 3rd ed. LJLM Press, Madison, WI, 595 pp.

Graham, L.E., M.J. Piotrowski, J.M. Graham & A. Satjarak. 2020. Molecular markers obtained from draft genomic sequence data characterize an isolate of *Oedogonium* (Oedogoniales, Chlorophyta) employed for biomass applications. *Phycologia* (in press).

Guiry, M.D. in Guiry M.D. & G.M. Guiry. 2019. AlgaeBase. World-wide electronic publication, National University of Ireland, Galway http://www.algaebase.org; searched on 14 July 2019.

Gupta, V.K. & A. Rastogi A. 2008a. Biosorption of lead(II) from aqueous solutions by non-living algal biomass *Oedogonium* sp. and *Nostoc* sp.–A comparative study. *Colloids Surfaces B:Biointerfaces* 64:170-178.

Gupta, V.K. & A. Rastogi. 2008b. Equilibrium and kinetic modeling of cadmium(II) biosorption by nonliving algal biomass *Oedogonium* sp. from aqueous phase. *J Hazard Mat* 153:759–766.

Gupta, V.K. & A. Rastogi. 2009. Biosorption of hexavalent chromium by raw and acid-treated green alga *Oedogonium hatei* from aqueous solutions. *J Hazard Mat* 163:396–402.

Gupta, V.K., A. Rastogi & A. Nayak. 2010. Biosorption of nickel onto treated alga (*Oedogonium hatei*): Application of isotherm and kinetic models. *J Colloid Interface Sci* 342:533–539.
Gupta 8a.b, 9, 10, 11

Harholt, J., I. Sørensen, J. Fangel, A. Roberts, W.G. Willats, H.V. Scheller, B.L. Petersen, J.A. Banks & P. Ulvskov. 2012. The glycosyltransferase repertoire of the spikemoss *Selaginella moellendorffii* and a comparative study of its cell wall. *PloS ONE* 7(5):e35846.

Haigler, C.H. & A.W. Roberts. 2019. Structure/function relationships in the rosette cellulose synthesis complex illuminated by an evolutionary perspective. *Cellulose* 26:227-247.

Huxley, R. 2003. *Oedogonium* Link 1820. In: *The freshwater algal flora of the British Isles. An identification guide to freshwater and terrestrial algae*. (ed. D.M. John, B.A. Whitton, & A.J. Brook). Pp. 413-433. Cambridge University Press, Cambridge.

Kubicki, J.D., H. Yang, D. Sawada, H. O'Neill, D. Oehme & D. Cosgrove. 2018. The shape of native plant microfibrils. *Sci Rep* 8:13983.

Kumar, M. & S. Turner. 2015. Plant cellulose synthesis: CESA proteins crossing kingdoms. *Phytochemistry* 112:91-99.

Lawton, R.J., R. de Nys, S. Skinner & NA. Paul. 2014. Isolation and identification of *Oedogonium* species and strains for biomass applications. *PLoS One* 9:e97373.

Lawton, R.J., A.J. Cole, D.A. Roberts, N.A. Paul, & R. de Nys. 2017. The industrial ecology of freshwater macroalgae for biomass applications. *Algal Res* 24:486-491.

Liu, L., C. Anderson, D. Pearl & S.V. Edwards. 2019. Modern phylogenomics: Building phylogenetic trees using the multispecies coalescent model. Chapter 7 In Anisimova, M. (ed.) *Evolutionary Genomics: Statistical and Computational Methods*, Methods in Molecular Biology, vol. 1910:211-239.

Machlis, L. 1973. The effects of bacteria on the growth and reproduction of *Oedogonium cardiacum*. *J Phycol* 9:342-344.

Mei, H., W. Luo, G.X. Liu & Z.Y. Hu. 2007. Phylogeny of Oedogoniales (Chlorophyceae, Chlorophyta) inferred from 18S rDNA sequences with emphasis on the relationships in the genus *Oedogonium* based on ITS-2 sequences. *Plant System Evol* 265:175-191.

Mihranyan, A. 2011. Cellulose from Cladophorales green algae: From environmental problem to high-tech composite materials. *J Appl Polymer Sci* 119:2449–2460.

Mikkelson, M.D., J. Harholt, P. Ulskov, I.E. Johansen, J.U. Fangel, M.S. Doblin, A. Bacic & W.G. Willats. 2014. Evidence for land plant cell wall biosynthetic mechanisms in charophyte green algae. *Ann Bot* 114:1217-1236.

Neveux, N., M. Magnusson, L. Mata, A.Whelan, R. de Nys R & N.A. Paul. 2016. The treatment of municipal wastewater by the macroalga *Oedogonium* sp. and its potential for the production of biocrude. *Algal Res* 13:284-292.

Nobles, D.R., D.K. Romanovicz, & R.M. Brown. 2001. Cellulose in cyanobacteria. Origin of vascular plant cellulose synthase? *Plant Physiol.* 127(2):529-542.

Piotrowski, M.J., J.M. Graham & L.E. Graham. 2020. Temperate zone cultivation of *Oedogonium* in municipal wastewater effluent to produce cellulose and oxygen. *J Indust Microbiol Biotechnol* (in press).

Polko, J.K. & J.J. Kleiber. 2019. The regulation of cellulose biosynthesis in plants. *Plant Cell* 31:282-296.

Roberts, D.A., R. de Nys & N.A. Paul. 2013. The effect of CO_2 on algal growth in industrial waste water for bioenergy and bioremediation applications. *PLoS ONE* 8: e81631.

Roberts, D.A., L. Shiels, J. Tickle, R. de Nys R & N.A. Paul. 2018 Bioremediation of aluminum from the waste water of a conventional water treatment plant using the freshwater macroalga *Oedogonium*. *Water* 10:626.

Satjarak A. & L.E. Graham. 2017. Whole genome sequencing of *Pyramimonas parkeae* reveals genes encoding carbohydrate active enzymes. *Journal of Phycology* 53:1072-86.

Speicher, T., P.A. Li & I.S. Wallace. 2018. Phosphoregulation of the plant cellulose synthase complex and cellulose synthase-like proteins. *Plants* 7:52.

Tsekos, I. 1999. The sites of cellulose synthesis in algae: diversity and evolution of cellulose-synthesizing enzyme complexes. *J. Phycol.* 35(4):635-655.

Ulvskov, P., Paiva, D.S., Domozych, D. & Harholt, J. 2013. Classification, naming and evolutionary history of glycosyltransferases from sequenced green and red algal genomes. *PloS ONE* 8(10):e76511.

Yin, Y., J. Huang & Y. Xu. 2009. The cellulose synthase superfamily in fully sequenced plants and algae. *BMC Plant Biology* 9:99.

Zulkifly, S., A. Hanshew, E.B. Young, P. Lee, M.E. Graham, M. Piotrowski & L.E. Graham. 2012. The epiphytic microbiota of the globally widespread macroalga *Cladophora glomerata* (Chlorophyta, Cladophorales). *Amer J Bot* 99:1541-1552.

PHYLOGENETIC ANALYSIS OF CELLULOSE BIOSYNTHESIS (*CESA*) GENES FROM A DRAFT GENOME FOR *OEDOGONIUM* (CHLOROPHYCEAE)[1]

Michael J. Piotrowski, *Linda E. Graham*[2]

Department of Botany, University of Wisconsin-Madison, 430 Lincoln Drive, Madison, Wisconsin, 53706 USA

and Anchittha Satjarak

Department of Botany, Chulalongkorn University, Bangkok, 10330 Thailand

[1]Received

[2]corresponding author: e-mail: lkgraham@wisc.edu, phone: +16082622640, fax: +16082627509

Key words: CesA; genomics; glycosyl transferases; *Oedogonium*.

Running header: *Oedogonium CesA* genes

Abbreviations: Bcs, bacterial cellulose synthases; *Bcs*, bacterial cellulose synthase gene; CesA, cellulose synthase; *CesA*, cellulose synthase gene; CSCs, cellulose synthesizing complexes; GTs, glycosyl transferases

Abstract

Local isolates of the fast-growing, herbivore- and pathogen-resistant, filamentous green alga *Oedogonium* (Chlorophyceae) have been effectively employed in cultivation systems designed to improve the quality of municipal wastewater before its discharge to natural environments, and at the same time generate O_2 and lipid-, protein-, and carbohydrate-rich biomass, such as cellulose, for industrial applications. Our previous studies indicated that, by comparison to other green algae, *Oedogonium* cellulose may have unusual macromolecular structural properties. To focus on *CesA* genes that encode cellulose synthases, we used shotgun genomic sequence to assemble a draft nuclear genome for an *Oedogonium* isolate (Lake Mendota strain) that we had previously generated and characterized by multiple taxonomic markers. 23 putative *CesA* sequences identified in the assembled *Oedogonium* draft genome were translated to proteins for sequence alignment and used for phylogenetic analysis, together with 108 other chlorophyte CesA proteins and one for a bacterial outgroup, a known cellulose producer. Some *Oedogonium* Lake Mendota strain CesAs formed early-diverging clades distinct from those of other chlorophycean algae; other CesAs were distinct from those of two other *Oedogonium* species for which database sequences are known, possibly explaining unusual features of *Oedogonium* Lake Mendota strain cellulose. These new molecular observations may aid the development of new applications and markets for *Oedogonium* biomass generated in cultivation systems engineered to reduce nutrient input to natural waters from existing and future wastewater treatment facilities, with the goal of improving the health of humans and aquatic ecosystems on a global basis.

INTRODUCTION

The fast-growing, herbivore- and pathogen-resistant chlorophyte *Oedogonium* (Oedogoniales, Chlorophyceae) produces attached or floating masses that are often conspicuous along shorelines of temperate-tropical freshwater bodies worldwide (Tiffany et al. 1927, McCracken et al. 1974). This genus, with 569 species listed in Algaebase (Guiry 2019), occurs in a wide spectrum of environmental conditions. Unbranched *Oedogonium* filaments readily undergo asexual reproduction by fragmentation and zoospore release, in addition to producing resistant zygospore stages in a sexual process (Rawitscher-Kunkel and Machlis 1962, Pickett-Heaps 1975). These reproductive features help to explain why *Oedogonium* has such a broad ecological distribution and why favorable environmental conditions lead to rapid development of large populations that become visible as mats.

Algal mats dominated by *Oedogonium* rapidly take up and thus reduce environmental concentrations of dissolved nutrients such as N and P (Whitford and Schumacher 1961, 1964). Metals are known to adsorb to *Oedogonium* surfaces (Gupta et al. 2008a, 2008b, 2009, 2010; Bakatula 2014). These features suggested potential use of *Oedogonium* in engineered cultivation systems to remove waste CO_2, N and P, and heavy metals from wastewaters to improve water quality before effluent discharge to natural environments (Cole et al. 2013, 2014, 2016, Francke et al. 1983, Neveux et al. 2016, Roberts et al. 2013, 2018), and at the same time generate biomass for bioenergy and other industrial applications, reviewed by Lawton et al. (2017). Consequently, efforts have been made to isolate, characterize, and compare *Oedogonium* strains for their suitability for use in diverse applications, a process that has revealed previously unrecognized genetic diversification and substantial variation in environmental tolerances (Lawton et al. 2014).

Cellulose has been cited among various types of useful materials that might be extracted from *Oedogonium* grown in wastewater remediation systems (Piotrowski et al. 2020). Like cell walls of the chlorophyte *Cladophora*, which commonly occurs with *Oedogonium* in freshwater periphyton, *Oedogonium* cellulose-rich walls are known to resist dissolution by acid-hydrolysis (Graham et al. 2013). Highly-crystalline cellulose extracted from the branched filamentous chlorophyte *Cladophora* has been proposed for a variety of industrial applications (reviewed by Mihranyan 2011), suggesting that *Oedogonium* cellulose may also find industrial uses. Chlorophyte celluloses are known to vary among genera, and to differ from celluloses produced by streptophytes–plants and closely-related charophycean green algae–in biophysical traits (Kubicki et al. 2018) arising from biochemical differences in the cell membrane proteins that make up cellulose-synthesizing complexes (Tsekos 1999, Polko and Kleiber 2019), whose subunits are encoded by *CesA* genes (Yin et al. 2009, Kumar and Turner 2015, Satjarak and Graham 2017, Chen et al. 2018, Speicher et al. 2018). Chlorophyte algae thus offer the potential for wastewater-linked production of distinctive types of cellulose that may have useful applications.

Cellulose-production at a temperate locale by a wastewater-grown isolate of *Oedogonium* defined by molecular marker sequences (Graham et al. 2020), has recently been quantified (Piotrowski et al. 2020). Unusual macromolecular features of *Oedogonium* cell wall cellulose produced in this engineered system have been noted (Piotrowski et al. 2020) and compared to cell wall cellulose structures of other green algae at the SEM level. Extracted *Oedogonium* cellulose was observed to lack conspicuous microfibrillar patterns known for other green algae and plants examined by SEM. To gain insight into this structural difference, we compared *CesA* gene sequences from *Oedogonium* to those known for other green algae and land plants.

CesA genes encode proteins that are classified as glycosyl transferases (GTs). These proteins catalyze the formation of glycosyl bonds between a donor sugar substrate and another molecule, typically another sugar. Consequently, GTs are key to the biosynthesis of glucans, and occur in cell membrane arrays known as CSCs (cellulose-synthesizing complexes). Biochemical analyses have shown that cellulose is the main component of the cell walls of streptophytes (plants and closely-related green algae) and many chlorophyte algae, although the structure of streptophyte and chlorophyte CSCs differ; like bacteria, chlorophytes produce linear CSCs, whereas those of streptophytes occur as rosettes (reviewed by Popper et al. 2011). Chlorophytes possess only gene sequences that encode the bacterial CSC type, but at least some streptophytes possess both rosette CSCs and genes related to the bacterial CSC type (Kumar and Turner 2015).

In the present study, we focused on *CesA* genes represented in draft whole genome sequence we had obtained for a local isolate of *Oedogonium* that we had generated for study of cellulose production in local municipal wastewater (Piotrowski et al. 2020), and characterized with the use of five molecular marker sequences (Graham et al. 2020). Such phylogenetic analysis revealed that the local *Oedogonium* isolate employed for draft genome sequencing was not con-specific with any *Oedogonium* species represented in genetic databases to date, and so is here denoted as *Oedogonium* sp., Lake Mendota isolate.

Materials and methods

Isolate production and cultivation

An isolate of *Oedogonium* was made from periphyton collected in 2009 from Lake Mendota (Dane County, WI, USA, 43.1097N, 89.4206W). Many single filaments were observed by means

of a dissecting microscope and fine forceps were used to transfer filaments free of conspicuous bacterial or eukaryotic epiphytes to sterile SD11 medium (Graham et al. 1982) into well slides, one filament per well. SD11 medium is a modification of D11medium formulated by Gerloff and Fitzgerald (1976) to reproduce the chemical milieu of hypereutrophic lakes, specifically Lake Mendota.

Isolated *Oedogonium* filaments were observed over the next week until motile zoospores appeared; these were individually isolated by micropipette into well slides containing sterile SD11. Zoospore development and release are triggered by environmental signals that include mineral nutrient concentration and light environment variation (Pickett-Heaps 1971). Newly-released zoospores are relatively free of epiphytes, so new vegetative filaments that develop from settled zoospores are free of conspicuous contamination. Zoospore isolation was key to our ability to generate unialgal cultures *Oedogonium* cultures. Axenic *O. cardiacum* cultures have been observed to undergo abnormal growth (Machlis 1973), suggesting that microbiota may aid algal growth, as we have inferred from metagenomic and other high-throughput DNA sequence analyses of periphytic *Cladophora glomerata* from Lake Mendota (Zulkifly et al. 2012, Graham et al. 2015, Braus et al. 2017). To avoid the potential for abnormal growth, we did not attempt to obtain axenic cultures of the Lake Mendota strain of *Oedogonium* that was employed in this study.

Vegetative filaments arising from isolated zoospores were used to produce stock unialgal cultures that were maintained in 250-500 mL Erlenmeyer flasks containing sterile SD11 medium. Stock-culture flasks were aerated with compressed air that was first cotton-filtered to prevent contamination with oil from compression machinery, and then hydrated by passage through a flask containing distilled water, to prevent excessive evaporation during the cultivation

period. To reduce the potential for microbial contamination of culture flasks during aeration, loose plugs of cotton were inserted into the external ends of glass tubing running through rubber flask stoppers, then SD11 medium was added to flasks and the culture flask-stopper assembly was autoclaved prior to algal inoculation. Stock cultures were maintained in a temperature-controlled (21˚C) walk-in culture room, with an irradiance level of 234 μmol quanta m^{-2} s^{-1} provided by cool white fluorescent lamps, on a 16:8 light:dark cycle.

The Lake Mendota isolate was identified as the genus *Oedogonium* based on presence of unbranched filaments anchored by a basal holdfast, barrel-shaped cells containing reticulate plastids, distinctive cell wall rings, and production of a single multiflagellate zoospore per vegetative cell, features illustrated in Graham et al. (2016). Species identification by means of structural characters alone was not possible because sexual stages important in making species distinctions were not expressed in lab cultures, and so has been characterized by commonly-used molecular markers (Graham et al. 2020).

DNA extraction and sequencing

Biomass for DNA extraction was grown using fresh cultures of *Oedogonium sp.* grown for a period of seven days in a climate-controlled growth chamber as described in Chapter 1. Biomass was collected, pooled, and 42 replicate DNA extractions conducted the same day. DNA preparations were done using the MPBio Fast DNA SPIN kit for soil (MP Biomedicals LLC, Solon, OH, USA), modified by adding 10 mg · mL−1 lysozyme in the initial step. After DNA collection, PCR was run on 42 replicate DNA extractions for 16S and 18S sequences using primers 16S (Pr001-2) and 18S (Pr003-4) respectively. Of the 42 replicate DNA extractions, only those that showed sequences for both 16S and 18S were used for further DNA sequencing,

because we wanted to obtain algal nuclear, chloroplast, mitochondrial, and bacterial sequences with our sequencing efforts.

Total DNA was prepared using the FastDNA® SPIN Kit for Soil (MP Biomedicals, Solon, OH, USA) and sequenced by Illumina Miseq and Hiseq platforms at the University of Wisconsin-Madison Biotechnology Center. Raw read data are from two parallel lanes of paired-end reads from Illumina Mi-Seq sequencing, constituting technical replicates from the same extracted DNA pool.

Data pre-processing, genome construction, and CesA *extraction*

The raw paired-end Illumina Miseq paired-end data consisted of 1,243,777,984 forward reads and 1,243,777,984 reverse reads, in total 2,487,555,968 reads. The sequences were trimmed using Trimmomatic (Bolger et al. 2014) v 0. The genome was then assembled using MEGAHIT (Li et al. 2015) v 1.2.6. The number of contigs was 88,083 (totaling 59,480,991 bp), with minimum contig length of 200 bp, maximum contig length of 63,095 bp, average contig length of 675 bp, and N 50 = 705 bp.

To select only contigs containing putative CesAs, we used all green algal CesA proteins archived in GenBank (accessed in July, 2019) as queries to perform tblastn searches against the *Oedogonium* assembly, using the threshold of expected value (e-value) of at least 1e-10. A blastx analysis was performed using putative *Oedogonium Ces A* nucleotide sequences, obtained in the previous step, as queries to search against NCBI non-redundant protein database (accessed in July 2019). Only sequences that returned as GT2 proteins were retained. The blast analyses suggested presence of 23 putative CesA sequences in the assembled *Oedogonium* draft genome.

CesA genes were extracted from contigs using the "extract regions" option implemented in Geneious v 9.0.4 (https://www.geneious.com/).

Phylogenetic analyses

For comparative analysis using phylogenetics, we first obtained all chlorophyte transcriptomes available on http://onekp.com/public_data.html (Matasci et al. 2014), then annotated the transcriptomes using HMMER method for CAZymes annotation available on dbCAN meta server (HMMER: e-value<1e-15, coverage >0.35) (Yin et al. 2012, Zhang et al. 2018), retaining only sequences annotated as cellulose synthases. The number of cellulose synthases varied among the 53 algal species employed for phylogenetic analysis; the total number of archived chlorophyte cellulose synthase sequences was 109. These sequences, in protein form, were employed, together with a bacterial outgroup (*Komagataeibacter xylinus*, NCBI accession number AAA85264.1), and 23 CesA protein sequences, for alignment using MAFFT (Katoh and Standley 2013) version 7.308, and alignment trimming using trimAL (Capella-Gutierrez et al. 2009) version 1.2. The LG model for protein alignment, based on use of IQ-TREE (Nguyen et al. 2014) v 1.6.10 available on CIPRES Science Gateway (Miller et al. 2010) was employed.

Maximum likelihood analysis was performed using RAxML-HPC (Stamatakis 2014) BlackBox v 8.2.12, available on CIPRES Science Gateway; RAxML was allowed to halt bootstrapping automatically. Bayesian inference was performed using MrBayes (Ronquist et al. 2012) on XSEDE version 3.2.6 available on CIPRES Science Gateway. For MCMC, the number of generations = 100,000, with 25% burnin. Trees were visualized using FigTree version 1.4.3 (http://tree.bio.ed.ac.uk/software/figtree).

RESULTS

In this study, 23 *Oedogonium* Lake Mendota strain CesA protein sequences were identified and aligned (Table 1) for comparison with CesA proteins reported for other chlorophytes (Table 2). QXXRW domains and DAD and DXD motifs associated with catalytic sites of cellulose synthase in bacteria and embryophytes were observed for most (Table 3).

Phylogenetic analyses showed that several of the *Oedogonium* Lake Mendota strain CesA proteins diverged very early in a chlorophyte tree. Sequences 1, 2, 16, 17, 18, 22 and 23 were the earliest-diverging chlorophyte CesA sequences in both ML (Fig. 1) and Bayesian analyses (Fig. 2). Other *Oedogonium* Lake Mendota strain CesA proteins clustered with other chlorophyte CesAs, but notably, did not cluster closely with CesAs for two other Oedogonium species for which CesA sequences occur in databases.

DISCUSSION

Cellulose is the most abundant component of the cell walls of many green algae and embryophytes. This polysaccharide is made up of microfibrils which are constructed from linear molecule of β-1,4-linked glucan chains held together by intra- and intermolecular hydrogen bonds and van der Waals forces. These molecules of β-1,4-linked glucan chains are synthesized at the plasma membrane by a membrane-bound complex locating on the protoplasmic face known as the cellulose synthesizing complex (CSC) or terminal complex (TC) as they are present at the end of the microfibrils (Tsekos 1999).

Cellulose synthesizing complexes are present in Cyanobacteria (Zaar 1979), Glaucophyta (Willison and Brown 1978), Rhodophyta (Tsekos et al.1999), Chlorophyta (Brown and Montezinos 1976), and Streptophyta (Okuda and Brown 1992, Hotchkiss and Brown 1987).

However, the shapes of these CSCs differ, which affects the structure and biophysical properties of cellulosic microfibrils (Giddings et al. 1980, Herth 1983, Tsekos 1999). The CSCs of chlorophyte algae that have been investigated occur as rectangular complexes consisting of rows of subunits, similar to CSCs reported for glaucophytes, rhodophytes, and photosynthetic stramenopiles (Zaar 1979, Willison and Brown 1978a, 1978b, Tsekos et al.1999). By contrast, streptophyte CSCs occur as rosettes, typically with sixfold rotational symmetry (Tsekos et al. 1999).

Most previous analyses of genes encoding CSC subunits involve streptophyte *CesA* – a gene that is known to encode CesA protein. Streptophyte rosette CSCs have been hypothetically linked to CesA-CesA, suggesting that the absence of rosette-shaped CSCs in non-streptophytes might due to absence of particular domains distinctive for streptophyte-CesA, such as the zinc-binding domain, plant-conserved regions, and a hypervariable region (Arioli et al. 1998, Peng et al. 2001, Kurek et al. 2002, Gardiner et al. 2003).

The universal of the presence of CSCs, along with their cellulose products, in cyanobacteria and Viridiplantae (Zaar 1979, Nobles et al. 2001) suggests that this *CesA* gene must be ancient. It has been hypothesized that Viridiplantae horizontally acquired *CesA* from a cyanobacterial endosymbiont (Nobles et al. 2001). Both bacterial and streptophyte *CesA*s occur in embryophytes such as spikemoss (Harholt et al. 2012), moss (Ulvskov et al. 2013), as well as the streptophyte algae (Mikkelsen et al. 2014).

We had earlier reported a *P. parkeae* GT2 protein sequence (CAMPEP_0191478436) that contains QXXRW domains and other residues (D and DXD) that are known to be catalytic regions of cellulose synthase. However, unlike other known CesAs, this wall-less prasinophyte sequence contained just a single transmembrane region. Phylogenetic analysis using ML showed

that this protein sequence, together with other *P. parkeae* GT2 proteins and other bacterial-type CesA sequences formed a monophyletic clade with high bootstrap support (Satjarak and Graham 2017). Phylogenetic results reported here show that prasinophyte CesAs occur throughout the chlorophyte tree, but surprisingly, at least seven of the *Oedogonium* Lake Mendota strain CesAs diverged earlier than those of prasinophytes, the earliest-diverging lineages of chlorophyte algae. These observations suggest that these seven early-diverging CesAs might represent horizontal gene transfer from bacteria, after divergence of the Lake Mendota strain from other Oedogonium species represented in CesA databases. Future explorations of *Oedogonium* CesAs may reveal more information about this transfer event, indicating whether other *Oedogonium* species might have the early-diverging CesAs or not. Other future work may indicate which modern bacterial species are most closely-related to the hypothesized CesA donor.

Our results indicated that *CesA* genes are present in *Oedogonium*, as was also the case for the prasinophyte *P. parkeae* (Satjarak and Graham 2017). However, noted in that previous study, the classification of genes as *CesA*s based on sequence similarity alone is not sufficient evidence to conclude that the functional orthology of these sequences has been conserved. The genomic data might contain related but degenerate sequences or sequences might be non-functional for other reasons. Our report emphasizes the need for functional studies of the proteins indicated by draft genomic analyses.

Fig. 1. Maximum-Likelihood tree inferred from predicted CesA proteins from chlorophyte algae, including the new *Oedogonium* sequences, with the cellulose-producing bacterial species *Komagataeibacteria xylinus* as an outgroup, using an LG amino acid substitution model.

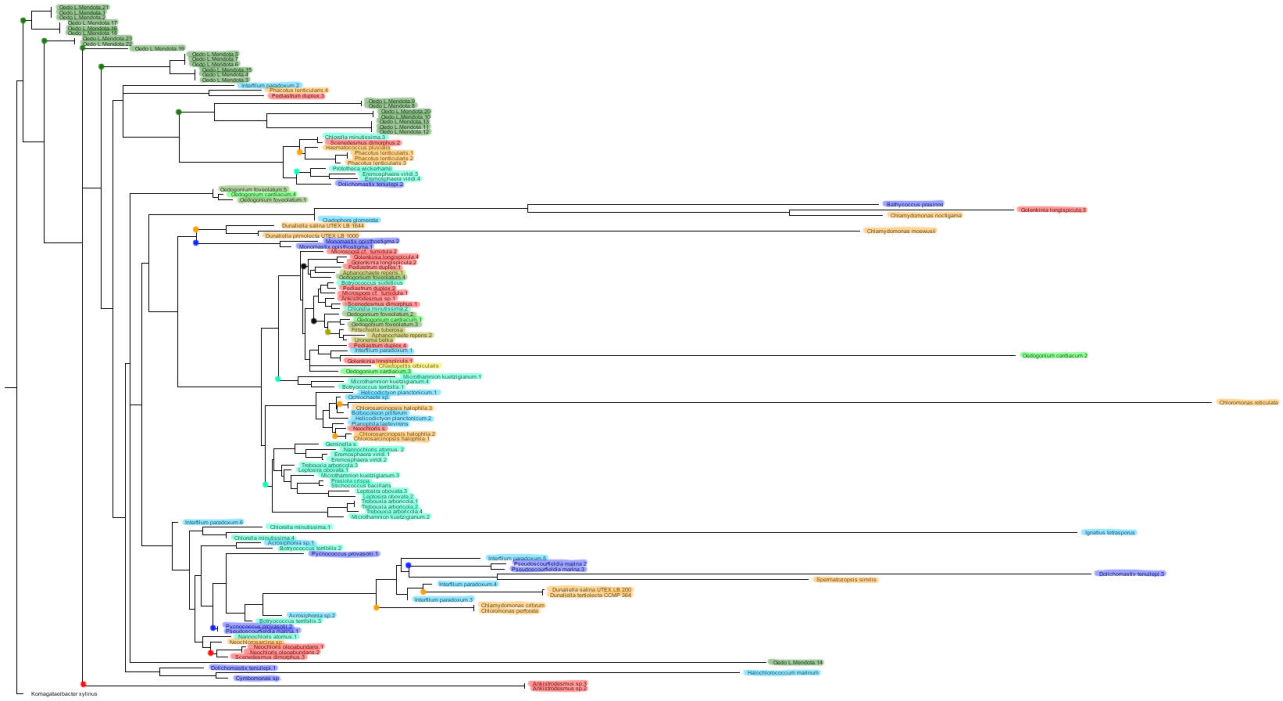

Fig. 2. Bayesian tree inferred for CesAs from chlorophyte green algae, including the new Oedogonium sequences and the cellulose-producing bacterial species *Komagataeibacteria xylinus* as an outgroup.

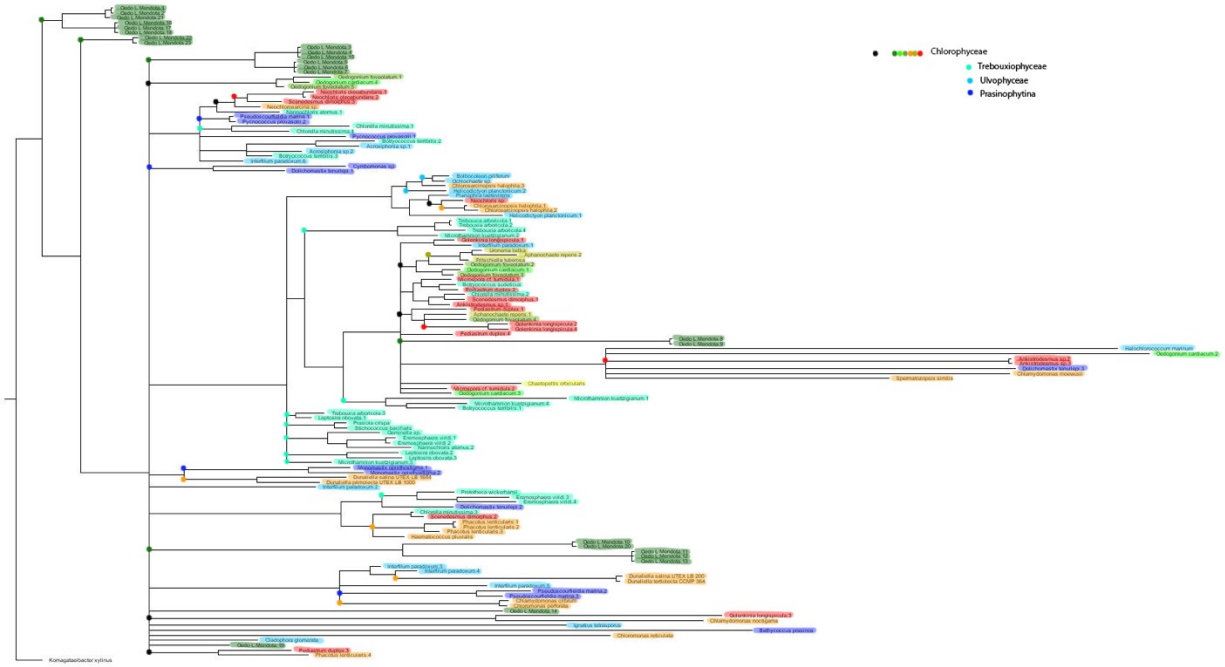

Table 1. Amino acid alignments for *Oedogonium* Lake Mendota strain CesAs

k141_17167_extraction_translation	AKAGNINHALAYVVIFDCGFLQLSLGWMDQGLAMVQTPHYFYSIQQGNDFFCGSCAVIRRTALESVETVTEDCHCSLRMQKGWRTAYLVPLAAGLATGQRMR--WGRGMIQ
k141_33200_extraction_translation	AKAGNINHALAYVVIFDCGFLQLSLGWMDQGLAMVQTPHYFYSIQQGNDFFCGSCAVIRRTALESVETVTEDCHCSLRMQKGWRTAYLVPLAAGLATGQRMR--WGRGMIQ
k141_261_extraction_translation	AKAGNVNNGLAFVLLLDANILRRTLPLFEADVGIVQTPQHFFNILPAKDACCGTSAVLRVEALVQAETVTEDMLTTFKLEEGWRTIFLEQLSSGLAPGQRAR--WCLGAVQ
k141_20281_extraction_translation	AKAGNVNNGLAFVLLLDANILRRTLPLFEADVGIVQTPQHFFNILPAKDACCGTSAVLRVEALVQAETVTEDMLTTFKLEEGWRTIFLEQLSSGLAPGQRAR--WCLGAVQ
k141_4039_extraction_translation	AKAGNVNNGLHFILLLDANILRRVLPLFDPKIGIVQTPQHFFNLLPCKDACCGTSAVFRVEALIKSETVTEDMLTTFRFLEGYKTAFLERLSLGLAPGQRSR--WCLGAIQ
k141_19651_extraction_translation	AKAGNVNNGLHFILLLDANILRRVLPLFDPKIGIVQTPQHFFNLLPCKDACCGTSAVFRVEALIKSETVTEDMLTTFRFLEGYKTAFLERLSLGLAPGQRSR--WCLGAIQ
k141_38248_extraction_translation	AKAGNVNNGLHFILLLDANILRRVLPLFDPKIGIVQTPQHFFNLLPCKDACCGTSAVFRVEALIKSETVTEDMLTTFRFLEGYKTAFLERLSLGLAPGQRSR--WCLGAIQ
k141_31786_extraction_translation	TKPRALNFGLDIIGIYDADQLLKVAATFPPRLGCLQGMLDFYNFLPGLVRLGGTTLFLRRDAVLEVHNVTEDADLGLRLARGWQTGMLS-VTMEEANKQRSR--WTKGYLM
k141_57104_extraction_translation	TKPRALNFGLDIIGIYDADQLLKVAATFPPRLGCLQGMLDFYNFLPGLVRLGGTTLFLRRDAVLEVHNVTEDADLGLRLARGWQTGMLS-VTMEEANKQRSR--WTKGYLM
k141_78262_extraction_translation	GKSDALNTGMTFILNMDGNSLRACIRHFNPRIGAVAGNVKVLNLAMARKAIPGPLGMFRKTVLQQADTFAEDADLTLKLLMGWQIAYEAAVAWVETPKQRYR--WTRGILQ
k141_13454_extraction_translation	RKADATNAGISLICIIDAEGLLRAVQPFDGTVIAVGGSIRIANFLGGRVAISGAFGLFRRDVLFEADSLGEDLELLVRLQRPHKVAYLEICCWTEAPNQRTR--WQQGGLQ
k141_22943_extraction_translation	RKADATNAGISLICIIDAEGLLRAVQPFDGTVIAVGGSIRIANFLGGRVAISGAFGLFRRDVLFEADSLGEDLELLVRLQRPHKVAYLEICCWTEAPNQRTR--WQQGGLQ
k141_37199_extraction_translation	RKADATNAGISLICIIDAEGLLRAVQPFDGTVIAVGGSIRIANFLGGRVAISGAFGLFRRDVLFEADSLGEDLELLVRLQRPHKVAYLEICCWTEAPNQRTR--WQQGGLQ
k141_53831_extraction_translation	SWQGVTRHRAAFLLFMDD----------DEVSTFVRAAQHSGA--------FRGAGPPPRHRSTRPILGVFQNALGDANMFMAW------RMAGFTLDRLQAAV--LAGLHLE
k141_6665_extraction_translation	----------FVLLLDANILRRTLPLFEADVGIVQTPQHFFNILPAKDACCGTSAVLRVEALVQAETVTEDMLTTFKLEEGWRTIFLEQLSSGLAPGQRAR--WCLGAVQ
k141_13570_extraction_translation	AKAGNLNHAMRYIAIFDCAFLQLTLGWLDKRIALVQTPHHFYSIQPGSDLFCGSCAVLRRTALEEVVTVTEDCHCALKMQQGWHTAYI----------
k141_56282_extraction_translation	AKAGNLNHAMRYIAIFDCAFLQLTLGWLDKRIALVQTPHHFYSIQPGSDLFCGSCAVLRRTALEEVVTVTEDCHCALKMQQGWHTAYI----------
k141_81164_extraction_translation	AKAGNLNHAMRYIAIFDCAFLQLTLGWLDKRIALVQTPHHFYSIQPGSDLFCGSCAVLRRTALEEVVTVTEDCHCALKMQQGWHTAYI----------
k141_36985_extraction_translation	-KAGNINHALRLVLVFDADFLQRTVGFFDEKVGLVQVPHHFFNIMACRDGSCGSNSLARRSALEEMDSITEDILTSIVLLQGWKTVYL----------
k141_2653_extraction_translation	----------LAMARKAIPGPLGMFRKTVLQQADTFAEDADLTLKLLMGWQIAYEAAVAWVETPKQRYR--WTRGILQ
k141_415_extraction_translation	AKAGNINHALAYVVIFDCGFLQLSLGWMDQGLAMVQTPHYFYS----------
k141_36942_extraction_translation	AKAGNINQALPLVAIFDCSFLQMTVGQFDPKLAMVQTPHHFLS----------
k141_53061_extraction_translation	AKAGNINQALPLVAIFDCSFLQMTVGQFDPKLAMVQTPHHFLS----------

Table 2. Chlorophyte taxa and outgroup used for phylogenetic analyses

Genera	Subphylum	Class	Order	Family
Chaetopeltis orbicularis	Chlorophytina	Chlorophyceae	Chaetopeltidales	Chaetopeltidaceae
Aphanochaete repens	Chlorophytina	Chlorophyceae	Chaetophorales	Aphanochaetaceae
Fritschiella tuberosa	Chlorophytina	Chlorophyceae	Chaetophorales	Fritschiellaceae
Uronema belka	Chlorophytina	Chlorophyceae	Chaetophorales	Uronemataceae
Chlamydomonas cribrum	Chlorophytina	Chlorophyceae	Chlamydomonadales	Chlamydomonadaceae
Chlamydomonas moewusii	Chlorophytina	Chlorophyceae	Chlamydomonadales	Chlamydomonadaceae
Chlamydomonas noctigama	Chlorophytina	Chlorophyceae	Chlamydomonadales	Chlamydomonadaceae
Chloromonas perforata	Chlorophytina	Chlorophyceae	Chlamydomonadales	Chlamydomonadaceae
Chloromonas reticulata	Chlorophytina	Chlorophyceae	Chlamydomonadales	Chlamydomonadaceae
Chlorosarcinopsis halophila	Chlorophytina	Chlorophyceae	Chlamydomonadales	Chlorosarcinaceae
Neochlorosarcina sp.	Chlorophytina	Chlorophyceae	Chlamydomonadales	Chlorosarcinaceae
Dunaliella primolecta UTEX LB 1000	Chlorophytina	Chlorophyceae	Chlamydomonadales	Dunaliellaceae
Dunaliella salina UTEX LB 1644	Chlorophytina	Chlorophyceae	Chlamydomonadales	Dunaliellaceae
Dunaliella salina UTEX LB 200	Chlorophytina	Chlorophyceae	Chlamydomonadales	Dunaliellaceae
Dunaliella tertiolecta CCMP 364	Chlorophytina	Chlorophyceae	Chlamydomonadales	Dunaliellaceae
Spermatozopsis similis	Chlorophytina	Chlorophyceae	Chlamydomonadales	Dunaliellaceae
Haematococcus pluvialis	Chlorophytina	Chlorophyceae	Chlamydomonadales	Haematococcaceae
Phacotus lenticularis	Chlorophytina	Chlorophyceae	Chlamydomonadales	Phacotaceae
Oedogonium cardiacum	Chlorophytina	Chlorophyceae	Oedogoniales	Oedogoniaceae
Oedogonium foveolatum	Chlorophytina	Chlorophyceae	Oedogoniales	Oedogoniaceae
Pediastrum duplex	Chlorophytina	Chlorophyceae	Sphaeropleales	Hydrodictyaceae
Microspora cf. *tumidula*	Chlorophytina	Chlorophyceae	Sphaeropleales	Microsporaceae
Golenkinia longispicula	Chlorophytina	Chlorophyceae	Sphaeropleales	Neochloridaceae
Neochloris oleoabundans	Chlorophytina	Chlorophyceae	Sphaeropleales	Neochloridaceae
Neochloris sp.	Chlorophytina	Chlorophyceae	Sphaeropleales	Neochloridaceae
Scenedesmus dimorphus	Chlorophytina	Chlorophyceae	Sphaeropleales	Scenedesmaceae
Ankistrodesmus sp.	Chlorophytina	Chlorophyceae	Sphaeropleales	Selenastraceae
Chlorella minutissima	Chlorophytina	Trebouxiophyceae	Chlorellales	Chlorellaceae
Geminella sp.	Chlorophytina	Trebouxiophyceae	Chlorellales	Chlorellaceae
Nannochloris atomus	Chlorophytina	Trebouxiophyceae	Chlorellales	Chlorellaceae
Prototheca wickerhamii	Chlorophytina	Trebouxiophyceae	Chlorellales	Chlorellaceae
Eremosphaera viridis	Chlorophytina	Trebouxiophyceae	Chlorellales	Oocystaceae
Microthamnion kuetzigianum	Chlorophytina	Trebouxiophyceae	Microthamniales	Microthamniaceae
Prasiola crispa	Chlorophytina	Trebouxiophyceae	Prasiolales	Prasiolaceae
Stichococcus bacillaris	Chlorophytina	Trebouxiophyceae	Prasiolales	Prasiolaceae
Botryococcus sudeticus	Chlorophytina	Trebouxiophyceae	Trebouxiales	Botryococcaceae
Botryococcus terribilis	Chlorophytina	Trebouxiophyceae	Trebouxiales	Botryococcaceae
Trebouxia arboricola	Chlorophytina	Trebouxiophyceae	Trebouxiales	Trebouxiaceae
Leptosira obovata	Chlorophytina	Trebouxiophyceae	Trebouxiophyceae ordo incertae sedis	Trebouxiophyceae incertae sedis
Cladophora glomerata	Chlorophytina	Ulvophyceae	Cladophorales	Cladophoraceae
Ignatius tetrasporus	Chlorophytina	Ulvophyceae	Ignatiales	Ignatiaceae

Halochlorococcum marinum	Chlorophytina	Ulvophyceae	Oltmannsiellopsidales	Oltmannsiellopsidaceae
Helicodictyon planctonicum	Chlorophytina	Ulvophyceae	Ulotrichales	Helicodictyaceae
Planophila laetevirens	Chlorophytina	Ulvophyceae	Ulotrichales	Planophilaceae
Acrosiphonia sp.	Chlorophytina	Ulvophyceae	Ulotrichales	Ulotrichaceae
Interfilum paradoxum	Chlorophytina	Ulvophyceae	Ulotrichales	Ulotrichaceae
Bolbocoleon piliferum	Chlorophytina	Ulvophyceae	Ulvales	Bolbocoleonaceae
Ochlochaete sp.	Chlorophytina	Ulvophyceae	Ulvales	Ulvaceae
Dolichomastix tenuilepi	Prasinophytina	Mamiellophyceae	Dolichomastigales	Dolichomastigaceae
Bathycoccus prasinos	Prasinophytina	Mamiellophyceae	Mamiellales	Bathycoccaceae
Monomastix opisthostigma	Prasinophytina	Mamiellophyceae	Monomastigales	Monomastigaceae
Pseudoscourfieldia marina	Prasinophytina	Pyramimonadophyceae	Pseudoscourfieldiales	Pycnococcaceae
Pycnococcus provasolii	Prasinophytina	Pyramimonadophyceae	Pseudoscourfieldiales	Pycnococcaceae
Cymbomonas sp.	Prasinophytina	Pyramimonadophyceae	Pyramimonadales	Pyramimonadaceae
Komagataeibacter xylinus		Alphaproteobacteria	Rhodospirillales	Acetobacteraceae

Table 3. *Oedogonium* Lake Mendota strain CesA regions: DXD regions in olive green, TED domains dark green, QXXRW motifs in yellow

Identity	AA Length	Sequence
k141_261 *Oedo* sp. L. Mendota 3	340	VDVFLCTYNEGPEILERSILCATRIAHRDLRVWVLDDGARDWVRDLAAEMGALYVRRVKGRHAKAGNVNNGLAHALNTGRPPQFVLLLDADFSAHRNILR RTLPLFREADVGIVQTPQHFFNPDPLQTGLLAAKTLPDEQRFFFNHILPAKDAWGAAFCCGTSAVLRVEALVQAGGMAVETVTEDMLTTFKLEEHGWRTI FLNEQLSSGLAPEGLSEYIGQRARWCLGAVQQVYTRWSFVGPARMSWVNRLSGLDTVLYWCTSFLARLMVLSAPILFWWFGIASFAASQEELIYWLAPHV LAGMLALGLLSQGRLVPLLSDVSQLLITFPVLATVARTLV
k141_415 *Oedo* sp. L. Mendota 21	167	FLGVGLLLAEVYAIIALVLAYFQTLWPLDRKPAPLPANPDEWPAVDVFIPSYNEPLDVVRPTVFAALALDWPPDKLNVYLLDDGRREDFRRFAEEVGCHY IIRPDNKGAKAGNINHALAQTSSEYVVIFDCDHVATRGFLQLSLGWMLRDQGLAMVQTPHYFYSPDP
k141_2653 *Oedo* sp. L. Mendota 20	129	SLWAKIQAVEYIEGLAMARKAQSYLRSVVIIPGPLGMFRKTVLQQAGGYDHDTFAEDADLTLKLLMRGWQIAYEPAAVAWVETPSRLLDLLKQRYRWTR GILQAIRKHASALWRPRKGGVNFFILWYML
k141_4039 *Oedo* sp. L. Mendota 5	277	WAWIFFTFETASILSSCLVYMFMSRRLDRSVHADKLYGSPLSTRPVDVFIATYNEGLEILERTLVGATSIDHPDVRVWVLDDGARPWVEQLAKDFGARYV KRVKGAHAKAGNVNNGLHVALSSEGRKPEFILLLDADFVAQRNILRRVLPLFEDPKIGIVQTPQHFFNPDPVQSNLLCTGAWPDEQRFFFNELLPCKDAW GAAFCCGTSAVFRVEALIKSGGMATETVTEDMLTTFRFLEHGYKTAFLNERLSLGLAPEGLAEYIGQRSRWCLGAIQ
k141_6665 *Oedo* sp. L. Mendota 15	269	KRQALNTGRPPQFVLLLDADFSAHRNILRRTLPLFREADVGIVQTPQHFFNPDPLQTGLLAAKTLPDEQRFFFNHILPAKDAWGAAFCCGTSAVLRVEA LVQAGGMAVETVTEDMLTTFKLEEHGWRTIFLNEQLSSGLAPEGLSEYIGQRARWCLGAVQQVYTRWSFVGPARMSWVNRLSGLDTVLYWCTSFLARLM VLSAPILFWWFGIASFAASQEELIYWLAPHVLAGMLALGLLSQGRLVPLLSDVSQLLITFPVLATVARTLV

k141_13454 *Oedo* sp. L. Mendota 11	338	PRISVIAPAFNEELSIAQSIQSLLSLQYPDLEVIVVNDGSKDRTMEILHDTFALVPAEREIDRALHGTRVLGTYASRDHDNLFVVDKENGRKADATNAGI SYSTGDLICIIDADSVIDPEGLLRAVQPFIEGDGTVIAVGGSIRIANGCKIHNGSVVEVGTGRDWLPLFQTLEYFRAFLGGRVASARLSMLLLISGAFGL FRRDVLFEAGGYQHDSLGEDLELLVRLQRIAFEQGRPHKVAYLPEICCWTEAPFTFEGVRNQRTRWQQGGLQVFFKHRKMLFNPRYGRLGMLAFPLLALE DLIGPIVELLGYVLMIVGLIFGILNSAVAVLFFLLTCV
k141_13570 *Oedo* sp. L. Mendota 16	224	YIQTSYPLDRKPVPMPIDPDTWPTVDIYVPSYNESLDLVRPTVLAAMNMDYPRDKLNVWILDDGRRPEFRDFAEECGCGYIIRPDNKGAKAGNLNHAMRH TTGEYIAIFDCDHAPTRAFLQLTLGWLIRDKRIALVQTPHHFYSPDPFERNLVRQRLVPNEGLLFYGAIQPGSDLWNASFFCGSCAVLRRTALEEVGGVP HVTVTEDCHCALKMQQKGWHTAYI
k141_17167 *Oedo* sp. L. Mendota 1	275	FLGVGLLLAEVYAIIALVLAYFQTLWPLDRKPAPLPANPDEWPAVDVFIPSYNEPLDVVRPTVFAALALDWPPDKLNVYLLDDGRREDFRRFAEEVGCHY IIRPDNKGAKAGNINHALAQTSSEYVVIFDCDHVATRGFLQLSLGWMLRDQGLAMVQTPHYFYSPDPFERNLAAGQRVPNEGLLFYGLIQQGNDFWGATF FCGSCAVIRRTALESVGGVPTETVTEDCHCSLRMQKKGWRTAYLRVPLAAGLATERLMLHIGQRMRWGRGMIQIL
k141_19651 *Oedo* sp. L. Mendota 6	277	WAWIFFTFETASILSSCLVYMFMSRRLDRSVHADKLYGSPLSTRPVDVFIATYNEGLEILERTLVGATSIDHPDVRVWVLDDGARPWVEQLAKDFGARYV KRVKGAHAKAGNVNNGLHVALSSEGRKPEFILLLDADFVAQRNILRRVLPLFEDPKIGIVQTPQHFFNPDPVQSNLLCTGAWPDEQRFFFNELLPCKDAW GAAFCCGTSAVFRVEALIKSGGMATETVTEDMLTTFRFLEHGYKTAFLNERLSLGLAPEGLAEYIGQRSRWCLGAIQ
k141_20281 *Oedo* sp. L. Mendota 4	338	VFLCTYNEGPEILERSILCATRIAHRDLRVWVLDDGARDWVRDLAAEMGALYVRRVKGRHAKAGNVNNGLAHALNTGRPPQFVLLLDADFSAHRNILRRT LPLFREADVGIVQTPQHFFNPDPLQTGLLAAKTLPDEQRFFFNHILPAKDAWGAAFCCGTSAVLRVEALVQAGGMAVETVTEDMLTTFKLEEHGWRTIFL NEQLSSGLAPEGLSEYIGQRARWCLGAVQQVYTRWSFVGPARMSWVNRLSGLDTVLYWCTSFLARLMVLSAPILFWWFGIASFAASQEELIYWLAPHVLA GMLALGLLSQGRLVPLLSDVSQLLITFPVLATVARTLV
k141_22943 *Oedo* sp. L. Mendota 12	338	PRISVIAPAFNEELSIAQSIQSLLSLQYPDLEVIVVNDGSKDRTMEILHDTFALVPAEREIDRALHGTRVLGTYASRDHDNLFVVDKENGRKADATNAGI SYSTGDLICIIDADSVIDPEGLLRAVQPFIEGDGTVIAVGGSIRIANGCKIHNGSVVEVGTGRDWLPLFQTLEYFRAFLGGRVASARLSMLLLISGAFGL FRRDVLFEAGGYQHDSLGEDLELLVRLQRIAFEQGRPHKVAYLPEICCWTEAPFTFEGVRNQRTRWQQGGLQVFFKHRKMLFNPRYGRLGMLAFPLLALE DLIGPIVELLGYVLMIVGLIFGILNSAVAVLFFLLTCV
k141_31786 *Oedo* sp. L. Mendota 8	321	FGLLFGMTALTFLGLTLLKIATAVAALRAPQDTTPPLDRADLPTISLLVALYGEAEIAPRLIRRLSALDYPRDRLDVIVLLESSDTATCTAIAGIDLPPW MRVIAVPDGRIRTKPRALNFGLDFTRGSIIGIYDAEDAPASDQLLKVAATFANAPPRLGCLQGMLDFYNPATNWIARCFTLEYAAWFRLFLPGLVRLGLP IPLGGTTLFLRRDAVLEVGAWDAHNVTEDADLGLRLARRGWQTGMLSSVTMEEANCRPVPWIKQRSRWTKGYLMTWLVHMRAPRALLRDLGLRRFAAVQV LIVGSLMQGIATPVFWSLWLV
k141_33200 *Oedo* sp. L. Mendota 2	275	FLGVGLLLAEVYAIIALVLAYFQTLWPLDRKPAPLPANPDEWPAVDVFIPSYNEPLDVVRPTVFAALALDWPPDKLNVYLLDDGRREDFRRFAEEVGCHY IIRPDNKGAKAGNINHALAQTSSEYVVIFDCDHVATRGFLQLSLGWMLRDQGLAMVQTPHYFYSPDPFERNLAAGQRVPNEGLLFYGLIQQGNDFWGATF FCGSCAVIRRTALESVGGVPTETVTEDCHCSLRMQKKGWRTAYLRVPLAAGLATERLMLHIGQRMRWGRGMIQIL
k141_36942 *Oedo* sp. L. Mendota 22	174	MVLMIGFVQTIWPLRRKPVPMPDDVSTWPSVAILIPSYNEPLSVVRPTVMAALAQDWPRDRLKVYILDDGRRQEFREFAELVGVTHITRDNNRHAKAGNI NQALPKTEGELVAIFDCDHIPNRSFLQMTVGQFLVDPKLAMVQTPHHFLSPDPFERNLGVFRSMPNEGALFYGL
k141_36985 *Oedo* sp. L. Mendota 19	134	KAGNINHALRHTHGDLVLVFDADFVAQRDFLQRTVGFFRDEKVGLVQVPHHFFNTDPVQANLGLFQKHADDQEFFFTDIMACRDGWGVAFSCGSNSLARR SALEEMGGIPTDSITEDILTSIVLLQRGWKTVYL
k141_37199 *Oedo* sp.	338	PRISVIAPAFNEELSIAQSIQSLLSLQYPDLEVIVVNDGSKDRTMEILHDTFALVPAEREIDRALHGTRVLGTYASRDHDNLFVVDKENGRKADATNAGI SYSTGDLICIIDADSVIDPEGLLRAVQPFIEGDGTVIAVGGSIRIANGCKIHNGSVVEVGTGRDWLPLFQTLEYFRAFLGGRVASARLSMLLLISGAFGL

L. Mendota 13		FRRDVLFEAGGYQHDSLGEDLELLVRLQRIAFEQGRPHKVAYLPEICCWTEAPFTFEGVRNQRTRWQQGGLQVFFKHRKMLFNPRYGRLGMLAFPLLALE DLIGPIVELLGYVLMIVGLIFGILNSAVAVLFFLLTCV
k141_38248 *Oedo* sp. L. Mendota 7	277	WAWIFFTFETASILSSCLVYMFMSRRLDRSVHADKLYGSPLSTRPVDVFIATYNEGLEILERTLVGATSIDHPDVRVWVLDDGARPWVEQLAKDFGARYV KRVKGAHAKAGNVNNGLHVALSSEGRKPEFILLLDADFVAQRNILRRVLPLFEDPKIGIVQTPQHFFNPDPVQSNLLCTGAWPDEQRFFFNELLPCKDAW GAAFCCGTSAVFRVEALIKSGGMATETVTEDMLTTFRFLEHGYKTAFLNERLSLGLAPEGLAEYIGQRSRWCLGAIQ
k141_53061 *Oedo* sp. L. Mendota 23	179	MVYAWLVLMIGFVQTIWPLRRKPVPMPDDVSTWPSVAILIPSYNEPLSVVRPTVMAALAQDWPRDRLKVYILDDGRRQEFREFAELVGVTHITRDNNRHA KAGNINQALPKTEGELVAIFDCDHIPNRSFLQMTVGQFLVDPKLAMVQTPHHFLSPDPFERNLGVFRSMPNEGALFYGL
k141_53831 *Oedo* sp. L. Mendota 14	214	MPLSLIHISPLVSVCMAAFNRHEPLAHAIASIERQDHPRLELILVDDASTDPATRQFLEALRPRFAARGWTLLRNAENSWQGVTRHRAAQAAQGEFLLFM DDDNAAWPDEVSTFVRAAQHSGADILTCQMQPFRGAGPPPRHRSTRPIGYFPVGPCPALGVFQNALGDANMFMRRSAWDRMAGFTLDRAYFEDWEFLQAA VLAGLHLECLPEIL
k141_56282 *Oedo* sp. L. Mendota 17	228	MTLSYIQTSYPLDRKPVPMPIDPDTWPTVDIYVPSYNESLDLVRPTVLAAMNMDYPRDKLNVWILDDGRRPEFRDFAEECGCGYIIRPDNKGAKAGNLNH AMRHTTGEYIAIFDCDHAPTRAFLQLTLGWLIRDKRIALVQTPHHFYSPDPFERNLVRQRLVPNEGLLFYGAIQPGSDLWNASFFCGSCAVLRRTALEEV GGVPHVTVTEDCHCALKMQQKGWHTAYI
k141_57104 *Oedo* sp. L. Mendota 9	321	FGLLFGMTALTFLGLTLLKIATAVAALRAPQDTTPPLDRADLPTISLLVALYGEAEIAPRLIRRLSALDYPRDRLDVIVLLESSDTATCTAIAGIDLPPW MRVIAVPDGRIRTKPRALNFGLDFTRGSIIGIYDAEDAPASDQLLKVAATFANAPPRLGCLQGMLDFYNPATNWIARCFTLEYAAWFRLFLPGLVRLGLP IPLGGTTLFLRRDAVLEVGAWDAHNVTEDADLGLRLARRGWQTGMLSSVTMEEANCRPVPWIKQRSRWTKGYLMTWLVHMRAPRALLRDLGLRRFAAVQV LIVGSLMQGIATPVFWSLWLV
k141_78262 *Oedo* sp. L. Mendota 10	309	DNQLPMISLVVPAYNEGLVIQPAIRSLLHLDYPNYEILVVNDGSTDDTYEKALVVARESTTVPVRVINKRNGGKSDALNTGMTQARGEFILNMDGDTKLS PNSLRACIRHFDNPRIGAVAGNVKVLNRESLWAKIQAVEYIEGLAMARKAQSYLRSVVIIPGPLGMFRKTVLQQAGGYDHDTFAEDADLTLKLLMRGWQI AYEPAAVAWVETPSRLLDLLKQRYRWTRGILQAIRKHASALWRPRKGGVNFFILWYMLFEGILWPFSTVLGSLFFAYVGLYYGVATFIFFWWLQLTLLDV IAAAYCVIV
k141_81164 *Oedo* sp. L. Mendota 18	228	MTLSYIQTSYPLDRKPVPMPIDPDTWPTVDIYVPSYNESLDLVRPTVLAAMNMDYPRDKLNVWILDDGRRPEFRDFAEECGCGYIIRPDNKGAKAGNLNH AMRHTTGEYIAIFDCDHAPTRAFLQLTLGWLIRDKRIALVQTPHHFYSPDPFERNLVRQRLVPNEGLLFYGAIQPGSDLWNASFFCGSCAVLRRTALEEV GGVPHVTVTEDCHCALKMQQKGWHTAYI

References

Arioli,T., Peng, L., Betzner, A.S., Burn, J., Wittke, W., Herth, W., Camilleri, C., Höfte, H., Plazinski, J., Birch, R., Cork, A., Glover, J., Redmond, J., Williamson, R.E. 1998. Molecular Analysis of Cellulose Biosynthesis in *Arabidopsis*. *Science* 279:717-720.

Bakatulaa, E.N., Cukrowskaa, E.M., Weiersbyeb, I.M., Mihaly-Cozmutac, L., Peterc, A., Tutu, H. 2014. Biosorption of trace elements from aqueous systems in gold mining sites by the filamentous green algae (*Oedogonium* sp.). *J. Geochemical Exploration* 144:492-503.

Banks, J.A., Nishiyama, T., Hasebe, M., Bowman, J.L., Gribskov, M., Albert, V.A., Aono, N., Aoyama, T., Ambrose, B.A., Ashton, N.W. & Axtell, M.J. 2011. The *Selaginella* genome identifies genetic changes associated with the evolution of vascular plants. *Science* 332:960-963.

Bolger, A.M., Lohse, M., & Usadel, B. 2014. Trimmomatic: A flexible trimmer for Illumina sequence data. *Bioinformatics*, btu170.

Braus, M.J., Graham, L.E., Whitman, T.L. 2017 Spatiotemporal dynamics of the bacterial microbiota on lacustrine *Cladophora glomerata* (Chlorophyta). *J. Phycol.* 53:1255–1262.

Brown, R M., Montezinos, D. 1976. Cellulose microfibrils: visualization of biosynthetic and orienting complexes in association with the plasma membrane. *Proc Natl Acad Sci U S A.* 73(1): 143–147.

Capella-Gutierrez, S., Silla-Martinez, J.M. & Gabaldon, T. 2009. TrimA1: a tool for automated alignment trimming in large-scale phylogenetic analyses. *Bioinformatics* 25:1972-1973.

Chen, H.-W., Persson, S., Grebe, M. & McFarlane, H.E. 2018. Cellulose synthase during cell plate assembly *Physiol. Plant*. 164:17-26.

Cole, M., Lindeque, P., Fileman, E., Halsband, C., Goodhead, R., Moger, J., Galloway, T.S. 2013. Microplastic ingestion by zooplankton. *Environ Sci Technol.* 47(12):6646-55.

Cole, M., Webb, H., Lindeque, P.K., Fileman, E.S., Halsband, C., Galloway, T.S. 2014. Isolation of microplastics in biota-rich seawater samples and marine organisms. *Sci Rep.* 4:4528.

Cole, M., Lindeque, P.K., Fileman, E., Clark, J., Lewis, C., Halsband, C., Galloway, T.S. 2016. Microplastics Alter the Properties and Sinking Rates of Zooplankton Faecal Pellets. *Environ Sci Technol.* 50(6):3239-46.

Francke, J.A., Den Oude, P.J. 1983. Growth of *Stigeoclonium* and *Oedogonium* species in artificial ammonium-N and phosphate-P gradients. *Aquatic Bot.* 15:375-380.

Gardiner, J.C., Taylor, N.G., Turner, S.R. 2003. Control of Cellulose Synthase Complex Localization in Developing Xylem. *The Plant Cell*. 15:1740–1748.

Gerloff, G.C., & Fitzgerald, G.P. 1976. The Nutrition of Great Lakes *Cladophora*. USEPA *Tech. Rep. EPA*. 600(3):76-099

Gertz, E.M., Yu, Y.K., Agarwala, R., Schäffer, A.A. & Altschul, S.F. 2006. Composition-based statistics and translated nucleotide searches: improving the TBLASTN module of BLAST. *BMC Biol.* 4:41.

Giddings, T.H., Brower, D.L. & Staehelin, L.A. 1980. Visualization of particle complexes in the plasma membrane of *Micrasterias denticulata* associated with the formation of cellulose fibrils in primary and secondary cell walls. *J. Cell Biol.* 84(2):327-339.

Graham, J. M., Auer, M. T., Canale, R. P. & Hoffmann, J. P. 1982. Ecological and mathematical modeling of *Cladophora* in Lake Huron: 4. Photosynthesis and respiration as functions of light and temperature. *J. Gr. L. Res*. 8:100-111.

Graham, L.E., Cook, M.E., Wilcox, L.W., Graham, J., Taylor, W., Wellman, C.H. & Lewis, L. 2013. Resistance of filamentous chlorophycean, ulvophycean, and xanthophycean algae to

acetolysis: Testing proterozoic and paleozoic microfossil attributions. *International Journal of Plant Sciences* 174:947- 957.

Graham, L.E., Knack, J.J., Graham, M.E., Graham, J.M., Zulkifly, S. 2015.A metagenome for lacustrine *Cladophora* (Cladophorales) reveals remarkable diversity of eukaryotic epibionts and genes relevant to materials cycling. *J. Phycol*. 51(3): 408-418.

Graham, L.E., Graham, J.M., Wilcox, L.W., Cook, M.E. 2016. Algae. 3rd ed.
LJLM Press, Madison, WI, 595 pp.

Graham LE, MJ Piotrowski, JM Graham, A Satjarak 2020 Molecular markers obtained from draft genomic sequence data characterize an isolate of Oedogonium (Oedogoniales, Chlorophyta) employed for biomass applications. Phycologia (accepted pending figure adjustments).

Guiry M.D. in Guiry M.D. & Guiry G.M. 2019. AlgaeBase. World-wide electronic publication, National University of Ireland, Galway. http://www.algaebase.org; searched on 14 July 2019.

Gupta, V.K. & Rastogi, A. 2008a. Biosorption of lead(II) from aqueous solutions by non-living algal biomass *Oedogonium* sp. and *Nostoc* sp.—A comparative study. *Colloids and Surfaces B: Biointerfaces* 64:170–178.

Gupta, V.K. & Rastogi, A. 2008b. Equilibrium and kinetic modeling of cadmium(II) biosorption by nonliving algal biomass *Oedogonium* sp. from aqueous phase. *J. Hazard. Mat*. 153:759–766.

Gupta, V. K. & Rastogi, A. 2009. Biosorption of hexavalent chromium by raw and acid-treated green alga *Oedogonium hatei* from aqueous solutions. *J. Hazard. Mat*. 163:396–402.

Gupta, S., Babu, B.V., 2009. Utilization of waste product (tamarind seeds) for the removal of Cr(VI) from aqueous solutions: Equilibrium, kinetics, and regeneration studies. *Journal of Environmental Management*. 90(10):3013-3022.

Gupta, V. K., Rastogi, A. & Nayak, A. 2010. Biosorption of nickel onto treated alga (*Oedogonium hatei*): Application of isotherm and kinetic models. *J. Colloid Interface Sci*. 342:533–539.

Harholt, J., Sørensen, I., Fangel, J., Roberts, A., Willats, W.G., Scheller, H.V., Petersen, B.L., Banks, J.A. & Ulvskov, P. 2012. The glycosyltransferase repertoire of the spikemoss *Selaginella moellendorffii* and a comparative study of its cell wall. *PloS ONE* 7(5):e35846.

Herth, W. 1983. Arrays of plasma-membrane “rosettes” involved in cellulose microfibril formation of *Spirogyra*. *Planta* 159(4):347-356.

Hotchkis, A.T., Brown, R.M., 1987. The association of rosette and globule terminal complexes with cellulose microfibril assembly in *Nitella translucens* var. *axillaris* (Charophyceae). *J. Phycol*. 23:220-37.

Katoh, K. & Standley, D.M. 2013. MAFFT multiple sequence alignment software version 7: improvements in performance and usability. *Mol. Biol. Evol.* 30:772-780.

Kumar, M., Turner, S. 2015. Plant cellulose synthesis: CESA proteins crossing kingdoms. *Phytochemistry*. 112: 91-99.

Mikkelson, M.D., Harholt, J., Ulskov, P., Johansen, I.E., Fangel, J.U., Doblin, M.S., Bacic, A., Willats, W.G. 2014. Evidence for land plant cell wall biosynthetic mechanisms in charophyte green algae. *Ann Bot*. 114:1217-1236.

Polko, J. & Kleiber J.J. 2019. The regulation of cellulose biosynthesis in plants. *Plant Cell* DOI: https://doi.org/10.1105/tpc.18.00760.

Kurek, I., Kawagoe, Y., Jacob-Wilk, D., Doblin, M., Delmer, D. 2002. Dimerization of cotton fiber cellulose synthase catalytic subunits occurs via oxidation of the zine-binding domains. *Proc Natl Acad Sci USA*. 99:11109-11114.

Kubicki, J.D., Yang, H., Sawada, D., O'Neill, H., Oehme, D. & Cosgrove, D. 2018. The shape of native plant cellulose microfibrils. *Sci. Rep*. 8:13983.

Lawton, R.J., de Nys, R., Skinner, S., Paul, N.A. 2014. Isolation and identification of *Oedogonium* species and strains for biomass applications *PLoS One.* 9:e90223.

Lawton, R.J., Cole, A.J., Roberts D.A., Paul, N.A., de Nys, R. 2017 The industrial ecology of freshwater macroalgae for biomass applications. *Algal Res.* 24:486-491.

Li, D., Liu, C.-M., Luo, R., Sadakane, K. & Lam, T.-W. 2015. MEGAHIT: an ultra-fast single-node solution for large and complex metagenomics assembly via succinct de Bruijn graph. *Bioinformatics* 31:1674-1676.

Machlis, L. 1973. The effects of bacteria on the growth and reproduction of *Oedogonium cardiacum. J. Phycol*. 9:342-344.

Matasci, N., Hung, L.-H., Yan, Z., Carpenter, E. J., Wickett, N. J., Mirarab, S., Nguyen, N., et al. 2014. Data access for the 1,000 plants (1KP) project. *Gigascience* 3:17.

McCracken, M. D., Gustafson, T. D. & Adams, M.S. 1974. Productivity of *Oedogonium* in Lake Wingra, Wisconsin. *Am. Midland Nat*. 92:247-254.

Mihranyan, A. 2011. Cellulose from Cladophorales green algae: From environmental problem to high-tech composite materials. *J. Appl. Polymer Sci*. 119:2449–2460.

Miller, M.A., Pfeiffer, W. & Schwartz, T. 2010. Creating the CIPRES Science Gateway for inference of large phylogenetic trees. In Gateway Computing Environments Workshop (GCE), *IEEE*. 1-8.

Neveuxa, N., Magnussona, M., Mataa, L., Whelan, A., de Nysa, R., Paul, N.A. 2016. The treatment of municipal wastewater by the macroalga *Oedogonium* sp. and its potential for the production of biocrude. *Algal Research*. 13: 284-292.

Nguyen, L.-T., Schmidt, H.A., von Haeseler, A. & Minh, B.Q. 2014. IQ-TREE: a fast and effective stochastic algorithm for estimating maximum-likelihood phylogenies. *Mol. Biol. Evol*. 32:268-74.

Nobles, D.R., Romanovicz, D.K. & Brown, R.M. 2001. Cellulose in cyanobacteria. Origin of vascular plant cellulose synthase? *Plant Physiol.* 127(2):529-542.

Okuda, K., Brown, M. 1992. A new putative cellulose-synthesizing complex of *Coleochaete scutata*. *Protoplasma*. 168(1–2):51–63.

Peng L, F Xiang, E Roberts, Y Kawagoe, LC Greve, K Kreutz, DP Delmer 2001 The experimental herbicide CGA 325' 615 inhibits synthesis of crystalline cellulose and causes accumulation of non-crystalline □-1.4-glucan associated with CesA protein. Plant Physiol 126:981-992.

Pickett-Heaps, J. 1971. Reproduction by zoospores in *Oedogonium*. *Protoplasma* 72:275-314.

Pickett-Heaps, J. 1975. *Green Algae*. Sinauer Associates Inc. Publishers, Sunderland, Massachusetts.

Piotrowski, M.J., Graham, J.M., Smith, B. & Graham, L.E. 2020. Temperate zone cultivation of *Oedogonium* in municipal wastewater effluent to produce cellulose and oxygen. *J. Indust. Micro. Biotechnol*. Revised after review and resubmitted.

Popper, Z. A., Michel, G., Hervé, C., Domozych, D. S., Willats, W. G., Tuohy, M. G., ... & Stengel, D. B. 2011. Evolution and diversity of plant cell walls: from algae to flowering plants. *Annual Review of Plant Biology* 62, 567-590.

Rawitscher-Kunkel, E., Machlis, L. 1962. The hormonal integration of sexual reproduction in *Oedogonium*. *Am J Bot*. 49:177-183.

Roberts, D. A., de Nys R. & Paul, N. A. 2013. The effect of CO2 on algal growth in industrial waste water for bioenergy and bioremediation applications. *PLoS ONE* 8: e81631.

Roberts, D.A., Shiels, L., Tickle, J., de Nys, R., Paul, N.A. 2018. Bioremediation of aluminum from the waste water of a conventional water treatment plant using the freshwater macroalga *Oedogonium*. *Water*. 10:626.

Ronquist, F., Teslenko, M., Van Der Mark, P., Ayres, D.L., Darling, A., Hohna, S., Larget, B., Liu, L., Suchard, M.A. & Hulsenbeck, J.P. 2012. MrBayes 3.2: efficient Bayesian phylogenetic inference and model choice across a large model space. *Systematic Biol*. 61:539-542.

Satjarak, A. & Graham, L.E. 2017. Whole genome sequencing of *Pyramimonas parkeae* reveals genes encoding carbohydrate active enzymes. *J. Phycol*. 53:1072-1086.

Speicher, T., Li, P.Z. & Wallace, I.S. 2018. Phosphoregulation of the plant cellulose synthase complex and cellulose synthase-like proteins. *Plants* 7:52.

Stamatakis, A. 2014. RAxML version 8: a tool for phylogenetic analysis and post-analysis of large phylogenies. *Bioinformatics* btu033.

Tiffany, L. H. & Transeau, E. N. 1927. *Oedogonium* periodicity in northern central states. *Trans. Am. Micros. Soc.* 46:166-174.

Tsekos, I. 1999. The sites of cellulose synthesis in algae: diversity and evolution of cellulose-synthesizing enzyme complexes. *J. Phycol.* 35(4):635-655.

Tsekos, I., Orologas, N., Herth, W. 1999. Cellulose microfibril assembly and orientation in some bangiophyte red algae: relationship between synthesizing terminal complexes and microfibril structure, shape, and dimensions. *Phycologia*. 38(3):217-224.

Ulvskov, P., Paiva, D.S., Domozych, D. & Harholt, J. 2013. Classification, naming and evolutionary history of glycosyltransferases from sequenced green and red algal genomes. *PloS ONE* 8(10):e76511.

Whitford, L.A., & Schumacher, G.J. 1961. Effect of current on mineral uptake and respiration by a fresh-water alga. *Limnol Oceanogr.* 6:423-425.

Whitford, L.A., & Schumacher, G.J. 1964. Effect of a current on respiration and mineral uptake in *Spirogyra* and *Oedogonium*. *Ecology.* 45:168-170.

Willison, J.H., Brown, R.M. 1978a. Cell wall structure and deposition in *Glaucocystis*. *J. Cell Biology*. 77 (1): 103.

Willison, J.H., Brown, R.M. 1978b. A model for the pattern of deposition of microfibrils in the cell wall of *Glaucocystis. Planta.* I41:51-58.

Yin, Y., Huang, J., & Xu, Y. 2009. The cellulose synthase superfamily in fully sequenced plants and algae. *BMC Plant Biology* 9(1):99.

Yin, Y., Mao, X., Yang, J., Chen, X., Mao, F. & Xu, Y. 2012. dbCAN: a web resource for automated carbohydrate-active enzyme annotation. *Nucleic Acids Res.* 40(W1):W445-W451.

Zaar, K. 1979. Visualization of pores (export sites) correlated with cellulose production in the envelope of the gram-negative bacterium *Acetobacter xylinum*. *J. Cell Biol.* 80:773-777.

Zhang, H., Yohe, T., Huang, L., Entwhistle, S., Wu, P., Yang, Z., Busk, P.K., Xu, Y. & Yin, Y. 2018. dbCAN2: a meta server for automated carbohydrate-active enzyme annotation. *Nucleic Acids Research* 46:W95-W101.

Zulkifly, S, Hanshew, A, Young, EB, Lee, P, Graham, ME, Graham ME, Piotrowski, M & Graham, LE. The epiphytic microbiota of the globally widespread macroalga *Cladophora glomerata* (Chlorophyta, Cladophorales). 2012. *Amer J. Bot* 99:1541-1552.

Authors: Michael J. Piotrowski · James M. Graham · Linda E. Graham

Title: Temperate Zone Cultivation of *Oedogonium* in Municipal Wastewater Effluent to Produce Cellulose and Oxygen

M. J. Piotrowski, L. E. Graham, J. M. Graham*

Department of Botany, University of Wisconsin-Madison,

430 Lincoln Drive, Madison, WI 53706, USA

*Corresponding author email jgraham@wisc.edu, phone 608-262-2640, fax 608-262-7509

Acknowledgements

The reported work was funded by United States Department of Agriculture National Institute of Food and Agriculture Small Business Innovation Research grant 2015-33610-2355 to the entity previously registered with the State of Wisconsin as AlgaExperts, LLC, now Algenomics, LLC, located at Suite 30A, 505 South Rosa Road, Madison, WI, 53717. Madison (WI) Metropolitan Sewerage District generously provided research space and resources; B. Smith, Z. Muscavitch, B. Pfleger, and A. Sanyal contributed technical expertise; S. Friedrich improved illustrations. All authors have agreed to submit this manuscript to the "Journal of Industrial Microbiology and Biotechnology."

Abstract

Cultivation of the filamentous chlorophyte *Oedogonium* in municipal wastewater effluent is known to improve water quality and yield lipid- and protein-rich biomass for industrial applications. Chlorophyte celluloses, whose molecular organization and physical traits differ from those of plants, represent yet another valuable extractive, and algal oxygen production is of economic value in wastewater treatment. Consequently, we explored cellulose- and oxygen-production from *Oedogonium* biomass batch-cultivated in treated secondary municipal wastewater effluent. We compared biomass, cellulose, and oxygen production outside and within an adjacent greenhouse, under differing dissolved CO_2 and pH conditions, and during temperate zone seasonal change from summer through fall. Overall production did not differ within or outside the greenhouse, but outside production was higher in summer and lower in fall as air temperatures declined. Batch cultivation offered advantages, but high levels of mixing and CO_2 were essential to maintain neutral pH for optimal algal growth and oxygen production.

Keywords Algae·Cellulose·Chlorophyta·*Oedogonium*·Wastewater.

Introduction

The fast-growing, herbivore- and pathogen-resistant chlorophyte *Oedogonium* (Oedogoniales, Chlorophyceae) generates conspicuous attached or floating masses along shorelines of temperate-tropical freshwater bodies worldwide, indicating that the >500 described and widely accepted species [10] together tolerate a wide spectrum of environmental conditions.

Microscopic unbranched *Oedogonium* filaments readily undergo asexual reproduction by fragmentation and zoospore release, in addition to producing resistant zygospore stages in a sexual process [25]. These reproductive features help to explain why *Oedogonium* has such a broad ecological distribution and why favorable environmental conditions lead to rapid development of large populations that become visible as mats.

Algal mats dominated by *Oedogonium* rapidly take up and thus reduce environmental concentrations of dissolved nutrients such as N and P [5]. Metals are known to adsorb to *Oedogonium* surfaces [1, 11-15]. These features have suggested potential for use of *Oedogonium* in industrial processes to remove waste CO_2, N and P, and heavy metals from wastewaters to improve water quality before discharge to natural environments [2-4, 27-28], and at the same time generate biomass for bioenergy [23, 26, 32] and other industrial applications, recently reviewed by Lawton et al. [17]. Consequently, efforts have been made to isolate, characterize, and compare *Oedogonium* strains for diverse industrial applications, a process that has revealed previously unrecognized genetic diversification and substantial variation in environmental tolerances [18].

Cellulose has been cited among various types of useful materials that might be extracted from *Oedogonium* biomass grown in wastewater [2]. We have shown that *Oedogonium* cellulose, like that of the chlorophyte *Cladophora*, which commonly occurs in periphyton with *Oedogonium*, is known to resist dissolution by acid-hydrolysis [8]. Highly-crystalline cellulose extracted from the branched filamentous chlorophyte *Cladophora* has been proposed for a variety of industrial applications [19-22], suggesting that *Oedogonium* cellulose is also likely to find industrial uses. Chlorophyte celluloses are known to vary among genera, and our work and that of others indicates that chlorophyte celluloses and genes encoding them differ from those of

streptophytes–plants and closely-related charophycean green algae–in biophysical traits arising from biochemical differences in the cell membrane proteins that make up cellulose-synthesizing complexes, which are encoded by *CESA* genes [16, 29-31]. Chlorophytes thus offer the potential for wastewater-linked production of diverse types of cellulose that may have distinctive applications. Despite this potential, cellulose-production by wastewater-grown *Oedogonium* has not previously been quantified, nor have the macromolecular features of *Oedogonium* cellulose been compared to those of other chlorophytes.

Likewise, oxygenation of wastewater effluents as the result of algal photosynthesis in *Oedogonium* cultivation systems has been recognized as beneficial and oxygen-demand reductions documented [23], but O_2 production by wastewater-cultivated *Oedogonium* has not been quantified. Molecular oxygen is a byproduct of the process of photosynthesis. A stream of oxygen-rich water arising from on-site algal cultivation could potentially be redirected to primary wastewater treatment to reduce oxygen demand, providing wastewater treatment facilities with an important economic benefit.

Dissolved CO_2 is a reactant in algal photosynthesis and is also an important determinant of growth medium pH, important because too low or high pH can be detrimental to algal growth. When carbon dioxide is present in natural waters, the pH will be acidic to neutral (pH 7.0), pH levels optimal for growth of many algal species. Carbon dioxide readily diffuses from the surrounding medium into algal cells without expenditure of energy, but as the external concentration of CO_2 declines below optimal levels, many algae begin taking up bicarbonate ion (HCO_3^-), which requires an expenditure of energy in the form of ATP. Once bicarbonate passes into an algal cell, carbon dioxide and hydroxide ion (OH^-) are released and the hydroxide ion returns to the medium, alkalinizing it [6]. Unless carbon dioxide is added to a batch culture, the

result of algal photosynthesis is to increase the pH of the medium, potentially beyond optimal algal growth conditions.

In addition to assessing *Oedogonium* batch production of biomass, cellulose, and oxygen with and without CO_2 amendments, we also examined the production of saturated and unsaturated fatty acids by lab-grown cultures of the same *Oedogonium* strain under three temperature conditions: 10, 20, and 30°C. These temperatures reflect spring-to-summer and summer-to-fall climatic transitions in temperate locales. Although a fatty acid profile for wastewater-cultivated *Oedogonium* samples pooled over a 3-month period has been reported [3], how such fatty acids might change during seasonal transition is also of interest. Information about seasonal fatty acid changes would be useful in developing strategies for processing and marketing an algal crop.

Here, we report the results of experiments designed to obtain quantitative estimates of algal biomass, cellulose, and oxygen production in a temperate locale, by a local *Oedogonium* strain that was batch-cultivated in treated wastewater effluent, both within and adjacent to a greenhouse, under varying conditions of dissolved CO_2, pH, and temperature, during seasonal transition from warm to cool conditions. We used information acquired in this study to calculate (model) the production of cellulose and oxygen by *Oedogonium* cultivated outdoors over a temperate zone growing season, or cultivated annually under greenhouse conditions, at a wastewater treatment facility with outflow typical of operations in non-urban communities worldwide.

Materials and Methods

Algal isolation, characterization, and maintenance

A new, local strain of *Oedogonium* was isolated for outdoor cultivation because local strains are already adapted to local environmental conditions [18]. *Oedogonium* sp. was isolated from periphyton collected from Lake Mendota (Dane County, WI, USA, 43.1097N, 89.4206W), using algal isolation methods similar to those we have previously described [9] (specified in Online Resource 1). The local isolate was identified as the genus *Oedogonium* based on presence of unbranched filaments anchored by a basal holdfast, barrel-shaped cells containing reticulate plastids, distinctive cell wall rings, and production of a single multiflagellate zoospore per vegetative cell, features illustrated in Graham et al. [6]. Species identification by means of structural characters alone was not possible because key sexual stages essential to making species distinctions were not expressed in lab cultures of the Lake Mendota isolate. For authentication purposes a dry culture sample was deposited under barcode number WIS-A-0000001 in the Wisconsin State Herbarium, Department of Botany, University of Wisconsin, Madison, WI https://herbarium.wisc.edu/; when rehydrated, this dry material displays structural features consistent with those of living cultures. For additional authentication, we used phylogenetic methods to evaluate five DNA barcode markers derived from our draft Illumina Mi-seq paired-end genome sequence for the new isolate to assess relationships, finding that our isolate is not con-specific with any *Oedogonium* species currently represented in molecular databases [7]. The following marker sequences for *Oedogonium* sp. Lake Mendota strain have been archived in NCBI GenBank: 18S rDNA (MN191507); 23S rDNA (MN191506); 28S rDNA (MN191505); *rbc*L (MN205324); ITS1+5.8S rDNA+ITS2 (MN191508). For the purposes of the current report, we indicate the isolate under study as "*Oedogonium* sp. (Lake Mendota)" or "the Lake Mendota isolate."

Production of algal inoculant for batch cultivation

Algal biomass for inoculation into experimental cultivation containers, also referred to as reactors, was generated under field conditions from laboratory-grown stock cultures grown in 24.6 l polyethylene terephalate (PET) Big Mouth Bubblers (Northern Brewer, LLC, Roseville, MN, USA). These inoculum containers, chosen for transparency to light, light-weight yet sturdy construction, low cost, and cleaning ease, were each fitted with a rubber stopper penetrated with a longer glass aeration tube and a shorter glass vent tube, both loosely plugged with sterile cotton to reduce potential for contamination.

To each 24.6 l inoculum container, 18.9 l of treated effluent was added and supplemented with vitamins and micronutrients in amounts consistent with the SD11 cultivation medium [9] that we used to produce lab-grown stock cultures. Lab-cultured *Oedogonium* biomass of 20-30 g wet weight was added to each inoculum container. Aeration tubes were attached to latex rubber tubing fitted with an 18-gauge syringe needle inserted into a central latex air supply line. Airflow was generated using Whisper 60 Aquarium Air Pumps (Tetra, Blacksburg, VA, USA) operated at 6 L/min, with air drawn directly from the outdoor environment. Inoculated containers were mounted off the ground to allow airflow, and roofed with fiberglass screening to prevent photo-inhibition and 10 mil plastic to deflect rain. Inoculum containers were spaced 15 cm apart in clusters of 6, each cluster spaced 45 cm apart to reduce shading (diagrammed in Online Resource 2). After a three-week growth period, the resulting algal biomass was used to inoculate experimental cultivation containers (reactors), and to generate additional biomass of algal inoculant for later experimental stages.

Study design

To gain insight into cultivation issues related to warm-to-cool season transition, five experimental stages of batch cultivation were operated sequentially over a period of four months during warm-cool temperature transition, starting in mid-August, and ending in early November of the same year. To gain insight into optimal cultivation periods during seasonal transition, two of the early experimental stages lasted 8 days and others lasted 12 days. To explore the potential for greenhouse enclosure to protect algal crops and possibly extend the cultivation season in temperate climates, at each experimental stage, three replicate cultivation containers (reactors) were located within an anchored greenhouse: Clear Span EZ-Build and Gro, High Tunnel, Cold Frame (ClearSpan Fabric Structures, South Windsor, CT, USA). Three replicate cultivation containers (reactors) were located immediately outside the greenhouse (see Online Resource 2). The greenhouse was equipped with vent fans but not otherwise cooled or heated. Stock inoculant cultures and CO_2 tanks employed during experimental stages were located adjacent to the greenhouse (see Online Resource 2).

Because the investigation was conducted outdoors, during seasonal transition from summer to fall, temperature and day length conditions necessarily varied among the five experimental stages over the study period; for example, average cultivation container water temperature decreased from a maximum of 30.6ºC to a minimum of 9.6ºC. Adaptive cultivation methods were also implemented over the study period: relatively low CO_2 and mixing during stage 1, low CO_2 and high mixing during stage 2, and high CO_2 plus high mixing in stages 3-5.

Batch cultivation containers (reactors) and medium

Batch cultivation containers (reactors) were constructed by cutting Schütz 1,250 l BOT/UN Certified IBC tanks (SCHUTZ Container Systems, Inc., NG, USA), into halves, so that each

piece accommodated 492 liters of cultivation medium, leaving a 15 cm headspace. To achieve continuous aeration and vertical mixing to prevent formation of zones of nutrient depletion or temperature stratification, the bottom periphery of each cultivation container was equipped with an aeration frame constructed from pvc plumbing pipe and latex tubing supplied air via Whisper 60 Aquarium Air Pumps (Tetra, Blacksburg, VA, USA) operated at 6 l/min. UXCELL Aquarium Fish Tank Mineral Bubble Air Stone Oxygen Diffusers (Kwai Fong, New Territories, Hong Kong) were employed to diffuse air into small bubbles.

The cultivation medium was treated effluent obtained from final discharge outflow from the Nine Springs Madison Metropolitan Sewerage District (MMSD), 1610 Moorland Road, Madison, WI 53713, USA. This final effluent was the product of secondary waste treatment, including primary aerobic digestion, sludge removal/particular separation, secondary clarification/particulate separation, and high intensity UV light exposure, according to standard industry practice. Because microscopic examination of this final effluent revealed particulates of sizes up to 1 mm, and microorganisms such as green algae and bacteria, we used additional treatments to reduce the potential for investigator infection, contamination of the desired crop by other algae, and particulate fouling of the algal biomass crop. Before use as a cultivation medium, final effluent was passed through a 10 μm particulate filter, followed by UV light exposure from a Viqua UV Max model E4 (Viqua, Guelph, Ontario, Canada). The maximum rating for effective UV sterilization by the UV Max E4 is 32.2 liters per minute, so a rate of 7.6 l/m was employed. Filtered, UV-treated effluent employed in batch cultivation containers (reactors) was not supplemented with mineral nutrients except CO_2 for pH control.

Batch cultivation container (reactor) inoculation and pH monitoring

A standard quantity of 120-130 g wet *Oedogonium* biomass was used to inoculate each of six experimental cultivation containers at the start of each of the five experimental stages. After inoculation, cultivation containers were covered with a layer of fiberglass screening, which helped to prevent photo-inhibition associated with high irradiance levels, and reduce entry of airborne debris. A pH monitor (MC122 pH Meter, Smart Monitoring System, Milwaukee Instruments, Inc., Rocky Mount, NC, USA) was mounted to the exterior of each cultivation container, with electrode placed directly into the container growth medium, to continuously monitor pH. An initial pH reading was recorded for each cultivation container. MC122 meters contain control elements for a plug running from the meter, which allows a secondary device to be switched on or off when a pH setpoint has been exceeded. A Red Sea CO_2 Control Solenoid Valve (Red Sea USA, Houston, TX, USA) was plugged into each pH meter. For cultivation containers that were experimentally supplemented with CO_2, when pH reached 8.0, solenoids forced CO_2 into the growth medium. Initially, CO_2 additions were made through UXCELL Aquarium Fish Tank Mineral Bubble Air Stone diffusers, but later through diffuser plates (DYPFP12m Pentair Aquatic Eco-Systems, Inc. Apopka, FL, USA) because the resulting curtains of smaller (4-40 μm bubbles) allowed for faster pH manipulation via CO_2 amendments.

CO_2 used for pH adjustment (and for algal photosynthesis) was supplied from 4.5 kg tanks (Airgas, Madison, WI, USA), using Victor Edge Series single stage regulators (Victor Technologies International, Denton, TX, USA). Regulators were set to 2.8 kg/cm^2, a level between the minimum 2.46 kg/cm^2 and maximum 3.5 kg/cm^2 ratings for the diffuser plates.

Irradiance and O_2 assessments

An initial measurement of irradiance, photosynthetically-active radiation (PAR), was made for each cultivation container using a QSL-100 Laboratory Quantum Solar Irradiance Meter (Biophysical Instruments Inc., San Diego, CA, USA). Subsequently, ambient and cultivation container PAR were recorded daily at three points four-hours apart, and cultivation container pH and temperature were recorded at the same times. Oxygen levels were determined with the use of dissolved oxygen electrodes (model 97-08-00, Orion Research, Cambridge, MA, USA).

Biomass collection and measurement

On the final day of each cultivation stage, wet biomass was manually harvested using a garden rake, and mass recorded after excess water was removed by employing fiberglass screening, then blotting. Biomass samples were examined by compound microscopy for assessment of crop integrity. Wet biomass was dried overnight in weigh boats in an oven at 60ºC, then dry biomass recorded, to obtain a wet-to-dry biomass regression.

Cellulose extraction and microscopic characterization

Cellulose was extracted from wastewater-cultivated *Oedogonium* biomass using a modification of established protocols for algal cellulose [19-22]. Cellulose extractions were performed in sterile Whirl-Paks (Nasco, Fort Atkinson, WI, USA), which are dimensionally-stable up to 80ºC. Algal biomass was first bleached at 60ºC by immersion in an L Isotemp Water Bath (Fisher Scientific, Waltham, MA, USA) for 3 h. The bleaching solution (~60 ml per gram of dry algal biomass) was 2.16 g $NaClO_2$ plus 6.0 ml of 100 mM acetic buffer solution (pH 4.0), in 54 mL distilled, reverse osmosis (RO) water. The acetic buffer solution was made by dissolving 0.48 ml glacial acetic acid, then 0.2 g sodium acetate, into 1000 ml of distilled RO water.

After 3 h of bleaching, algal biomass was visually assessed, and if visible pigments remained, bleaching was continued for an additional 3 h. This process was repeated until samples had fully bleached. Bleached biomass was rinsed to pH neutrality in a stream of distilled RO water over 10 μm mesh. Excess 0.5 M NaOH was then added to new Whirl-Pak bags containing samples, and bags returned to the 60ºC water bath overnight. A final milling and acid treatment step specified in the Mihranyan et al. [20] procedure was not applied, to allow microscopic assessment of extracted cellulose. Instead, extraction was completed by washing cellulose remains to pH neutrality and drying at 60 ºC overnight in weigh boats, for subsequent mass determinations. For each replicate, the ratio of dry *Oedogonium* biomass that had survived the extraction procedure was calculated.

A Zeiss Axioplan epifluorescence microscope equipped with crossed polarizers for detection of birefringence and UV filter G365 FT395 LP420 for assessment of Calcofluor White staining was used to ascertain that the extraction product demonstrated properties of cellulose, and that extraction had removed materials other than cellulose. Light microscopic images were recorded using a Nikon D300s digital camera and Camera Control Pro software (Nikon, Melville, NY, USA). SEM was employed to determine surface macromolecular features of *Oedogonium* cellulose. SEM was performed at the University of Wisconsin-Milwaukee, by metal-coating dry samples of extracted *Oedogonium* cellulose with 5nM Iridium, then imaging with a Hitachi S-4800 Ultra High Resolution Cold Cathode field emission Scanning Electron Microscope (FE-SEM) operated at 5kV.

Statistical analysis

The biomass data were analyzed to determine whether or not a significant difference in cellulose production occurred inside vs outside the greenhouse over the entire study period. For this purpose Welch's approximate t was calculated as $t' = (X_1 - X_2)/ \sqrt{(s_1^2/n_1 + s_2^2/n_2)}$ with 20 degrees of freedom. In this equation, X_1 was the mean biomass within the greenhouse and X_2 the mean biomass outside the greenhouse; s_1 was the corresponding variance of the biomasses inside the greenhouse and s_2 the corresponding variance of biomasses outside the greenhouse; n_1 and n_2 were the number of data points in each set. Analysis of variance (ANOVA) was used to evaluate the effect of temperature on greenhouse production. A time-series regression analysis was conducted of increasing biomass productivity on temperature.

Fatty acid extraction and analysis

For fatty acid analysis, stock cultures were laboratory-grown at 10ºC, 20ºC, and 30ºC, a temperature range that reflected seasonal temperature environments experienced during experimental outdoor and greenhouse cultivation (August-November, 2015). This period paralleled the timeframe of a study of fatty acids produced by *Oedogonium intermedium* cultivated outdoors in wastewater effluent in Australia, which involved pooled samples likewise taken during warm-to-cool season transition (March-June, 2015) [3], thereby facilitating comparison. Fatty acid analysis followed procedures used in our previous study of fatty acids produced by four diatoms isolated from the same freshwater lake source [9] as the *Oedogonium* isolate employed in the present study, facilitating comparisons.

Modeling cellulose production

Detailed climate data taken over the study period were used together with dry biomass productivity predicted for *Oedogonium* (Lake Mendota strain), under the assumption that about 35% of dry biomass can be extracted as cellulose, to calculate potential annual cellulose production by a small (40,000 gal/day) temperate zone municipal wastewater treatment plant operated 1) outdoors over a spring-fall outdoor growing season, and 2) year-round, under greenhouse conditions in which near-optimal illumination and temperature conditions were maintained. The outdoor growing season was assumed to encompass a time period from the last 10 days of March through the first 10 days of November, based on outdoor temperature measurements observed during the experimental study.

Modeling O_2 production

O_2 production data obtained in our experiments were used to model net O_2 production in a wastewater treatment system using the following assumptions: 310 cultivation containers (each reactor containing 492 l of treated effluent) in a greenhouse, with a plant outflow of 151,400 l/day. The particular number of cultivation containers employed for calculations was based upon numbers obtained in our cellulose production modeling exercise. In our experimental studies, the initial inoculum of *Oedogonium* into each cultivation container was 120-130 g wet biomass (equivalent to 18-19.5 g dry biomass). Assuming an oxygen production rate of 15 mg O_2/g dry biomass h (a level indicated by experimental results), this amount of algal inoculum was calculated to produce 270-292 mg O_2 in one hour and 3,240-3,510 mg O_2 after 12 h. Under these assumptions, the algal inoculum alone could potentially generate an oxygen concentration in each 492 l cultivation container volume of 6.6-7.1 mg O_2 per l in just over 12 h from the time of inoculation (3,240-3,510 mg O_2 per 492 l cultivation container). These levels of oxygen are close

to saturation for oxygen in water at 20ºC (8 mg O_2 per l). This information was used to estimate the oxygen concentration generated by the wet biomass equivalent of 40 g dry biomass, which is the biomass level at which full oxygen saturation occurs.

Data availability

All data generated or analyzed during this study are included in this article [and its supplementary information in Online Resources].

Results

Biomass and cellulose production

Replicate and mean dry biomass and cellulose production in each of five sequential experimental stages that varied in CO_2 supplementation, mixing, and seasonal conditions are recorded in Online Resource 3. Welch's approximate t' = 0.6376 indicated lack of significant difference in overall biomass production inside vs outside the greenhouse. Similar comparisons of biomasses generated within and external to the greenhouse in each of the five experimental stages did not yield results that indicated significant difference (Fig. 1). However, dry biomasses did vary among experimental stages, in response to seasonal temperature changes (Fig. 2).

Over the study period, during which vent fans were operated within the greenhouse, the mean water temperature in cultivation containers located within the greenhouse interior was 2-3°C higher than the mean water temperature of cultivation containers located outside. Biomass productivity was higher outside the greenhouse when temperatures were high (>28°C) but was higher inside the greenhouse when outside temperatures fell below about 14°C. For example,

during experimental stage 4 the biomass production inside the greenhouse at 17°C was higher than outside at 13.5°C.

The optimum observed temperature for biomass production by *Oedogonium* sp. (Lake Mendota strain) at the experimental site was around 22°C (see Fig. 2). Temperatures above and below this level resulted in a significant decrease in biomass production. For example, shortly after experimental stage 1 began, a three-day summer heat wave with air temperatures above 30°C occurred, causing the temperature inside the greenhouse to rise to a level that killed most of the algae, resulting in low biomass productivity. A similar lower level of productivity was observed in experimental stage 5, which experienced reduced fall temperatures.

Over the entire experimental period, the percentage of cellulose in dry biomass ranged from 24% to 58% (see Online Resource 3). A significantly higher percentage of cellulose occurred in the first two experiments, under conditions of higher temperature and lower CO_2 availability (Fig. 3). ANOVA analysis of temperature and cellulose production within the greenhouse indicated a significant effect ($F = 8.386$, $p<0.01$) (Online Resource 4).

pH data

During experimental stage 1 (low CO_2, low mixing) and experimental stage 2 (low CO_2, high mixing), cultivation container (reactor) pH had risen above 10 by the end of the experiment. By contrast, neutral pH conditions more favorable to algal growth occurred during experimental stages 3-5, which were operated under high CO_2 and high mixing conditions (Fig. 4).

Oxygen

Oedogonium growth in wastewater drove the concentration of dissolved oxygen in the surrounding medium to high levels (>12 mg O_2/l). Oxygen concentrations reached 11 mg O_2/l during stage 3, at least 12 mg O_2/l during stage 4, and more than 13 mg O_2/l during stage 5 (Figure 5).

Cellulose microscopy

The Lake Mendota isolate of *Oedogonium* produced robust cell walls (Fig. 6a) rich in cellulose, indicated by birefringence when viewed with crossed polarizers (Fig. 6b), and blue-white epifluorescence after staining with Calcofluor White and viewed under UV excitation (Fig. 6c). Retention of distinctive cell-wall structural features such as cell wall rings after the cellulose-extraction process demonstrated that the cellulose crop originated from *Oedogonium*. When viewed by SEM (Fig. 6d), the surfaces of *Oedogonium* cellulose appeared relatively smooth, lacking conspicuous cross-hatched fibrillar macromolecular structure. Microscopic examination also illustrated that the extraction process had removed cellular materials other than cellulose.

Fatty acids

The proportions of saturated fatty acids produced by lab-grown cultures of the Lake Mendota strain of *Oedogonium* varied over cultivation temperatures of 10, 20, and 30ºC (Table 1). Among fatty acids detected, concentrations of C16 (palmitic acid) and C18:1 (oleic acid) were highest, though the highest concentration of the unsaturated oleic acid occurred at 10 ºC, whereas the highest concentration of the saturated palmitic acid was reached at 30ºC. Similarly, the less-abundant unsaturated C18 and C20 fatty acids we detected in the Lake Mendota isolate of

Oedogonium were present at higher concentration in cultures grown at 10ºC than in those grown at 20ºC or 30ºC.

Cellulose production model

Detailed climate data for the Nine Springs wastewater treatment plant (Dane Co., WI) (Online Resource 5) together with predicted dry biomass productivity for *Oedogonium* throughout an entire growing season, based on productivity observed in this study over five experiments conducted over the summer-to-fall transition (Fig. 7), allow modeling of larger scale production. If productivity were based on a single cultivation container operating outside over a period including the last 10 days of March through the first 10 days of November, the dry biomass productivity of *Oedogonium* can be estimated at 624 g. If three growth cycles were conducted each month over this period, a single cultivation container operated outdoors would produce an estimated 1792 g of dry biomass and 627 g of cellulose, assuming that about 35% of *Oedogonium* dry biomass is cellulose. If the source of nutrients for *Oedogonium* growth is the outflow from a wastewater treatment plant, many cultivation containers would be necessary to process the daily outflow, which can vary from thousands of liters per day for a small operation to millions of liters per day for a city. If we consider a small wastewater treatment plant having an outflow of 151,400 l/day, given that cultivation containers used in this study hold 492 l, about 310 cultivation containers of this volume, distributed in a closely-spaced land footprint of 380 m^2, could hold the entire daily effluent output. Assuming daily replacement of container fluid contents, the dilution rate for 310 cultivation containers would be once per day ($D = 1.0\ day^{-1}$). If the same outflow volume of 151,400 l/day were processed through 155 cultivation containers, the dilution rate would be $D = 2.0\ day^{-1}$. Assuming that 310 cultivation containers were operated

outdoors from late March through early November, a wastewater treatment plant processing 151,400 l/day could potentially generate 1792 g of dry biomass per cultivation container (555,520 g in 310 cultivation containers). Assuming that extractable cellulose is 35% of dry *Oedogonium* (Lake Mendota strain) biomass, operating 310 cultivation containers could generate 194,432 g cellulose annually. The value of this crop would depend upon the commercial application.

If a greenhouse of at least 750 m^2 (to avoid placing cultivation containers near walls and allow walkways) were constructed to house 310 cultivation containers, *Oedogonium* production could be conducted year-round, allowing maintenance of near-optimal temperature and illumination conditions to maximize biomass productivity. In the four experiments we conducted within a greenhouse, maximum observed productivity was 132 g dry biomass per average 10-day growth period. Assuming that three such growth periods could be completed in each month, 396 g dry biomass could be produced per month per cultivation container, and 310 cultivation containers could yield 122,760 g dry biomass per month, and 1,473,120 g dry biomass per year. In this scenario, assuming that cellulose represents about 35% of dry biomass, the potential annual cellulose production would be 515,592 g. Construction and operation costs would be location-dependent.

Oxygen production model

A dry biomass of 40 g of *Oedogonium* (Lake Mendota strain) could potentially produce 600 mg O_2/h and 7200 mg O_2 in 12 h, which represents an oxygen concentration of 14.6 mg O_2 per l in a 492 l cultivation container under semi-continuous cultivation. Experimental observations were that maximum oxygen concentrations were 11-14 mg O_2 per l. When the dry biomass of

Oedogonium exceeds about 40 g, potential oxygen production exceeds the supersaturated state; the excess must escape into the air.

Discussion

Study results indicated high potential for temperate-zone *Oedogonium* batch cultivation systems (reactors) to substantially decrease wastewater treatment plant oxygenation costs, in conjunction with production of biomass for extraction of cellulose, fatty acids, and other valuable organic materials. Such products might help to subsidize the costs of: 1) reducing nutrient input to natural waters from existing wastewater treatment facilities, thereby improving water quality, and 2) constructing new wastewater treatment facilities in remote or underdeveloped areas currently lacking modern wastewater treatment, thereby improving the health of humans and aquatic ecosystems.

Batch cultivation of *Oedogonium* cellulosic biomass in municipal wastewater

By contrast to continuous flow cultivation systems, batch cultivation of *Oedogonium* in municipal wastewater offers benefits that potentially include lower energy requirements, no need for filtration to prevent algal outflow, retention of CO_2 or other amendments needed for maximal algal growth, biomass quarantine, scalability, and the opportunity for linkage into semi-continuous flow systems. The present study of batch cultivation of *Oedogonium* sp. (Lake Mendota) in wastewater effluent indicated that higher levels of mixing and CO_2 were essential to maintain a neutral pH environment for optimal growth and biomass accumulation (Online resource 6). This result is consistent with previous observations [28] that CO_2 amendments likewise employed to stabilize pH generated a 10% increase in sequestration of the metal Al

from municipal wastewater by outdoor cultivated *Oedogonium*, though authors of that study noted that this level of remediation might not justify the costs of CO_2 additions if Al removal is the primary goal.

When cellulose extraction is a primary goal, our results indicated that overall cellulose harvest was highest when *Oedogonium* biomass production was greatest. We found that wastewater-cultivated *Oedogonium* is a consistently good source of extractable cellulose, even during seasonal transition. In the current study, the proportion of cellulose to biomass was observed to be at least 24% and under some conditions reached nearly 60%. However, different environmental conditions were associated with higher biomass production vs higher proportions of cellulose; at the temperate experimental site employed in 2015, biomass production of the Lake Mendota strain was highest at 22°C under conditions of high CO_2 and mixing, whereas the greatest proportions of cellulose-to-biomass were observed under higher temperature conditions and lower CO_2 availability. Further testing would be required to determine the relative influences of temperature vs CO_2 on cellulose-to-biomass proportions, but a possible explanation might be that higher than optimum temperature might reduce algal growth while allowing cellulose production, thereby yielding biomass having a relatively high proportion of cellulose. If this explanation were valid, cellulose crop production involving the Lake Mendota strain might be accomplished in stages: a first stage of cultivation at 22°C with CO_2 supplementation to maximize biomass, followed by a period of exposure to higher temperature to maximize cellulose content.

The results of our study suggest the possibility that greenhouse-protected cultivation might continue into cooler seasons even when external temperatures occurring in late fall, winter, and early spring are too low for outside biomass cultivation. Comparisons of

Oedogonium strain responses to natural temperature regimes in Australia indicated that particular strains were better able to tolerate lower temperatures [18]. Local strains that vary in optimal growth temperature might be employed in sequences that correspond with changes in seasonal conditions. Batch cultivation containers might be equipped with sensor-linked stock tank heaters to maintain cultivation medium temperature at optimal levels, and sensor-linked supplementary lighting might be employed to extend winter day length. Although our observations suggest that in warmer times of the year outdoor cultivation can be more effective than greenhouse cultivation, we also noted that temperate summer heat waves can substantially reduce algal productivity. In locales subject to heat waves, greenhouses equipped with flexible screening might be employed to reduce heat load and light stress on wastewater-cultivated *Oedogonium*.

Oxygen production by wastewater-cultivated *Oedogonium*

Our observations suggested that cultivation of cellulose-rich *Oedogonium* in municipal wastewater not only aids effluent remediation, but also generates oxygen-rich water. Modeling results indicate that after a first full day of operation, wastewater effluent in cultivation containers would be supersaturated with oxygen, and thus represent a source of low-nutrient, oxygen-rich water that could potentially be returned to an earlier stage in wastewater treatment to reduce costs. Siting algal cultivation containers close to both discharge effluent cultivation media and primary wastewater treatment might foster the post-harvest transfer of O_2-rich water before significant degassing occurs.

Seasonal changes in fatty acids produced by wastewater-cultivated *Oedogonium*

A previous fatty acid analysis of *Oedogonium* (*O. intermedium*) cultivated outdoors in wastewater effluent involved pooled and homogenized samples taken over a three-month period during warm-cool season transition of 2015 [3]. Our analysis of fatty acids production by *Oedogonium* cultivated under controlled laboratory conditions allowed us to distinguish variation related to temperature shifts (30, 20, 10ºC) consistent with warm-to-cool season transition of our outdoor study (August-November, 2015). In our lab study, among fatty acids detected, concentrations of C16 (palmitic acid) and C18:1 (oleic acid) were highest, though the highest concentration of the unsaturated oleic acid occurred at 10 ºC, whereas the highest concentration of the saturated palmitic acid was reached at 30ºC. Similarly, the less-abundant unsaturated C18 and C20 fatty acids we detected in the Lake Mendota isolate of *Oedogonium* were present at higher concentration in cultures grown at 10ºC than in those grown at 20ºC or 30ºC. These results suggest that lower temperatures might induce higher concentrations of unsaturated fatty acids, a finding that might indicate optimal harvest periods for extraction of unsaturated fatty acids.

By comparison, in our previous study of fatty acids produced by four diatom isolates (from the same temperate lake source as the *Oedogonium* isolate used in the current study) biomass cultivated at 21ºC was dominated by C16:1 (palmitoleic acid) [9]. At this temperature, and in a similar growth medium, the diatom *Cyclotella meneghiniana* produced about twice the concentration of C16:1 [9] as *Oedogonium* sp. (Lake Mendota) produced of C16 at 20ºC, or C18:1 at 10ºC. Given that *Cyclotella* was observed to produce even higher levels of unsaturated fatty acids under Si amendments, diatom cultivation in wastewater effluents might be economically preferable to *Oedogonium* cultivation for fatty acid extraction alone. But if

Oedogonium is cultivated in wastewater effluent for cellulose extraction and/or O_2 production, fatty acids might prove to be of additional benefit.

In summary, our comparison of algal biomass production in batch cultivation containers did not indicate significant difference between biomass production inside and outside a greenhouse over a period starting in late August and extending through early November (warm-to-cool season) study period. However, the pattern of algal biomass production indicated the importance of some type of greenhouse system to maintain biomass production rates during suboptimal late fall through early spring conditions. Batch cultivation offers advantages, but our study indicated that carbon dioxide additions are required to boost biomass production and maintain pH in a range optimal for algal growth, thereby increasing oxygen production for potential use in other parts of the wastewater treatment process. Gaseous emissions from wastewater treatment, which include CO_2 [24] might be explored as possible sources of CO_2 for algal cultivation, and photovoltaics might be examined as a potential source of energy for optimizing cool-season temperature and illumination in greenhouse conditions.

Author contributions

All authors contributed to study design and materials preparation. MJP performed data collection, MJP and JMG performed data analysis, and LEG wrote the first manuscript draft. All authors commented on previous versions of the manuscript, and read and approved the final manuscript.

Disclosure of potential conflicts of interest

The work was supported by United States Department of Agriculture National Institutes of Food and Agriculture Small Business Innovation Research grant 2015-33610-2355 to the entity previously registered with the State of Wisconsin as AlgaExperts, LLC, now Algenomics, LLC, located at Suite 30A, 505 South Rosa Road, Madison, WI, 53717, for which all authors are co-members. None of the authors is under any publication restriction. The authors declare that they have no conflicts of interest. This article does not contain any studies with human participants or animals performed by any of the authors.

References

1. Bakatula EN, Cukrowska EM, Weiersbye, IM, Mihaly-Cozmuta L, Peter A, Tutu H (2014) Biosorption of trace elements from aqueous systems in gold mining sites by the filamentous green algae (*Oedogonium* sp.). J Geochem Explor 144:492-503.
2. Cole AJ, Mata L, Paul, NA, de Nys R (2014) Using CO_2 to enhance carbon capture and biomass applications of freshwater macroalgae. GCB Bioenergy 6:637-645.
3. Cole AJ, Neveux N, Whelan A, Morton J, Vis M, de Nys R, Paul NA (2016) Adding value to the treatment of municipal wastewater through the intensive production of freshwater macroalgae. Algal Res 20:100-109.
4. Ellison MB, de Nys R, Paul NA, Roberts DA (2014) Growth and metal bioconcentration by conspecific freshwater macroalgae cultured in industrial waste water. PeerJ 2:e401: DOI 10.7717/peerj.401.
5. Francke JA, Den Oude PJ (1983) Growth of *Stigeoclonium* and *Oedogonium* species in artificial ammonium-N and phosphate-P gradients. Aquatic Bot 15:375-380.
6. Graham LE, Graham JM, Wilcox LW (2016) Algae. LJLM Press, Madison, WI

7. Graham LE, Piotrowski MJ, Graham JM, Satjarak A (2020) Molecular markers obtained from draft genomic sequence data characterize an isolate of *Oedogonium* (Oedogoniales, Chlorophyta) employed for biomass applications (submitted).
8. Graham LE, Cook ME, Wilcox LW, Graham J, Taylor W, Wellman CH, Lewis L (2013) Resistance of filamentous chlorophycean, ulvophycean, and xanthophycean algae to acetolysis: Testing Proterozoic and Paleozoic microfossil attributions. Int J Plant Sci 174:947-957.
9. Graham JM, Graham LE, Zulkifly SB, Pfleger BF, Hoover SW, Yoshitani Y (2011) Freshwater diatoms as a source of lipids for biofuels. J Ind Microbio Biotechnol. DOI 10.1007/s10295-011-1041-52
10. Guiry MD, Guiry GM (2019) AlgaeBase. World-wide electronic publication. National University of Ireland, Galway.
11. Gupta VK, Rastogi A (2008a) Biosorption of lead(II) from aqueous solutions by non-living algal biomass *Oedogonium* sp. and *Nostoc* sp.–A comparative study. Colloids Surfaces B:Biointerfaces 64:170-178.
12. Gupta VK, Rastogi A (2008b) Equilibrium and kinetic modeling of cadmium(II) biosorption by nonliving algal biomass *Oedogonium* sp. from aqueous phase. J Hazard Mat 153:759–766.
13. Gupta VK, Rastogi A (2009) Biosorption of hexavalent chromium by raw and acid-treated green alga *Oedogonium hatei* from aqueous solutions. J Hazard Mat 163:396–402
14. Gupta VK, Rastogi A, Nayak A (2010) Biosorption of nickel onto treated alga (*Oedogonium hatei*): Application of isotherm and kinetic models. J Colloid Interface Sci 342:533–539.

15. Gupta SS, Bhattacharya KA (2011) Kinetics of adsorption of metal ions on inorganic surfaces: A review. Adv Colloid Interface Sci 162:39-52.

16. Kumar M, Turner S (2015) Plant cellulose synthesis: CESA proteins crossing kingdoms. Phytochemistry 112:91-99.

17. Lawton RJ, Cole AJ, Roberts DA, Paul NA, de Nys R (2017) The industrial ecology of freshwater macroalgae for biomass applications. Algal Res 24:486-491.

18. Lawton RJ, de Nys R, Skinner S, Paul NA (2014) Isolation and identification of *Oedogonium* species and strains for biomass applications PLoS One 9:e90223.

19. Mihranyan A (2011) Cellulose from Cladophorales green algae: From environmental problem to high-tech composite materials. J Appl Polymer Sci 119:2449–2460.

20. Mihranyan A, Edsmana K, Strømme M (2007) Rheological properties of cellulose hydrogels prepared from *Cladophora* cellulose powder. Food Hydrocolloids 21:267-272.

21. Mihranyan A, Nyholm L, Garcia Bennett AE, Strømme M (2008) A novel high specific surface area conducting paper material composed of polypyrrole and *Cladophora* cellulose. J Phys Chem B 112:12249–12255.

22. Mihranyan A, Llagostera AP, Karmhag R, Strømme M, Ek R (2004) Moisture sorption by cellulose powders of varying crystallinity. Int J Pharm 269:433–442.

23. Neveux N, Magnusson M, Mata L, Whelan A, de Nys R, Paul NA (2016) The treatment of municipal wastewater by the macroalga *Oedogonium* sp. and its potential for the production of biocrude. Algal Res 13:284-292.

24. Parravicini V, Svardal K, Krampe J (2016) Greenhouse gas emissions from wastewater treatment plants. Energy Procedia 97:246-253.

25. Pickett-Heaps J (1975) Green algae: structure reproduction and evolution in selected genera. Sinauer, Sunderland, MA

26. Ramola B, Kumar V, Nanda M, Mishra Y, Tyagi T, Gupta A, Sharma N (2019) Evaluation, comparison of different solvent extraction, cell disruption methods and hydrothermal liquefaction of *Oedogonium* macroalgae for biofuel production. Biotechnology Reports 24 https://doi.org/10.1016/j.btre.2019.w00340

27. Roberts DA, de Nys R, Paul NA (2013) The effect of CO2 on algal growth in industrial waste water for bioenergy and bioremediation applications. PLoS ONE 8: e81631.

28. Roberts DA, Shiels L, Tickle J, de Nys R, Paul NA (2018) Bioremediation of aluminum from the waste water of a conventional water treatment plant using the freshwater macroalga *Oedogonium*. Water 10:626 doi:10.3390/w10050626

29. Satjarak A, Graham LE (2017) Whole genome sequencing of *Pyramimonas parkeae* reveals genes encoding carbohydrate active enzymes. J Phycol 53:1072-1086

30. Ulvskov P, Paiva DS, Domozych D, Harholt J (2013) Classification, naming and evolutionary history of glycosyltransferases from sequenced green and red algal genomes. PLoS One 8:e76511.

31. Yin Y, Huang J, Xu Y (2009). The cellulose synthase superfamily in fully sequenced plants and algae. BMC Plant Biology 9:99.

32. Zhu Y, Kwong EW, van Eyk PJ, de Nys R, Wang D, Ashman PJ (2015) Pyrolysis characteristics and char reactivity of *Oedogonium* sp. and Loy Yang coal. Energy Fuels 29:5047-5055.

Table 1 Fatty acid production by lab-cultivated *Oedogonium* sp. (Lake Mendota) at temperatures of 10, 20, and 30ºC, representing the temperature range during outdoor cultivation during summer-to-fall (August-November) transition. Lipid volumes are represented as µg/ml of the sample volume(s) tested; values reported are micrograms of each fatty acid present in one ml of extracted fatty acid profile from the original sample of algal biomass.

Fatty acids	10ºC (µg/ml)	20ºC (µg/ml)	30ºC (µg/ml)
C14 Myristic	0.56	1.09	1.14
C16:1 Palmitoleic	10.63	5.62	3.88
C16:0 Palmitic	19	21.97	24.3
C18:3 Linoleic	1.48	1.13	1.58
C18:1 Oleic	20.41	9.88	10.39
C18 Stearic	0.37	0.60	0.81
C20:5 8,11,14 Eicosapentaenoic acid	1.86	1.37	1.18
C20:5 11,14,17 Eicosapentaenoic acid	3.46	1.18	0.92

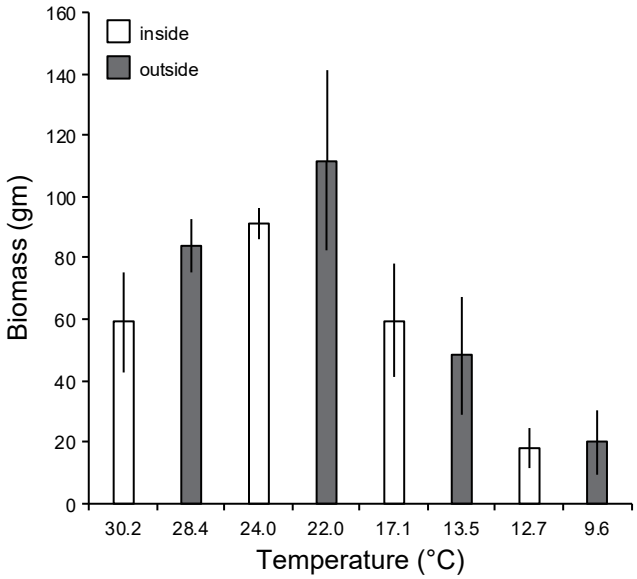

Fig. 1 Production of dry *Oedogonium* biomass inside vs outside greenhouse in each of five sequential experimental stages conducted during transition from summer to fall (error bars denote the standard deviations of the means).

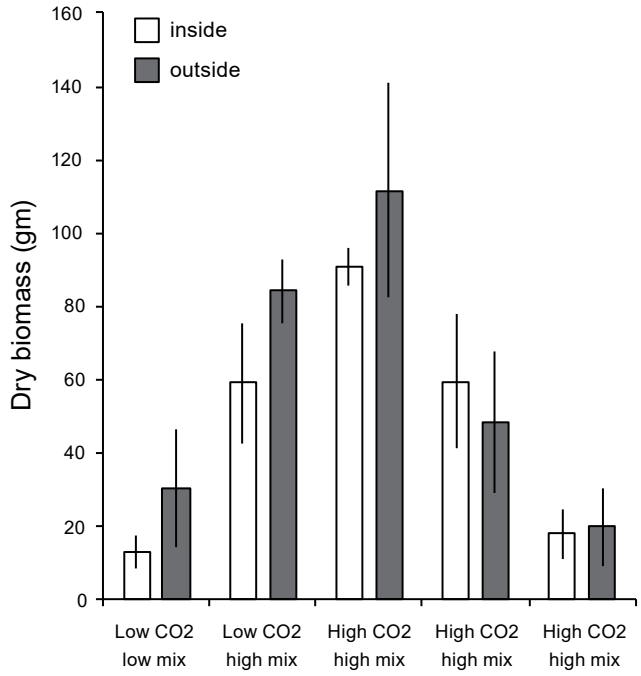

Fig. 2 Temperature and standard deviations of the means for sequential experimental stages 2-5 conducted during seasonal change from summer to fall, showing that temperatures inside the greenhouse were consistently higher than outside

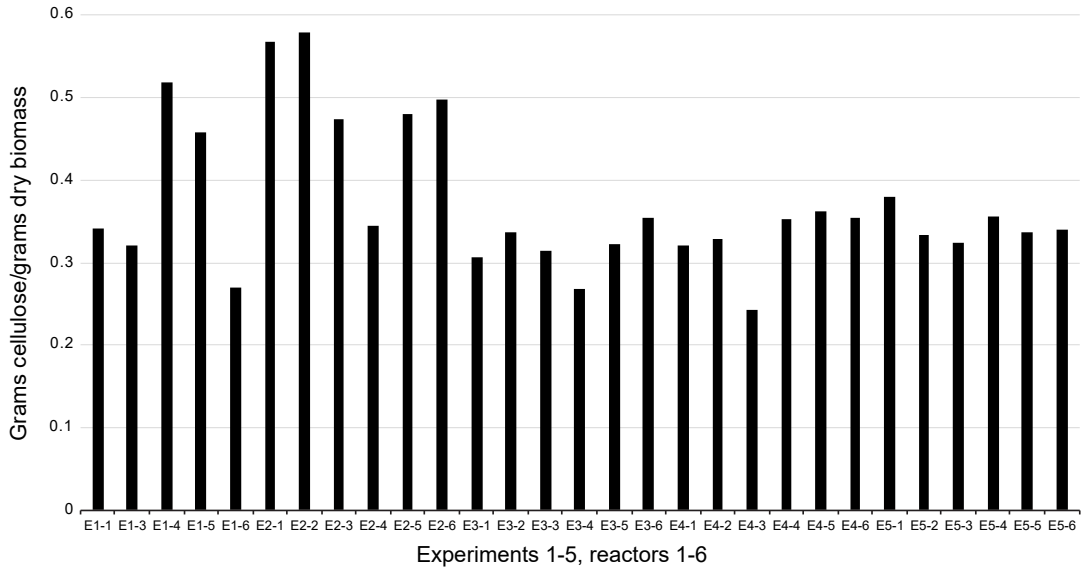

Fig. 3 Changes in the proportion of cellulose-to-total dry biomass ratio in 5 sequential experiments conducted during summer to fall seasonal transition

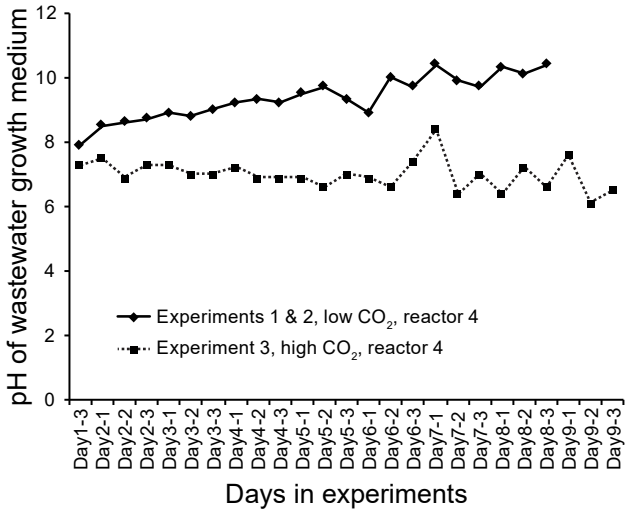

Fig. 4 Profile of pH changes assessed 3 times a day over a period of 9 days in experimental cultivation container (reactor) number 4, in experimental stage 2 with lower CO_2 (diamonds) and experimental stage 3 with higher CO_2 conditions (squares)

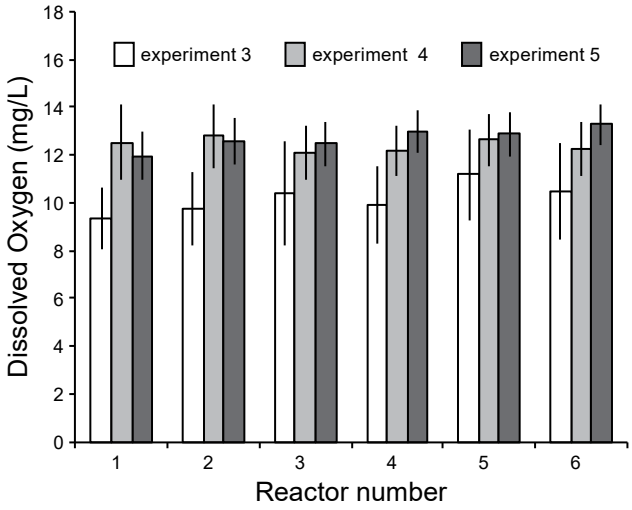

Fig. 5 Oxygen production (with standard deviation of the means) in replicate cultivation containers in experimental stages 3-5, showing that oxygen content was consistent and high during seasonal transition from warmer to cooler conditions

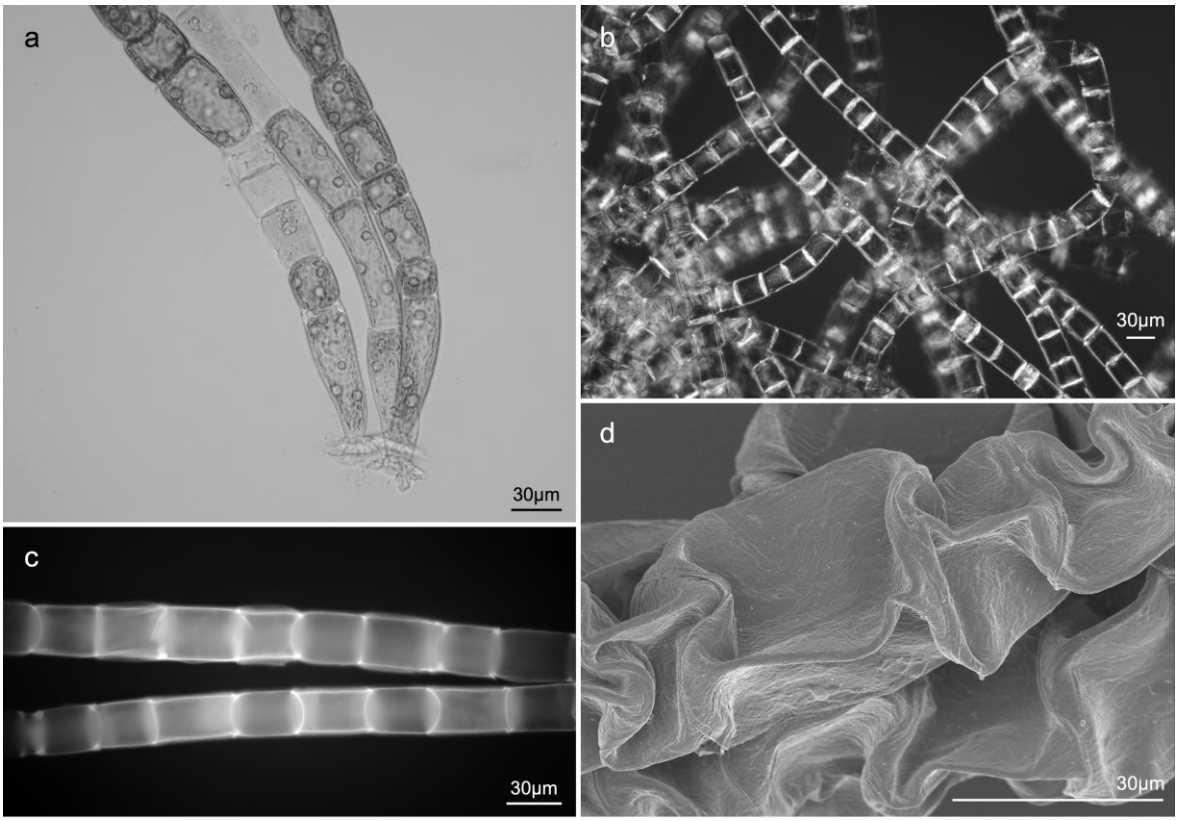

Fig. 6 *Oedogonium* (Lake Mendota strain) microscopy. **a** bright field view of typical unbranched filaments, showing characteristic basal holdfast and barrel-shaped cells with reticulate, pyrenoid-bearing chloroplasts, **b** View in crossed-polarizers of extracted cellulose, showing retention of filament structure and cell-wall birefringence, **c** Epifluorescence view in UV excitation of extracted cellulose stained with Calcofluor White, a fluorescence reaction that is generally characteristic of cellulose, **d** SEM view of extracted cellulose, showing relatively smooth surface lacking obvious fibrillar macromolecular structure

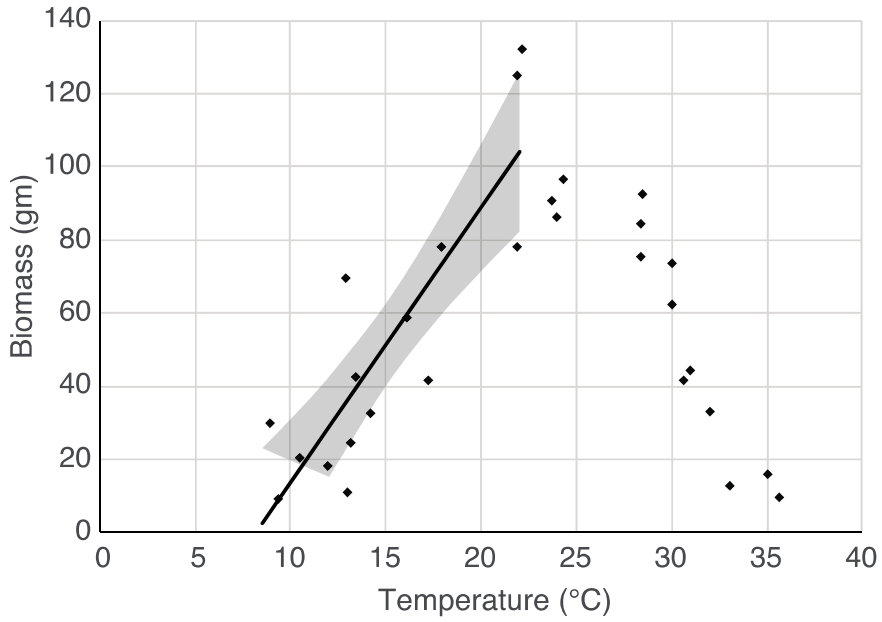

Fig. 7 Time-series regression of *Oedogonium* sp. (Lake Mendota strain) biomass on temperature during positive growth, with 95% confidence envelope. Biomass decrease at temperatures above 25ºC show that maximum biomass productivity had been achieved at the particular temperate locale

Online Resources Supplementary Materials Captions

Online Resource 1 Algal isolation and laboratory stock cultivation methods

Online Resource 2 Arrangement of inoculation culture containers (A), replicate batch cultivation containers (reactors) (1-3) within greenhouse (B) and replicate batch cultivation containers (reactors) (4-6) outside greenhouse, and carbon dioxide supplies (C)

Online Resource 3 Table of replicate and mean algal biomass, cellulosic biomass, and cellulose productivity

Online Resource 4 Analysis of variance (ANOVA) of cellulose production and temperature

Online Resource 5 Temperature, photoperiod, and *Oedogonium* sp. (Lake Mendota strain) biomass at the temperate zone Nine Springs wastewater treatment facility (Dane Co., WI, USA)

Online Resource 6 Supplementary tables (S1-S9) showing daily temperature data for experimental stages 2-5 and daily pH data for experimental stages 1-5

EPIBACTERIAL DENSITY VARIATION WITH HOST SURFACE CELLULOSIC MICROFIBRIL FEATURES OF THREE SPECIES REPRESENTING DIFFERENT GREEN ALGAL CLASSES [1]

Michael J. Piotrowski

Department of Botany, University of Wisconsin, Madison, WI 53706

and Linda E. Graham[2]

Department of Botany, University of Wisconsin, Madison, WI 53706

[1]Received.

[2]Author for correspondence: email lkgraham@wisc.edu, phone 1 608-262-2640, fax 1 608 262-

Running title:

ABSTRACT

Understanding factors that determine and predict the formation of epibacterial communities (biofilms) on surfaces of biological hosts is an important aspect of natural ecology, and also has implications for medical and industrial applications. Surface texture is known to affect microbe attachment and biofilm formation. We hypothesized that known class-specific differences in green algal cell wall cellulose structures that determine host surface texture might influence epibacterial colonization. To quantitatively explore such relationships, we employed SEM and fluorescence microscopy to assess natural epibacterial density for standard surface areas for three

structurally-similar green algal species known to have cellulose-rich cell walls, sampled from ecologically-similar freshwater habitats: 1) an *Oedogonium* morphotype (Chlorophyceae) we had previously isolated for draft genome sequencing, sampled from the same site and on the same day as 2) *Cladophora glomerata* (Ulvophyceae) for which we had previously employed metagenomics to assess microbiomes and whose cellulosic features are known to differ from those of plants, and 3) *Nitella tenuissima* representing the streptophyte algae, whose cellulosic features are known to resemble those of land plants. SEM confirmed that the latter two algal hosts had differing, but highly-textured surfaces with epimicrobiota densities that were not significantly different from each other, but were at least an order of magnitude higher than for the low-texture surfaces of *Oedogonium*. These differences, corroborated by fluorescence microscopy, indicated a previously unrecognized mechanism by which host phylogenetic grouping and genotype, specifically variations in the genes that encode cellulose synthesizing complexes, can influence algal microbiomes, thereby allowing prediction of epimicrobiota features.

INTRODUCTION

Advances in high-throughput sequencing have fostered the ability to survey microbiota associated with physical environments such as soil and ice, as well as biofilms associated with surfaces of diverse biological hosts, including freshwater algae and plants (reviewed by Graham et al. 2018). Such studies have stimulated a new research frontier, comprehending general factors key to microbiome assembly (e.g. Golford et al. 2018). One factor known to influence the development and composition of bacterial biofilms is nanoscale surface texture, a feature

considered key to managing and manipulating bacterial attachment in industrial and medical contexts (e.g., Ammar et al. 2015, Feng et al. 2015, James et al. 2019). Many types of green algae produce cellulose-rich cell walls that vary in macromolecular structural features arising from differences in genes that encode cellulose synthases. Consequently, we hypothesized that differences in algal surface textures arising from genetically-determined cellulosic structural variation might influence the establishment and persistence of epibacterial populations.

Biochemical analyses have shown that cellulose, the most abundant biopolymer on Earth (reviewed by McNamara et al. 2015), is a major component of cell walls (reviewed by Popper et al. 2011) at the surfaces of many chlorophytes (the green algal phylum Chlorophyta) and streptophytes (Streptophyta = the paraphyletic green algal class Charophyceae + land plants (e.g. Fang et al. 2017). Chlorophytes and streptophytes are known to differ substantially in the macromolecular arrangement of cellulose-synthesizing proteins (GT2 glycosyltransferases), which are encoded by nuclear cellulose synthase genes (*CesA*), and occur at the cell membrane in arrays known as cellulose synthesizing complexes (CSCs). Chlorophyte CSCs form rectangular arrays of cellulose-synthesizing particles that generate relatively thick microfibrils, and are hypothesized to have descended from linear CSCs characteristic of cellulose-producing bacteria (Nobles et al. 2001).

By contrast, streptophyte CSCs typically occur in the form of rosettes composed of six trimeric lobes that spin out microfibrils consisting of 18 strands of cellulose; such microfibrils are notably thinner in cross-section than those known for chlorophytes (reviewed by Tsekos 1999, Roberts et al. 2002, Roberts and Roberts 2004, Mikkelsen et al. 2014, Haigler and Roberts 2019). The *CesA* genes encoding streptophyte cellulose have been intensively explored (Persson et al. 2005,

Sethaphong et al. 2013, Gonneau et al. 2014, Olek et al. 2014, Slabaugh et al. 2014, Polko and Kleiber 2019). However, streptophytes are also known to possess genes encoding bacterial-type cellulose synthases, whose functions have been unclear (Pear et al. 1996, Ulvskov et al. 2013, Mikkelsen et al. 2014, Kumar and Turner 2015).

CesA-CesA interactions have been proposed to underlie the distinctive rosette-shapes of streptophyte CSCs; the absence of rosette-shaped CSCs in chlorophytes examined so far has been hypothesized to result from the lack of one or more CesA domains distinctive for streptophytes, namely a zinc-binding domain, a plant-conserved region, and a hypervariable region (Arioli et al. 1998, Peng et al. 2001, Kurek et al. 2002, Gardiner et. al. 2003). Such CesA domain differences underlie dramatic differences in the macromolecular organization of cellulose-synthesizing complexes, which in turn determine nanoscale cell wall cellulosic microfibril features. Variation in cellulosic microfibril organization has been hypothesized to help explain differences in cell wall degradability that can influence the formation of fossil remains (Graham et al. 2013).

Macromolecular shapes of plant cellulosic microfibrils are also considered important for industrial applications, so have been a recent research focus. For example, functional theory modeling has suggested that the 18 cellulose strands generated by each rosette CSC occur in angiosperm microfibrils as five layers in a 34443 arrangement, though other topologies were regarded as possible (Kubicki et al. 2018). Macromolecular features of cellulose produced by the marine/freshwater chlorophyte *Cladophora* (class Ulvophyceae) have also been investigated in light of potential industrial applications deriving from exceptionally high crystallinity (e.g. Xiang et al. 2016). By contrast, little is known about macromolecular features of cellulosic microfibrils generated by members of class Chlorophyceae, which includes a large number of freshwater

genera, including the widespread, abundant genus *Oedogonium*. This chlorophyte has been the subject of recent studies aimed at using easily-harvested filamentous green algae to improve the quality of wastewater effluent before discharge to natural systems, and at the same time generate useful materials that might subsidize wastewater remediation costs (reviewed by Lawton et al. 2017, Piotrowski et al. 2020b).

CSC variation noted to occur within green algal classes likely results from the evolutionary diversification of cellulose synthase genes. Nobles et al. (2001) hypothesized that early Viridiplantae (green algae + land plants) acquired bacterial-type *CesA* genes by horizontal transfer from cyanobacteria ancestral to green plastids. Bacterial genes that encode cellulose synthase occur as the *Bcs* operon containing *BcsA* and *BcsB*, which are sometimes fused; both genes are considered crucial for the synthesis of bacterial-type cellulose because mutation of either is reported to result in the absence of cellulose production (Hu et al. 2015). *BcsA* encodes the protein responsible for production of the linear cellulose glucan chain, while *BscB* encodes an activator of cellulose synthesis (Romling et al. 2015), which may be employed to produce extracellular mucilage. A plant homolog of BcsB has not been identified, possibly because in plants, newly-produced cellulose does not traverse the cell wall (reviewed by Haigler and Roberts 2019). Despite the significance of relationships between CSC proteins and cellulose microfibril structure, the evolutionary processes by which rectangular chlorophyte CSCs or rosette streptophyte CSCs might have arisen from ancestral bacterial-type CSCs are not well understood. *CesA* genes of early-diverging green algae, represented by modern prasinophytes, have recently been investigated to illuminate this issue.

For example, genomic and transcriptomic evidence for the presence of a Bcs-like protein in the early-diverging prasinophyte *Pyramimonas parkeae*, which lacks a cellulosic cell wall (Satjarak and Graham 2018), was consistent with GenBank evidence that Bcs-encoding sequences generally occur in the genomes of prasinophytes, including two *Ostreococcus* species, *Micromonas commoda*, and *Bathycoccus prasinos*. However, *P. parkeae* Bcs, though inferred to display QXXRW, Ds, and DXD motifs distinctive for CesA, was unusual in having only a single transmembrane region. The inferred *P. parkeae* protein formed a poorly-supported clade with a protein sequence (XP_013894101) from the chlorophyte *Monoraphidium neglectum,* which has been annotated as a cellulose synthase (Bogen et al. 2013).

In the current study, we sought to gain insight into possible effects of *CesA*-determined features of cellulose microfibril structure on densities of epibacteria occupying surfaces of common green algae representing different taxonomic classes known to differ in CSC architecture. That such influences might occur had been suggested by our own preliminary microscopic observations and images published by others (e.g. Pickett-Heaps 1975), indicating that bacterial biofilms seemed to occur more commonly on the cellulosic surfaces of charalean species representing streptophyte algae and Ulvophyceae (Chlorophyta) than on Chlorophyceae of similar ecology and similar body structure but differing in cellulosic cell wall texture.

To accomplish this goal, we assessed epibacterial densities in replicate, equivalent areas of SEM images of similarly-processed natural hosts of similar body type sampled from biogeographically-close, temperate freshwaters. Hosts included a filamentous species of *Oedogonium* (Chlorophyceae) that we had previously characterized by multiple taxonomic marker gene sequences (Graham et al. 2020), and employed for draft genome sequencing focusing on cellulose synthase-associated genes (thesis Chapter 2) and industrial applications

(thesis Chapter 3). Epibacterial densities were compared to those of two additional freshwater filamentous species whose microbiomes or microbiota we had previously characterized by high-throughput sequencing, namely *Cladophora glomerata* (Zulkifly et al. 2012, Graham et al. 2015, Braus et al. 2017) representing the green algal class Ulvophyceae, and *Nitella tenuissima* (Knack et al. 2015) representing charalean streptophyte algae. These filamentous green algal hosts are all common in nature and all are known to produce cellulose-rich walls whose surfaces vary in texture and are not extensively covered by mucilage, and so interact directly with potential epibacterial colonists. Zygnematalean streptophyte algae were not employed for this study because our previous TEM and molecular studies had shown that such species commonly produce extensive mucilage that may harbor microbes (Fisher and Wilcox 1996, Fisher et al. 1998), but that isolates cellulose cell wall surfaces from such direct association with the microbiota.

For the comparative study of epimicrobiota, *Oedogonium* was selected to represent the monophyletic class Chlorophyceae (Buchheim et al. 2012) because previous TEM, histochemistry, and cell wall immunolabeling studies had indicated that the vegetative cell walls of *Oedogonium bharuchae* are dominated by cellulose not obviously covered by other materials (Estevez et al. 2008), and previous extensive TEM observations of vegetative *Oedogonium* (and related *Bulbochaete*) (Pickett-Heaps 1975) had suggested low levels of surface biofilm formation. Neither cellulose microfibril nor CSC structure (from which key microfibril features might be inferred) have previously been described for *Oedogonium* or other representatives of class Chlorophyceae. A GT2 protein inferred from genomic sequence data for the chlorophycean *Monoraphidium neglectum* annotated as a cellulose synthase (Bogen et al. 2013) and some other

database sequences, allowed comparisons with cellulose synthase proteins inferred from our draft genomic sequence for *Oedogonium* (thesis Chapter 2). Although genomic databases (http://www.cazy.org (Lombard et al. 2014) also include putative *CesA* sequence from the Chlorophyceae *Chlamydomonas* and *Volvox*, their cell walls lack cellulose (reviewed by Domozych et al. 2012).

For our comparative analysis of epimicrobiota, *Cladophora glomerata* represented class Ulvophyceae, because this environmentally-widespread species is recognized for cellulose-rich cell walls having industrial utility (e.g. Zhang et al. 2018), as well as notable resistance to chemical and environmental degradation, features hypothetically linked to high crystallinity of distinctively large cellulosic microfibrils (Graham et al. 2013). Rectangular CSC architecture and cross-sectional microfibril dimensions have been described for the related ulvophycean genus *Valonia* (review by Okuda and Mizuta 1993). Other Chlorophyta lineages, such as paraphyletic class Trebouxiophyceae, earlier-diverging Chlorodendrophyceae and Pedinophyceae, and eight or so clades of prasinophyte green algae (Fang et al. 2017), were not represented in this study because species having comparable ecological features (freshwater, filamentous) are environmentally uncommon; with few exceptions, species classified in these early-diverging Chlorophyta lineages are unicellular or colonial (Graham et al. 2016).

In the current study, *Nitella tenuissima* represented charalean streptophyte green algae, a choice consistent with the recent availability of genomic data for *Chara braunii* (Nishiyama et al. 2018), which can co-occur in freshwater littoral environments. The inclusion of *N. tenuissima* is also justified by the availability of information about CSC architecture and microfibril cross-

sectional dimensions for *Nitella* and unicellular *Micrasterias* (Streptophyta, Desmidiales) (reviewed by Okuda and Mizuta 1993, Huang et al. 2019). Previous ultrastructural studies of filamentous *Chara fibrosa* indicated that epibacteria commonly form biofilms on environmentally-exposed walls of young vegetative cells (Pickett-Heaps 1975). In addition, we had documented presence and taxonomically characterized similar epibacterial biofilms on surfaces of young vegetative cells of *N. tenuissima* (Knack et al. 2015). *Ces*A genes including regions encoding embryophyte-specific domains (e.g. an N-terminal zinc-binding domain) have been described from the unicellular streptophyte alga *Mesotaenium caldariorum* (Roberts et al. 2002). A CAZyme-database GT2 protein inferred from draft genomic sequence for the earlier-diverging, cellulose-walled charophycean species *Klebsormidium flaccidum* (Klebsormidiales) (Hori et al. 2014) may be a CesA (Satjarak and Graham 2018). These and other GT2s mined from genomic studies of streptophyte algae (e.g. Taujale and Yin 2015) are of interest for comparison to those of the moss *Physcomitrella patens*, a model system commonly employed to represent early-diverging embryophytic streptophytes (e.g. Tran et al. 2018, review by Moody 2019). Such information, together with metagenomics-derived microbiome data for streptophyte algae and early-diverging modern plants (Knack et al. 2015)–may eventually provide insight into genomic influences on phenotype, namely how *CesA* variation may have influenced the assembly of early land plant microbiomes. The current study is an investigation of the potential for class-level green algal taxonomy, which is known to correspond with genetically-controlled differences in cell wall cellulosic features, to predict an aspect of algal microbiomes, namely the relative sizes of epimicrobiota populations.

MATERIALS AND METHODS

Sampling. Green algae sampled for this study were collected from geographically-close temperate freshwater locales during times of maximal growth, and processed similarly using sterile liquids and agitation to remove loosely-attached materials, leaving tightly-adherent, agitation-resistant biofilms. Detailed collection site metadata and specific cleaning methods have been published for *Cladophora glomerata* (Zulkifly et al. 2012) and *Nitella tenuissima* (Knack et al. 2015); similar methods were employed for the *Oedogonium* species employed in this study. Periphyton samples containing a mixture of *C. glomerata* and *Oedogonium* were collected on the same day in May, 2019, from the littoral zone of Lake Mendota, Dane Co. WI (43°4.53'N, 89°35.5'W). Early-season sampling allowed assessment of bacterial biofilms that had not been extensively overgrown by eukaryotic epibiotic species, such as diatoms. Samples of the streptophyte alga *Nitella tenuissima* had been collected from shallow benthic locales of Lake Tomahawk, Oneida Co., WI (45°50'23.29"N, 89°40'39.25"W) in August, 2012, a period when epimicrobiota largely consisted of bacterial taxa (Knack et al. 2015).

Sample processing prior to imaging. In all cases, samples were fixed shortly after collection with 2% EM grade glutaraldehyde (Polysciences Inc., Warrington, PA) in 0.05-0.2 M phosphate buffer at pH 7, rinsed three times with the same buffer, then dehydrated in an ethanol series to 95% EtOH. For scanning electron microscopy, EtOH-dehydrated samples were critical-point dried, attached to stubs using carbon tape, then coated with iridium before examination. For epifluorescence examination, glutaraldehyde-fixed and ethanol-dehydrated algal samples collected at the same time as those used for SEM were treated with a 50 μg/ml solution of the DNA-binding fluorochrome DAPI (4',6'-diamidino-2-phenylindole) to increase the contrast of bacterial cells.

Imaging for epibacterial population assessment. SEM images were made with use of a Hitachi S-4800 ultra-high-resolution cold cathode field emission SEM operated at 5 kV, at the University of Wisconsin–Milwaukee Electron Microscopy Laboratory. For quantitative assessment of epibacterial populations on surfaces of the three green algal species under study, images were randomly made, except that fields including eukaryotic microbes were avoided because the larger eukaryotes formed an over-story that obscured under-story bacterial films. SEM images of *Oedogonium* and *Cladophora glomerata* were made from samples made from the same Lake Mendota (WI) locale and on the same late-spring day in 2019. SEM images were also generated of cell wall surface cellulosic macrostructure of *Cladophora glomerata* and *Oedogonium* sp. in the same samples, for comparison of surface texture. SEM images for *Nitella tenuissima* were made from material on stubs prepared in a previous year from material collected from a different WI locale, because, to our knowledge, *N. tenuissima* does not currently occur in conspicuous populations in Lake Mendota.

Fluorescence images were made using a Zeiss Axioplan fluorescence microscope equipped with UV excitation filters (G365 FT395 LP420), a Nikon D300s digital camera, and Camera Control Pro software (Nikon, Melville, NY). Previous metagenomic studies had indicated that Lake Mendota *Cladophora* is dominated by the species *C. glomerata* (Graham et al. 2015), and all fluorescence images indicated filament structure consistent with that species. By contrast, more than one species of *Oedogonium* likely occurs in Lake Mendota periphyton, judging from variation in cellular dimensions, traits commonly employed to distinguish species of this genus. *Oedogonium* filaments having cellular features similar to those of a strain earlier isolated from the same site that had been cultivated and taxonomic markers obtained for other studies (Graham et al. 2020, Piotrowski et al. 2020a,b), exhibited yellow cell wall fluorescence that fostered

detection. Epibacterial populations were not assessed for co-occurring *Oedogonium* filaments of other species, distinguished by differing cellular features. Random algal filaments were imaged at high resolution when filament surfaces were not occluded by other algae or debris. Equal numbers of images were collected for *Oedogonium* and *Cladophora glomerata* sampled on the same day, for bacterial counts and statistical analysis. Fewer fluorescence images were available for *N. tenuissima*, which had been collected and processed at an earlier time period; such images were not employed for comparative epibacterial counts.

Epibacterial population counts and statistical analyses. Replicate SEM images of bacteria-dominated biofilms for each of the three green algal representatives were employed to generate bacterial density estimates from equal surface areas at the same magnification, then means and standard deviations were calculated, and single factor ANOVA was used for pairwise comparisons. For counts of epibacteria from fluorescence images of co-occurring *Oedogonium* and *C. glomerata*, a 20X objective lens proved optimal for assessing the largest area of algal surface while also enabling detection of unicellular coccoid bacteria. Bacteria were counted from a standard two-dimensional area of algal filament, employing a standard rectangular area of 25 mm X 200 mm (= 500 mm^2) drawn onto a transparent plastic sheet, which was then taped to a computer display screen. The length of this area was used to define a standard length of algal filament. The width of this area corresponded with 50 μm width and 400 μm of magnified *Cladophora* filaments; area 2 X 10^4 μm^2. *Oedogonium* filaments in the field sample were consistently ~20 μm in width, so filament area counted was 0.4 of that for *Cladophora*. A correction factor was employed in order to make statistical comparisons for equivalent areas of algal surface. The Student's t-test was used to make pairwise-comparisons of fluorescence epibacterial counts.

RESULTS

Bright-field light microscopy indicated the presence of bacteria on surfaces of the three species of filamentous green algae employed for this study (Fig. 1a-c), but this imaging method is too low in contrast and resolution to allow accurate quantitative assessments. Fluorescence microscopy of DAPI-stained samples (Fig. 1d-f) increased the contrast of epibacteria, allowing counts deemed more accurate than possible with bright-field microscopy, but less accurate than counts acquired from SEMs, from which a greater proportion of the standard host surface area can be accurately assessed (Fig. 1g-i).

SEM. Bacterial counts made from equivalent areas of algal surfaces viewed at the same SEM magnification are shown in Table 1. Statistical properties of these counts are shown in Table 2. Table 3 shows that epibacterial population counts on surfaces of *Cladophora glomerata* and *Nitella tenuissima* were not significantly different, but that epibacterial populations on surfaces of these two species were significantly different from and an order of magnitude higher than those on surfaces of the *Oedogonium* taxon studied.

SEM comparison of surface textures of co-occurring *Cladophora glomerata* and *Oedogonium* (Lake Mendota strain) (Fig. 2) revealed a dramatic difference. Relatively large cellulosic microfibrils of *C. glomerata* formed a coarse meshwork of relatively high surface texture, whereas cellulosic surfaces of *Oedogonium* were more finely-textured.

DAPI-staining and fluorescence microscopy. The mean number of bacteria detected in a standard area of *Cladophora* filament surface (2×10^4 μm^2) was 91.1 (range 62-125). Because *Oedogonium* filament widths were 2/5 those of *Cladophora*, a correction factor was employed to normalize *Oedogonium* counts to the same standard area; using this correction factor, the mean

bacterial count was 10 (range 0-20), ~ an order of magnitude lower than for *Cladophora*. Results obtained from the use of fluorescence microscopy were confounded by bright epifluorescence arising from algal nuclear DNA, which occluded views of some surface epibacteria. At the fluorescence microscopic level, elongate bacteria were more easily distinguished than were individual cocci occurring in groups. For these reasons, fluorescence microscopy counts are underestimated by comparison to those obtained by means of SEM. Even so, the more rapid speed with which differential bacterial counts can be made with fluorescence microscopy indicates possible utility for producing general estimates.

DISCUSSION

Our observations that epibacterial populations on cell walls of natural *Oedogonium* samples were consistently lower than those present on co-occurring *Cladophora glomerata* (Zulkifly et al. 2012, Graham et al. 2015) or those of another filamentous green alga, the streptophyte *Nitella tenuissima* (Knack et al. 2015) were consistent with the near-complete absence of evidence for epibacteria from many published TEM, SEM, and LM views of *Oedogonium* (and related *Bulbochaete*) (e.g. Pickett-Heaps 1975). These observations supported the hypothesis tested by our comparative imaging study of epibiota, namely, that cell wall features of at least some *Oedogonium* species are less amenable to bacterial attachment, leading to reduced epibacterial biofilm development, by comparison to ecologically-similar, filamentous green algal species representing phylogenetically-distinct classes. SEM revealed that the surface texture of *Oedogonium* is of a finer nature than that of *Cladophora*, a feature that may help to explain lower bacterial epibiont populations on the former genus. These results are consistent with those observed in a study of bacterial attachment and biofilm formation on alumina surfaces

constructed to have nanopores of diameters ranging from 15 to 100 nm; in that case, pathogenic bacteria were less able to colonize surfaces having the smaller pore diameters (Feng et al. 2015).

Variations in green algal cellulosic surface texture that we and others have observed seem likely related to differences in the organization of cell membrane cellulose-synthesizing complexes (CSCs), which generate cellulose fibrils, and are encoded by *CesA* genes. The CSC organization of studied species of chlorophyte green algae has been known to dramatically differ from that of streptophyte green algae (Okuda and Mizuta 1993, Tsekos 2002), and, so far as is known, seems relatively consistent within green algal classes. The current study suggests that algal cellulosic surface features differ among common filamentous representatives of different green algal classes in ways that may help predict the extent to which bacterial epibionts are able to colonize algal surfaces, thereby forming biofilms. Such information could prove useful in ecological assessments of the impacts of algal microbiota, and the development of medical/industrial applications of celluloses extracted from different types of green algae. Additional studies of green algal CSCs, *CesA* genes, macromolecular aspects of cellulose organization, and epimicrobiota populations are needed to test the generality of the observations reported here.

It is possible that cell wall components other than cellulose also influence the formation of bacterial biofilms on algae and plants. Chlorophytes and streptophytes are known to differ in non-fibrillar cell-wall carbohydrates such as hemicelluloses and matrix carboxylic polysaccharides. Xyloglucans and mannans occur in the cell walls of representatives of both green lineages (though in different ratios), while glucuronans and ulvans seem to only occur in chlorophytes, and mixed-linkage glucans and pectins may be associated only with streptophytes (reviewed by Popper et al. 2011). It is also possible that chemical exudations from the studied

algae and plants affect bacterial biofilms. Though not tested in this study, the possible roles of non-fibrillar cell wall constituents might be examined by comparing biofilm formation on axenically-cultured living filaments with biofilm formation on celluloses extracted from the same species. The roles of chemical exudations might be revealed by comparative studies of bacterial colonization of dead (e.g. autoclaved) versus living host surfaces.

ACKNOWLEDGEMENTS

We thank H. A. Owen for assistance with SEM expertise, S. Friedrich for assistance with image and graphical figures, and NSF grant DEB1119944 for financial support during the period in which *Nitella tenuissima* materials were sampled from nature and processed for SEM.

REFERENCES

Ammar Y, D Swailes, B Bridgens, J Chen 2015 Influence of surface roughness on the initial formation of biofilm. Surface Coatings Technol. 284:410-416.

Arioli T, L Peng, AS Betzner, J Burn, W Wittke, W Herth, C Camelleri, H Hofte, J Pazinski, R Birch, A Cork 1998 Molecular analysis of cellulose biosynthesis in *Arabidopsis. Science* 279:717-720.

Braus MJ, TL Whitman, LE Graham 2017 Spatiotemporal dynamics of bacterial microbiota and methanotrophic bacteria on lotic *Cladophora glomerata* (Chlorophyta). *J Phycol* 53:1255-1262.

Buchheim MA, DM Sutherland, T Schleicher, F Förster, M Wolf 2012 Phylogeny of Oedogoniales, Chaetophorales, and Chaetopeltidales (Chlorophyceae): inferences from sequence-structure analysis of ITS2. Ann Bot 109:109-116.

Domozych DS, M Ciancia, JU Fangel, MD Mikkelsen, P Ulvskov, WGT Willats 2012 The cells walls of green algae: a journey through evolution and diversity. Front Plant Sci 3:82.

Bogen C, A Al-Dilaimi, A Albersmeier, J Wichmann, M Grundmann, O Rupp, KJ Lauersen, O Blifernez-Klassen, J Kalinowski, A Goesmann, JH Mussgnug 2013 Reconstruction of the lipid metabolism for the microalga *Monoraphidium neglectum* from its genome sequence reveals characteristics suitable for biofuel production. BMC Genom 14:926.

Estevez, JM, PI Leonardi, JS Alberghina 2008 Cell wall carbohydrate epitopes in the green alga *Oedogonium bharuchae* f. minor (Oedogoniales, Chlorophyta). J Phycol 44:1257-1268.

Fang L, F Leliaert, Z-H Zhang, D Penny, B-J Zhong 2017 Evolution of the Chlorophyta: Insights from chloroplast phylogenomic analyses. J System Evol 55:322-332.

Feng G, Y Cheng, S-Y Wang, DA Borca-Tasciuc, RW Worobo, CI Morau 2015 Bacterial attachment and biofilm formation on surfaces are reduced by small-diameter nanoscale pores: How small is small enough? Biofilms Microbiomes 1:15022.

Fisher MM, LW Wilcox 1996 Desmid-bacterial associations in *Sphagnum*-dominated Wisconsin

peatlands. J Phycol 32:543-549.

Fisher MM, LW Wilcox, LE Graham 1998 Molecular characterization of epiphytic bacterial communities on charophycean green algae. Appl Environ Microbiol 64:4384-4389.

Gardiner JC, NG Taylor, SR Turner 2003 Control of cellulose synthase complex localization in developing xylem. *Plant Cell* 15:1740-1748.

Golford JE, N Lu, D Bajic, S Estrela, M Tikhonov, A Sanchez-Gorostiaga, D Segrè, P Mehta, A Sanchez 2018 Emergent simplicity in microbial community assembly. Science 361:469-474.

Gonneau M, T Desprez, A Guillot, S Vernhettes, H Hofte 2014 Catalytic subunit stoichiometry within the cellulose synthase complex. *Plant Physiol* 166:1709-1712.

Graham L, ME Cook, LW Wilcox, JM Graham, W Taylor, CH Wellman, L Lewis 2013 Resistance of filamentous chlorophycean, ulvophycean, and xanthophycean algae to acetolysis: Testing Proterozoic and Paleozoic microfossil attributions. *Int J Plant Sci* 174:947-957.

Graham LE, JJ Knack, ME Graham, JM Graham, S Zulkifly 2015 A metagenome for lacustrine *Cladophora* (Cladophorales) reveals remarkable diversity of eukaryotic epibionts and genes related to materials cycling. *J Phycol* 51:408-418.

Graham LE, JM Graham, LW Wilcox, ME Cook 2016 Algae. LJLM Press, Madison, WI.

Graham LE, JM Graham, LW Wilcox, Me Cook, P Arancibia-Avila, JJ Knack 2018 Evolutionary roots of plant microbiomes and biogeochemical impacts of nonvascular autotroph-microbiome systems over deep time. *Int J Plant Sci* 179:505-522.

Graham LE, MJ Piotrowski, JM Graham, A Satjarak 2020 Molecular markers obtained from draft genomic sequence data characterize an isolate of *Oedogonium* (Oedogoniales, Chlorophyta) employed for biomass applications. *Phycologia* (accepted pending figure adjustments).

Haigler CH, AW Roberts 2019 Structure/function relationships in the rosette cellulose synthesis complex illuminated by an evolutionary perspective. *Cellulose* 26:227-247.

Hori K, F Maruyama, T Fujusawa, T Togashi, N Yamamoto, M Seo, S Sato et al. 2014 *Klebsormidium flaccidum* genome reveals primary factors for plant terrestrial adaptation. *Nature Comm* 5:3978.

Hu L, CJ Grim, AA Franco, KG Jarvis, V Sathyamoorthy, MH Kothary, BA McCardell, BD Tall 2015 Analysis of the cellulose synthase operon genes, *bcsA*, *bcsB*, and *bcsC* in *Cronobacter* species: Prevalence among species and their roles in biofilm formation and cell-cell aggregation. Food Microbiol 52:97-105.

Huang, S., Kiemle, S.N., Makarem, M., Kim, S.H., 2019. Correlation between crystalline cellulose structure and cellulose synthase complex shape: a spectroscopic study with unicellular freshwater alga *Micrasterias*. *Cellulose* doi:10.1007/s10570-019-02793-3

James GA, L Boegli, J Hancock, L Bowersock, A Parker, MB Kinnney 2019 Bacterial adhesion and biofilm formation on textured breast implant shell materials. *Aesth Plast Surg* 43:490-497.

Knack JJ, LW Wilcox, P-M Delaux, J-M Ané, MJ Piotrowski, ME Cook, JM Graham, LE Graham 2015 Microbiomes of streptophyte algae and bryophytes suggest that a functional suite of microbiota fostered plant colonization of land. *Int J Plant Sci* 176:405–420.

Kubicki JD, H Yang, D Sawada, H O'Neill, D Oehme, D Cosgrove 2018 The shape of native plant microfibrils. *Sci Rep* 8:13983.

Kumar M, S Turner 2015 Plant cellulose synthesis: CESA proteins crossing kingdoms. *Phytochemistry* 112:91-99.

Kurek I, Y Kawagoe, D Jacob-Wilk, M Doblin, D Delmer 2002 Dimerization of cotton fiber cellulose synthase catalytic subunits occurs via oxidation of the zine-binding domains. *Proc Natl*

Acad Sci USA 99:11109-11114.

Lawton RJ, AJ Cole, DA Roberts, NA Paul, R de Nys 2017 The industrial ecology of freshwater macroalgae for biomass applications. *Algal Res* 24:486-491.

Lombard V, HG Ramulu, E Drula, PM Coutinho, B Henrissat 2014 The carbohydrate-active enzymes database (CAZy) in 2013. *Nucleic Acids Res* 42:D490-5.

McNamara JT, JL Morgan, J Zimmer 2015 A molecular description of cellulose biosynthesis. *Annu Rev Plant Biol* 84:895-921.

Mikkelson MD, J Harholt, P Ulskov, IE Johansen, JU Fangel, MS Doblin, A Bacic, WG Willats 2014 Evidence for land plant cell wall biosynthetic mechanisms in charophyte green algae. *Ann Bot* 114:1217-1236.

Moody LA 2019 The 2D to 3D growth transition in the moss *Physcomitrella patens*. *Curr Opin Plant Biol* 47:88-95.

Nishiyama and 37 others 2018 The *Chara* genome: Secondary complexity and implications for plant terrestrialization. *Cell* 174:448-464.

Nobles, D.R., Romanovicz, D.K., Brown, R.M. 2001. Cellulose in cyanobacteria. Origin of vascular plant cellulose synthase? *Plant Physiol.* 127(2):529-542.

Norris, JH, X Li, S Huang, AML Van de Meene, ML Tran, E Killeavy, AM Chaves, B Mallon, D Mercure, H-T Tan, RA Burton, MS Doblin, SH Kim, AW Roberts 2017 Functional specialization of cellulose synthase isoforms in a moss shows parallels with seed plants. *Plant Physiol* 175:210-222.

Okuta K, S Mizuta 1993 Diversity and evolution of putative cellulose-synthesizing enzyme complexes in green plants. *Jap J Phycol* 41:151-173.

Olek AT, C Rayon, L Makowski, HR Kim, P Ciesielski, J Badger, LN Paul, S Ghosh, D Kihara, M Crowley, ME Himmel, JT Bolin, NC Carpita 2014 The structure of the catalytic domain of a plant cellulose synthase and its assembly into dimers. *Plant Cell* 26:2996-3009.

Pear JR, Y Kawagoe, WE Schreckengost, DP Delmer, DM Stalker 1996 Higher plants contain homologs of the bacterial celA genes encoding the catalytic subunit of cellulose synthase. *Proc*

Natl Acad Sci USA 93:12637-12642.

Peng L, F Xiang, E Roberts, Y Kawagoe, LC Greve, K Kreutz, DP Delmer 2001 The experimental herbicide CGA 325' 615 inhibits synthesis of crystalline cellulose and causes accumulation of non-crystalline β-1.4-glucan associated with CesA protein. *Plant Physiol* 126:981-992.

Persson S, H Wei, J Milne, GP Page, CR Somerville 2005 Identification of genes required for cellulose synthesis by regression analysis of public microarray data sets. *Proc Natl Acad Sci USA* 102:8633-8638.

Pickett-Heaps JD 1975 Green Algae. Structure, Reproduction and Evolution in Selected Genera. Sinauer, Sunderland, MA.

Piotrowski MJ, LE Graham, A Satjarak 2020a Phylogenetic analysis of cellulose biosynthesis (*CesA*) genes from a draft genome for *Oedogonium* (Chlorophyceae). *J Phycol* (manuscript).

Piotrowski MJ, JM Graham, B Smith, LE Graham 2020b Temperate zone cultivation of *Oedogonium* in municipal wastewater effluent to produce cellulose and oxygen. *J Indust*

Microbiol Biotechnol (conditionally accepted).

Polko JK, JJ Kleiber 2019 The regulation of cellulose biosynthesis in plants. *Plant Cell* 31:282-296.

Popper ZA, MG Herve, DS Domozych, WG Willats, MG Tuohy, B Kloareg, DB Stengel 2011 Evolution and diversity of plant cell walls: from algae to flowering plants. *Annu Rev Plant Biol* 62:567-590.

Roberts AW, E Roberts 2004 Cellulose synthase (CesA) genes in algae and seedless plants. *Cellulose* 11:419-435.

Roberts AW, EM Roberts, DP Delmer 2002 Cellulose synthase (CesA) genes in the green alga *Mesotaenium caldariorum. Eukaryotic Cell* 1:847-855.

Romling U, MY Galperin 2015 Bacterial cellulose biosynthesis: diversity of operons, subunits, products, and functions. *Trends Microbiol* 23:545-557.

Satjarak A, LE Graham 2017 Whole genome sequencing of *Pyramimonas parkeae* reveals genes encoding carbohydrate active enzymes. *J Phycol* 53:1072-1086.

Sethaphong L, CH Haigler, JD Kubicki, J Zimmer, D Bonetta, S DeBolt, YG Yingling 2013 Tertiary model of a plant cellulose synthase. *Proc Natl Acad Sci USA* 110:7512-7517.

Slabaugh E, L Sethaphong, C Xiao, J Amick, CT Anderson, CH Haigler, YS Yingling 2014 Computational and genetic evidence that different structural conformations of a non-catalytic region affect the function of plant cellulose synthase. *J Exp Bot* doi:10.1093/jxb/eru383.

Taujale R, Y Yin 2015 Glycosyltransferase family 43 is also found in early eukaryotes and has three subfamilies in charophycean green algae. *PLoS One* 10:e0128409.

Tran, ML, TW McCarthy, H Sun, S-Z Wu, JH Norris, M Bezanilla, L Vidale, CT Anderson, AW Roberts 2018 Direct observation of the effects of cellulose synthesis inhibitors using live cell imaging of Cellulose Synthase (CESA) in *Physcomitrella patens*. *Sci Rep* 8:735.

Tsekos I 2002 The sites of cellulose synthesis in algae: Diversity and evolution of cellulose-synthesizing enzyme complexes. *J Phycol* 35:635-655.

Ulvskov P, DS Palva, D Domozych, J Harholt 2013 Classification, naming and evolutionary history of glycosyltransferases from sequenced green and red algal genomes. *PLoS ONE* 8:e76511.

Whitford LA, GJ Schumacher 1961 Effect of current on mineral uptake and respiration in a fresh-water alga. *Limnol Oceanogr* 6:423-425.

Whitford LA, GJ Schumacher 1964 Effect of a current on respiration and mineral uptake in *Spirogyra* and *Oedogonium*. *Ecology* 45: 168-170.

Xiang X, W Gao, L Chen, W Lan, JY Zhu, T Runge 2016 A comparison of cellulose nanofibrils produced from *Cladophora glomerata* algae and bleached eucalyptus pulp. *Cellulose* 23:493-503.

Zulkifly S, A Hanshew, EB Young, P Lee, ME Graham, M Piotrowski, LE Graham 2012 The epiphytic microbiota of the globally widespread macroalga *Cladophora glomerata* (Chlorophyta, Cladophorales). *Amer J Bot* 99:1541-1552.

Table 1. Ten replicate epibacterial counts from equivalent surfaces of three green algal species under SEM.

	Bacterial Counts		
Image #	*Cladophora*	*Nitella*	*Oedogonium*
1	832	347	41
2	957	319	56
3	486	274	56
4	489	490	55
5	472	246	17
6	325	307	56
7	394	206	52
8	234	435	112
9	246	249	31
10	412	607	75

Table 2. Statistical properties of comparative SEM epibacterial counts.

Cladophora		*Nitella*		*Oedogonium*	
Mean	484.7	Mean	348	Mean	55.1
Standard Error	74.7373252	Standard Error	39.88622709	Standard Error	8.08077279
Median	442	Median	313	Median	55.5
Standard Deviation	236.3401739	Standard Deviation	126.1313249	Standard Deviation	25.55364727
Range	723	Range	401	Range	95

Minimum	234	Minimum	206	Minimum	17
Maximum	957	Maximum	607	Maximum	112
Count	10	Count	10	Count	10

Table 3. Single-factor ANOVA pairwise comparisons of SEM epibacterial counts.

Groups	Count	Sum	Average	Variance
Cladophora	10	4847	484.7	55856.68
Nitella	10	3480	348	15909.11

ANOVA

Source of Variation	SS	df	MS	F	P-value	F crit
Between Groups	93434.45	1	93434.45	2.603871606	0.123996556	4.413873419
Within Groups	645892.1	18	35882.89444			
Total	739326.55	19				

Groups	Count	Sum	Average	Variance
Cladophora	10	4847	484.7	55856.68
Oedogonium	10	551	55.1	652.99

ANOVA

Source of Variation	SS	df	MS	F	P-value	F crit
Between Groups	922780.8	1	922780.8	32.65921937	2.03153E-05	4.413873419
Within Groups	508587	18	28254.83333			
Total	1431367.8	19				

Groups	Count	Sum	Average	Variance

Nitella	10	3480	348	15909.11
Oedogonium	10	551	55.1	652.99

ANOVA

Source of Variation	SS	df	MS	F	P-value	F crit
Between Groups	428952.05	1	428952.05	51.7992344	1.06798E-06	4.413873419
Within Groups	149058.9	18	8281.05			
Total	578010.95	19				

Fig. 1 Representative views of bacterial epibiota on cellulose-rich surfaces of *Oedogonium* sp. (Chlorophyceae) (a-c), *Cladophora glomerata* (Ulvophyceae) (d-f) and *Nitella tenuissima* (Streptophyta) (g-i) with three imaging methods. Left column: Bright-field light microscopy. Middle column: fluorescence microscopy showing DAPI staining response in UV excitation, Right column: representative SEMs.

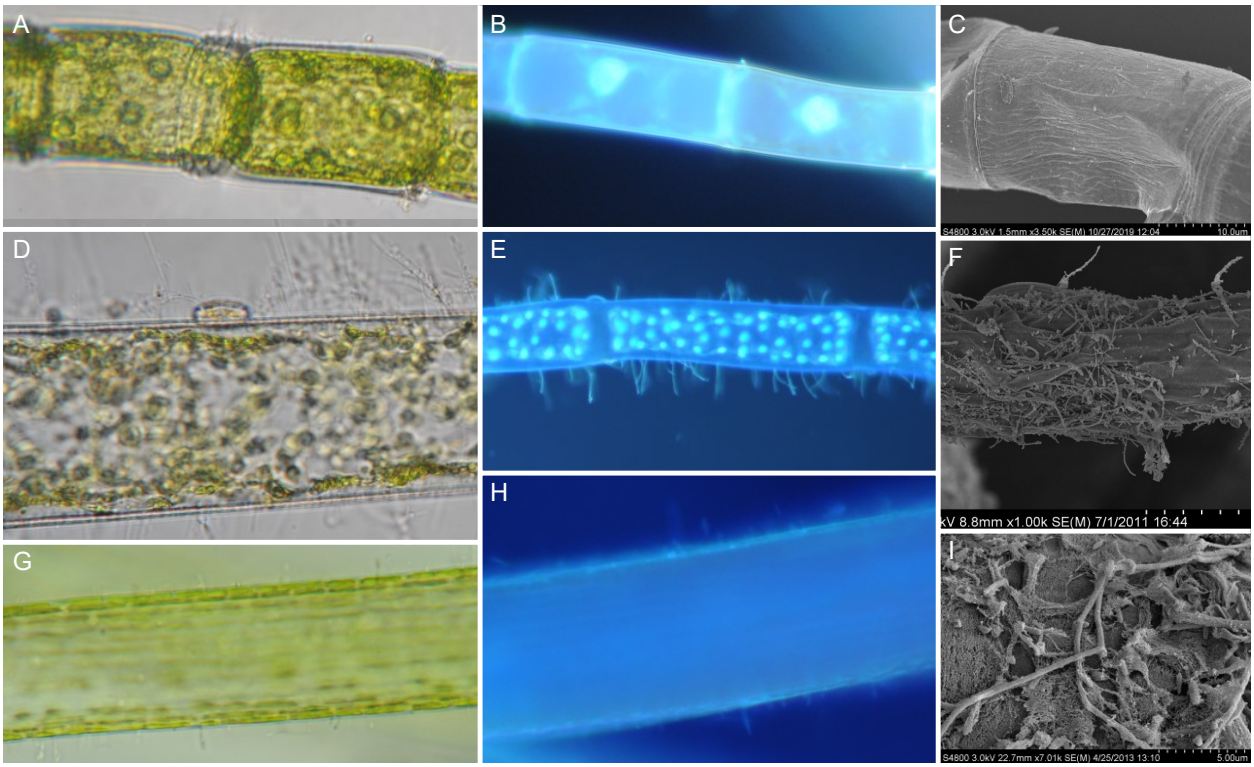

Fig. 2 SEM view of surface porosity of *Oedogonium* sp. (Chlorophyta, Chlorophyceae) at left, compared to *Cladophora glomerata* (Chlorophyta, Ulvophyceae) at right.

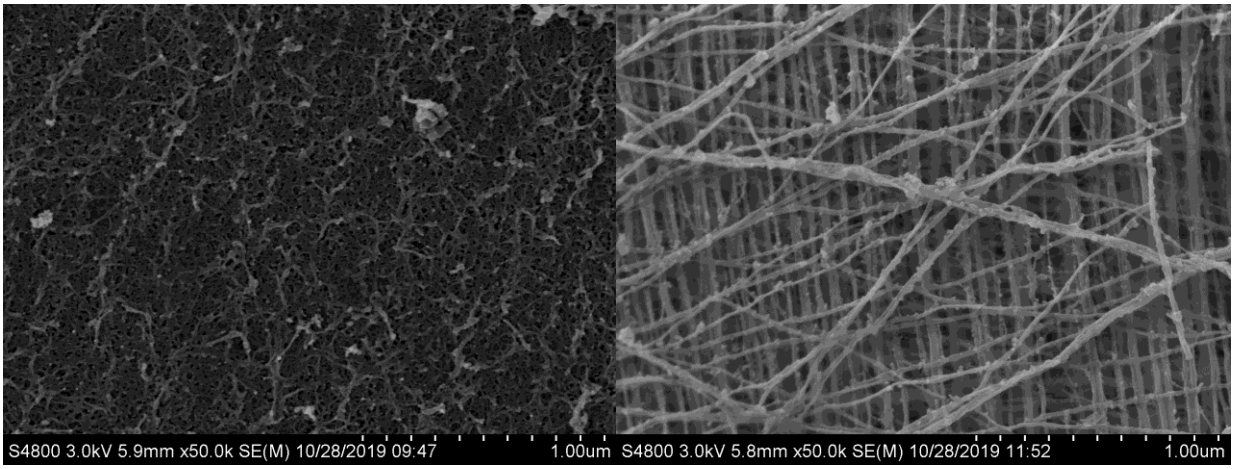

Chapter 5. Epilogue

The four previous chapters of this thesis–related by a focus on algal cellulose and its potential industrial applications–provide answers to specific questions, but also indicate future research directions. This epilogue summarizes the results of the three main areas of thesis research: a molecular analysis of cellulose synthesizing genes in draft genome sequence for a local isolate of the species-rich genus *Oedogonium* (Chapter 2), local industrial scale-up cultivation of the same isolate to produce a cellulose crop in nutrient-rich wastewater effluent (Chapter 3), and a comparative analysis of bacterial epimicrobiota associated with local *Oedogonium* populations to consider potential applications for industrially-produced cellulose (Chapter 4). For each topic, publication plans are indicated and suggestions for future investigation are made.

Chapter 1 provided an introduction to this thesis by focusing on the organismal system under study, an isolate of the cellulose-rich chlorophyte *Oedogonium* that had been generated in the Graham lab from local Lake Mendota, then characterized by means of five molecular marker gene sequences. This new locale isolate was key to molecular and industrial-scale growth studies described in Chapters 2 and 3. Genomic sequencing and gene analysis work on the new isolate could be accomplished with reduced concern that investigators elsewhere might "scoop" the work, a very real issue for Ph.D. thesis work. Further, the local isolate is more likely to be well-adapted to local climate conditions, a feature of significance for the outdoor cultivation study. Information provided in Chapter 1 enables other workers interested in such topics to generate

and use molecular markers to characterize more *Oedogonium* isolates, few species of which are represented in molecular databases. A related manuscript has been conditionally accepted by *Phycologia*, an international journal focused on algal biology, with publication expected in 2020.

Chapter 2 described the production of draft genome sequence for the local *Oedogonium* isolate to focus on genes associated with cellulose biosynthesis–*CesA* genes–for comparative evolutionary analyses. The Lake Mendota strain of *Oedogonium* was determined to possess 23 types of cellulose synthase sequences related to *Bcs* genes characterized in a previous Graham lab study of the chlorophyte *Pyramimonas parkeae*, and those identified from other chlorophytes, but that differed in ways possibly related to distinctive macromolecular features characterizing *Oedogonium* cellulose. Genomic sequence employed in this study, generated on the Illumina platform, was highly fragmented despite care employed during DNA extraction. A likely explanation for genomic fragmentation is the widespread presence of repeat regions; future re-sequencing efforts that employ long-read platforms might allow sequencing through such repeat regions, allowing more polished genome construction for this chlorophyte. A manuscript based on this thesis chapter will be generated for submission to an algae-related journal in which the lab has previously published genomic work on green algae.

Chapter 3 described the use of the Lake Mendota *Oedogonium* isolate in industrial-scale batch systems deployed at the local Madison Metropolitan Sewerage District water-treatment facility. This study built upon knowledge generated during the candidate's master's research project: cultivation of the same isolate under controlled, varying environmental conditions at the UW-Madison Biotron facility. The outdoor cultivation scale-up project indicated the feasibility

of producing a large cellulose crop whose sale could mitigate effluent remediation costs, and the added advantage of generating oxygen-enriched water that could profitably be recycled to primary wastewater treatment processes. The results were consistent with previous Biotron-generated data indicating the strong relationship of temperature and daylength to algal and cellulose crop production levels, and allowed modeling of crop production magnitude at larger scales. These models could be tested by conducting similar, larger-scale studies at wastewater treatment facilities, to generate effluent of improved water quality for discharge to natural systems, at reduced cost. In view of regulatory concerns associated with existing US wastewater treatment infrastructure, the construction of experimental larger-scale algae-linked systems might need to occur in locales currently lacking treatment infrastructure, such as remote areas or economically less-developed nations. A manuscript has been conditionally accepted by an engineering journal that previously published applied work on algae from the lab; the manuscript should be published in early 2020.

Chapter 4 described the use of imaging technologies to quantitatively test the hypothesis, based on long-term informal observations, that relatively smooth, non-fibrillar cell wall surfaces of the Lake Mendota strain of *Oedogonium* are less likely to be colonized by bacteria than are surfaces of co-occurring algae representing two other major lineages (classes) of green algae, whose cellulosic cell walls are more-highly textured. Results generated with the use of two imaging techniques were consistent in supporting that hypothesis, suggesting that distinctively smooth *Oedogonium* cellulose might be useful for applications in which bacterial colonization is undesirable. These results suggest potential markets for cellulose extracted from *Oedogonium* cultivated in large-scale industrial settings, as described in Chapter 3. Together with information

from Chapter 2, the results described in Chapter 4 also illustrate how genotypic variation affects phenotypic variation in ways relevant to aquatic microbial ecology. A manuscript similar to this chapter might be submitted to a journal focusing on algae or a materials sciences publication.

In future, emerging molecular sequencing and imaging technologies could be employed to more fully understand relationships among cellulose synthase gene structure, cellulose microfibril dimensions and organization, and algal cell surface features that affect degree of microbial colonization. The distinctive features of *Oedogonium* cellulose revealed by this study suggest that similar studies of diverse chlorophytes might indicate additional types of celluloses useful for industrial application. To identify such celluloses, more complete (polished, not draft) genome sequences assembled from long-reads could be generated for chlorophyte algae.